Integrated computer vision for autonomous marine operations.

SDPO.17.023.m.

N. Jacobsen

TU Delft
Delft University of Technology

Integrated computer vision for autonomous marine operations.

A thesis for the degree Master of Science in Marine Technology; Ship Design, Production and Operation at Delft University of Technology.

SDPO.17.023.m.

N. Jacobsen

August 14, 2017

Head Thesis Committee:
ir. K. Visser, Sbn b.d.

Daily Supervisor:
dr. ir. M. Godjevac

Graduation Committee:
dr. ir. A. Vrijdag
dr. ir. Y. Pang

Version 3.1
Delft
Master graduation thesis
Delft university of technology
Royal Netherlands Naval Academy

TU Delft Delft University of Technology

Abstract

In this graduation thesis the feasibility of a camera as sensor for nautical operations is investigated. In aerospace and automotive industries autonomous vehicles are already widely tested and used. However the marine industry has fallen behind in this development. Therefore this research is focussing on automation in the maritime sector. First a system was developed which measures distance and heading from a video feed. Thereafter simulink models were made to develop a system that autonomously can perform nautical operations. For this research multiple operations have been modeled. First of all the platform approach and the replenishment approach. In these operations the system should be able to approach a stationary or moving target. Also station keeping after the approach is required. The complexity of the operations was increased with the choice for follow the leader from the maneuvering operations. Finally the avoidance of upcoming collisions was modeled. The models for all of these operations were first developed and tested with an offline model. This enabled a quick and accurate controller tuning. The first real test for these models was done in a ship handling simulator. Here the models were tested and the influence of environmental conditions was measured. In the simulator all models performed quite well. However the performance is largely limited by the choice for the camera and environmental conditions. The most interfering conditions are lateral incoming waves, fog and light. Models for small scale testing were developed, but the communication between different components and the control system proved to be a large issue. Therefore these models could not be tested. All in all this research shows that after improving system component, a camera system can very well be used as a sensor for autonomous operations at sea.

Contents

List of Figures

List of Tables

Introduction

For many years people have been sailing the seas of the world. For just as long researchers have been investigating and developing new methods to assist the seafarers, making their jobs a little more easy. New sensors and new systems have been introduced in the nautical industry, first recommending the use of these systems and later the use of these systems was obliged by the IMO[1]. Historically shipping was the main mode of transport. Only in more recent years aviation and automotive industries have caught up with the marine industry.

However in recent years the development of new technologies in the marine industry have come to an hold, while the other two were developing more and more. Resulting in first remote operated vehicles and more recently autonomous vehicles. But in these areas of autonomous vehicles the nautical industry is far behind the other two.

This research is therefore focussing on developing a system for the first steps of automating ships. Thus there will not be a fully automated vessel, but some common or less common operations will be automated. For these operations one can think of collision avoidance or the final stages of an approach. For example platform approaches or the approach of an other vesssel, like navies do for replenishing at sea.

On ships a wide variety of sensors is being used, some of these sensors could very well be used for autonomous vessels. But to be able to fully replace the human factor on the bridge of a vessel, also a camera system should be pressent. It soon became clear that a camera is not only suited for target classification, but can also be used instead of a radar system for target detection and tracking. Thereby reducing the amount of transmitted detectable signals, which is beneficial for military use.

Therefore this research will focus on the use of a camera system for detection, tracking and classification on autonomous vessels. So the camera will be used for everything that is happening around the vessel. Other sensors will still be used to determine the state of the own vessel. For example the vessel heading and position.

Goal

The main goal of this research is to develop a camera system which is capable of performing autonomous operations at sea when integrated with a vessel. The camera system will be based on the computer vision principle. Thus the computer will process the camera feed and calculate the required target information.

This target information is then compared to desired passing distance or required approach distance and heading. The controll system will then make sure that the vessel will react if one of the calculated parameters is not in complience with the requested situation. So the camera system should be able to perform detection and tracking. But the full system should also be able to calculate the rotational speeds, for all thrusters, for appropriate controll.

In this research, next to the development of this system, also the feasibility of a camera system as main nautical sensor is investigated. This leads to the main research question: Is a camera a reliable sensor for autonomous operations at sea? So in other words can a camera system take over tasks from widely used sensors like radar.

Approach

For the approach of this research, the choice was made to make a distinction in to three pillars. The first pillar is an offline model. In an offline model the vessel motion is estimated according to the equations of motions[2]. The offline model does not make use of a camera, but the camera input is estimated based on the motion of the vessel. This type of modeling can help in understanding vessel behaviour and tuning of the controll system. An offline model is a quick and easy way to develop the algorithm before it is connected to a real vessel.

The second pillar is simulator testing. The simulator gives a real representation of what operators on a bridge see. A camera was placed on the bridge panel of the simulator. From the camera feed a computer calculated the desired vessel settings, speed and heading for example. These settings were than manually changed on de controll panel of the simulator. The benefit of the simulator is that in a short period of time many operations can be simulated and the environmental conditions can be changed instantly.

Finally the third pillar is based on small scale testing. Small scale testing is important because this is the only way of testing a fully autonomous operation. This is the only way in which the computer vision software will calculate target data, the controll system calculates the vessel settings and these settings are instantly followed by the vessel. Thereafter the camera system is constantly monitoring the progress and the system should be able to autonomously perform the operation. This is the only method were a fully closed loop is working with an actual vessel attached.

In this paper first a thorough overview will be given on the preliminary research done before the start of this thesis project[3]. Thereafter system requirements will be stated for all operations and all pillars. Thereafter each pillar will be discussed in depth seperately. Thus the development of the system and the results obtained from testing. Finally the feasabilty of the camera system is discussed and recommendation for further research or implementations is done.

1 Problem statement

In the introduction the subject of this graduation thesis was presented. Next to this the introduction also elaborates on what to expect in this thesis. In this chapter a more in depth insight will be given on the objective. Finally this chapter will also present the main and support research questions. For these questions the relevance to the subject is discussed. These questions determine the direction in which the research is heading.

1.1 Objective

Allready very early it was decided that this research would be about autonomous shipping. However on this subject there has not been a lot of research, which means that the possibilities for this thesis are unlimited. Therefore this research will focus on the developement of a system for the automation of certain nautical tasks. There were multiple reasons for the choice to use a camera as a main sensor for this system. First of all this sensor is not yet used in the marine industry. Which leads to the opportunity to investigate if this sensor is suitable for the task. During sailing target identification is required in order to perform the required evasive action. The camera system is suitable for target identification, unlike the traditional sensors. The traditional sensors also emit detectable signals. The camera is a passive sensor, which can lead to a tactical advantage in naval applications. Finally the models for autonomous tasks have to be tested in the simulator, at small scale and at full scale. Therefore a system was required that is portable and can work in all of these testing facilities. The traditional sensors are large and can not easilly be connected to a laptop with the operational models. Also when testing in the simulator a camera is the only sensor that still can work when taken into the simulator. The simulator of course also produces the sensor values, but it is not possible to connect a computer to the simulator system to obtain these values. Therefore this research focusses on the use of a camera system for autonomous shipping.

1.2 Research questions

First of all the objective has lead to the main research question: Is a camera a reliable sensor for autonomous operations at sea? With this question the focus will not only be on the use of the camera system. But this research will also investigate operability, sensitivity and feasibility. Next to this research question, support questions will be used in order to eventually come to the final conclusion on the main question. In the remainder of this chapter the support questions will be presented.

Once in awhile vessel collisions take place at sea. Usually this could have been prevented when the watch personel on either vessel would have been better observing. In these cases an early warning system or an automated response system could also aid in preventing the incident. This has raised the question whether the camera system is able to act as an early warning or automated response system. Therefore the following research question will be investigated. Can the camera system improve safety at sea?

Generally all observations during watch keeping were performed by the watch keeping personel itself. The sensors are only used as an indication and to back up the observations. With the introduction of the camera system one would like to know to what extent the system could be used for navigation. Therefore the following research question was formulated: Is the camera system able to take over from humans and traditional sensors? This question consists of two part, firstly the human tasks and secondly the tasks performed by the traditional sensors. In this case the tasks by humans are traditionally clasification and decision making. The traditional sensors take care of all measurements which will lead to the decision making. For the target classification a camera system will most likely be required. Therefore the ability of also take over the measurement task with the same system is investigated. In order to also implement dicision making a control system is required.

In the marine industry system operability is strongly influenced by the environmental conditions. Therefore this research will also focus on the operability of the camera system. The research question for this subject is: What is the influence of the environmental conditions on the camera system? For these environmental conditions the influence of seastate, fog, precipitation and light are investigated.

For the developement of the entire system including the control system an offline model could be used. In the offline model all vessel behaviour as well as disturbances can be modeled. When the model is correct, for the vessel type and configuration, the control system tuning can be done with the offline model. Hereby saving a lot of testing time. Which has lead to the question: Is it possible to obtain a stable response by controller tuning with the use of an offline model? Different vessels can have different configurations. But also sometimes during operation some thrusters can fail or become unavailable for some time. These configuration changes can also be implemented in the offline model. Therefore the following research question is also focussing on the offline model. What is the influence of a configuration change on the vessel behaviour and control?

For the testing of the models for autonomous shipping multiple operations were chosen. These operations are; platform approach, replenishment approach, follow the leader and collision avoidance . The model complexity is increasing form one operation to the next. Therefore the research question will be: Is it posssible to autonomously perform platform approach, replenishment approach, follow the leader and collision avoidance operations?

From the traditional sensors the lesson can be taken that in the marine environment different type of noise will influence the measurements. Therefore it is likely that also the camera system will be influenced by these types of noise. Video processing can change multiple aspects of the video image. Which has lead to the research question: Can video processing improve image quality and increase system performance?

2 Preliminary research

As an introduction to this research assignment, a Literature study was done as part of an individual research assignment[3]. In this chapter an overview of this preliminary research will be given, which will elaborate more on the main findings. The heading of this thesis research was mainly based on the results obtained from the preliminary research. This chapter is added in order to understand some choices made in this thesis.

2.1 Theoretical

The theoretical part of the preliminary research can be split into three parts. The first part of the research was focussing on which nautical tasks should be selected to be automated. Secondly the variety of sensors was discussed in order to find suitable sensors and to determine the heading of the main research. Finally research was done on some of the challenges that have to be overcome when automating tasks in a nautical environment.

2.1.1 Tasks

The first task that was selected was plain navigation. This task may be the most fundamental, but may as well be the most challanging to perform autonomously. For this there can be multiple targets to detect and track with various sizes and shapes. Another challenge are the large number of rules and regulations to comply to[4]. The detection and avoidance of smaller objects was considered as a separate task, but it works in the same way as collision avoidence. The difference lies only in the size of the object and whether or not the object is moving.

The second task that was considered was platform support operations. In this case the choice was made to use the platform approach as an operation for the main research. In this operation the vessel is approaching a stationary target. Because the target is stationary this operation is relatively easy. That is also why this operation can act as a baseline from which the more challenging operations can be developed.

The third task is the naval replenishment operation. This operation is build upon the platform approach. The difference here is that the target vessel is moving and that the approach will not be exactly behind the target. This operation was chosen because of the slight increase in operation complexity.

The next task was naval manouvring. This task can be made more or less complex depending on the kind of maneuvers the target vessel is performing. Therefore it was chosen to not fully perform this operation. Only one aspect of this operation will be used for further research. The part that was chosen is follow the leader. In this case the vessel has to stay in the wake of the target vessel and follow all it‘s speed and heading changes.

2.1.2 Sensors

For the preliminary research the multiple sensors were discussed. The main point of view was to investegate whether or not these sensors could be suitable for automation. Another important feature was to determine which sensors can practically be used for different types of tests during the research. First of all the sensors used in autonomous cars were discussed. Some of these sensors can be used, but most of them have to be changed in order to cope with the different range needed for marine operations. For example the car used Lidar and ultrasound[5], were a ship would use radar. The camera system used on cars could however be usefull.

For potitioning GPS is the most used sensor. For full scale autonomous vessel this will have to be used. But the accuracy is generally not good enough for small scale tests. However with small hardware and software changes centimeter accurate GPS should be possible[6]. Another possibility is to measure the relative position to a landmark with radar or camera. With this relative position and the true position of the landmrk the vessel position can be determined. However this requires a large database and an accurate classification system.

Next the detection of other vessels and navigational hazzards was discussed in the paper. Typically a radar will be used to detect and track other vessels. Navigational hazzards are generally too small to be detected by radar due to the signal noise in which the target disappears. Therfore a camera system could be usefull in detecting [7] and tracking [8][9] these objects. An extra help in detecting smaller objects with a camera, is to take the own motion of the vessel into account[10]. This algorithm takes multiple image frames and determines which objects move and which objects only appear to move due to vessel motion. The objects that actually do not move belong to the background and the objects that are moving by itself should be investigated further.

Finally the sensors for determining distance and heading to vessels and object were mentioned in the paper. Generally this is also done by radar systems. However it is also possible to calculate the distance to an object in the water by only using a single frame from the video feed[11][12]. Mainly because of this feature the choice was made to shift the focus on using a camera system as primary sensor for the research. The camera system can be used for testing at full scale, small scale and in the Ship Handling Simulator. Figure 2.1 shows the principle of calculating distance from the camera frame. After the figure quation 2.1 will show how the distance is calculated with the use of this figure.

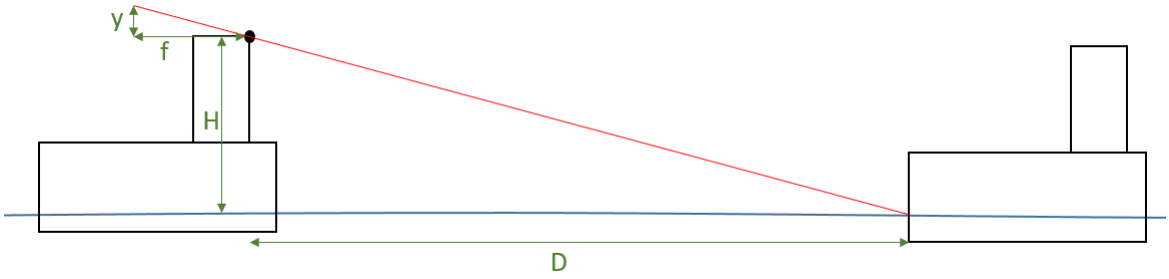

Figure 2.1: Triangle method for calculating the distance from a camera image.

$$D = \frac{f * H}{y} \tag{2.1}$$

In order to use this method the resolution of the camera should be high enough to detect the pixel position at which the target vessel intersects with the water level. Additionally the height 'H', with respect to the water level, at which the camera is placed should be known. But this is a vessel parameter, thus this value should be known. Furthermore two typical parameters from the camera should be known. The focal distance 'f' has to be used. Finally the image height 'y' is needed. To calculate the distance, this height should have the same unit as the camera height and the focal distance. Therefore the image height is calculated by multiplying the number of pixelf in y by the pixel diameter. The pixel diameter and the focal distance are dependent on the camera that is used.

A similar approach is taken to calculated the target bearing from the video feed. Only this time the triangle system is rotated 90 degrees to horizontal position. This time only the camera specific characteristics are used. This time not the vertical pixel position is used, but the horizontal pixel number from the centre 'x'. First figure 2.2 will show the situation. Thereafter in equation 2.2 the formula to calculate the bearing iss presented. 4.11

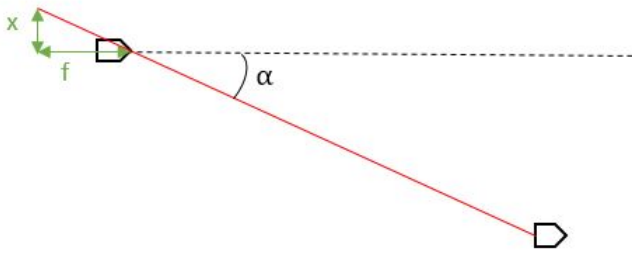

Figure 2.2: Triangle method for the calculation of the bearing from a camera image.

$$\alpha = atan\left(\frac{x}{f}\right) \tag{2.2}$$

2.1.3 Challenges

When a sensor like a camera system will be used in a harsh marine environment, there are some challenges which have to be overcome. The effect on the system will largely depent on the choices made for the sensor type and other sensor characteristics[13]. The challenging conditions will be mentioned first, followed by the sensor property which can reduce the effect.

The first challenge will be vessel movement. Usually a camera is positioned on a fixed location, or for example on a car with limited movements. However on a vessel, due to seastate, the camera will move with six degrees of freedom. The movements are surge, sway, heave, yaw, pitch and roll for linear movements and rotations. A possibility to overcome this issue is to stabilize the camera, but this will add to system complexity.

The seastate will not only cause vessel movements, but also signal noise will be a result of the seastate. The waves can cause false targets, but also targets can seem to disappear within the waves. Other causes of noise can come from precipitation and fog. Both weather phenomena will reduce the ability to make a distinction between target and background. In order to reduce the noise, caused by the waves, a filter could be added to the system. The noise caused by the waves will have a relative heigh frequency compared to vessel observations. The best suitable filters for this type of noise will be the low pass filter or the notch filter[14]. Both filters can filter out frequencies, while noise usually has a high frequency compared to the signal only the target signal will remain.

The weather phenomena also have another influence next to the introduction of noise. These phenomena will also reduce the light intensity, light intensity is also reduced during twilight periods twice a day. Of course when it is dark the camera system will not be able to detect any targets, but also with reduced light camera performence can be influenced. The use of a camera with a global shutter system can improve image quality in low light conditions. When a camera chip is used which produces a digital output, the image can be enhanced by software. By using a camera with three reception chips, one for each colour (red, green, blue), a better image quality can be obtained. Finally by increasing the size of each pixel, more light can be captured and thus improving the quality.

So when taking these influences into account the best camera system can be chosen. The CMOS (Complementary Metal-Oxide Semiconductor) camera sensor chip is perfered over the CCD (Charge Coupled Device)[15]. A CMOS sensor is equiped with a rolling shutter, but the digital output enables digital image enhancement[16]. The camera should also consist of a three chip configuration with large pixels. Finally the system should also contain some type of filter for noise reduction.

2.2 Matlab analysis

The final part of the preliminary research was based on understanding more of the image processing functionalities in Matlab simulink. With some of these functions a distance measurement system can be developed, however in order to use this system some parameter analysis is necesarry. In the first part of this section the Matlab functions are discussed, the second part is elaborating on the analysis.

2.2.1 Matlab functions

The Simulink modeling tool from Matlab has multiple functionalities that can be used for image processing. First of all the video feed has to be loaded into Simulink. This can be done by the 'from video device' function. In order to show what the functions do with the video image, an image from the ship handling simulator will be used. The test set up in the simulator will be discussed in chapter 5, where the simulator testing is discussed. Figure 2.3 shows the direct video image from the video device block.

Figure 2.3: Plain image as it enters Simulink.

As mentioned before a camera chip detects three colours, red, green and blue. So for every pixel a value for each colour is known, the value represents how much light of that colour was captured. These three values can be combined into one number via the formula given in equation 2.3. This equation is embedded in the colour space conversion function in Simulink.

$$Intensity = \begin{bmatrix} 0.299 & 0.587 & 0.114 \end{bmatrix} \begin{bmatrix} R \\ G \\ B \end{bmatrix} \tag{2.3}$$

The pixel value is now converted into an intensity value, where zero represents black and one represents white. The image is now transformed into a gray scale intensity image. Figure 2.4 shows this intensity image from the simulator image.

Figure 2.4: Intensity image from the colour space conversion block.

In order to develop a distance measurement system the gray scale image has to be converted to a binairy image. In a binairy image the pixels can either have a value of one or zero. The Simulink block that performs this conversion is the autothreshold block. As the name suggest, the block determines a threshold value based on the incoming gray scale image. Based on the threshold value the block assignes either a one or a zero tho each pixel. Figure 2.5 presents the resulting binairy image.

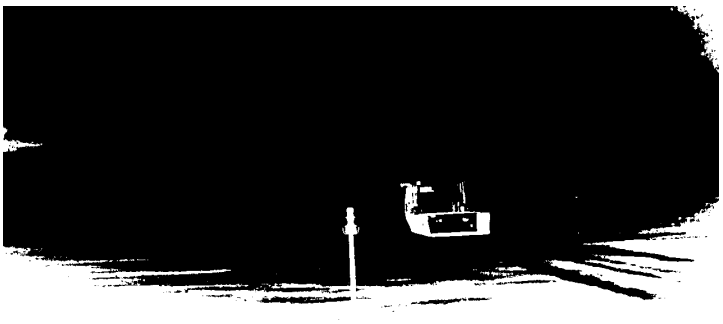

Figure 2.5: Binairy image from the autothreshold block.

The block that will use the binairy image is the Blob analysis block from the simulink library. This block is able to detect a group of white pixels, for example the vessel in the image. Groups that are touching the edge of the image can be neglected. Also the number of detected groups can be selected. As well as the size of the group, so that small targets can be neglected.

The blob analysis block can have multiple outputs, the specific outputs can be selected. The block can output the centre point of the blob. Also the bounding box can be an output, which is the smallest rectangle that can be fitted arround the blob. The length of the major and minor axis can be selected as an output. The orientation of these axis depends on the shape of the blob and thus the orientation is also an option. The area, which is the number of pixels in the blob, is the next option. Finally the block can give the number of blobs in the perimiter of the blob. These functions can aid the system in tracking targets. These functions can be used in order to calculate the required target information.

2.2.2 Analysis

In order to calculate the distance, two variables are needed: focal distance and image height. The image height has to be calculated by the product of the pixel diameter and the number of pixels. The number of pixels is the only value that can be obtained from image processing. The focal distance and pixel diameter are camera specific parameters. However both are usually not released by the manufacturer. These two parameters are combined in a camera parameter C. Equation 2.4 shows how equation 2.1 is transformed to feature the camera parameter.

$$D = \frac{f * H}{y} = \frac{f * H}{n * d} = \frac{C * H}{n} \tag{2.4}$$

This equation shows that the camera parameter is calculated by dividing the focal distance by the pixel diameter. Because these values are not known for the used camera the camera parameter has to be calculated by reversing equation 2.4, the result is found in equation 2.5.

$$C = \frac{D * n}{H} \tag{2.5}$$

A simple Simulink model was made which uses the Blob analysis block to calculate the camera parameter. The block gives the pixel number needed for the equation (n). The webcam was placed on a box wich puts the centre of the camera at a height of 10.7 centimeter (H). A white piece of paper was placed at multiple distances D based on the lines of laminate pieces on the floor (D). Table 2.1 shows the results for the camera parameter at different distances multiple times.

Camera Parameter	**Camera height 10,7 cm**			
Distance (cm)	**46.8**	**65.3**	**83.8**	**102.3**
	1261.842	1262.699	1261.586	1274.756
	1258.136	1263.598	162.693	1275.083
	1262.321	1265.867	1262.089	1274.838
	1258.894	1262.155	1261.973	1275.324
	1260.131	1261.752	1261.452	1274.897
Average	1260.2652	1263.2146	1261.959	1274.9798
First 3	1261.812932			
All	1265.10465			

Table 2.1: Camera parameters at multiple distances.

From this table it shows that the camera parameter for the first three distances produces almost the same values. However for the final distance the parameter produces a different value. That is also the reason that two averages are calculated as can be seen in the table. The next step is testing these parameters by measuring distances. This is done for more distances measured with a tapeline. The results for these measurments are presented in table 2.2.

Distance (cm)	**Matlab parameter**	
Ruler	**1261.812932**	**1265.10465**
40	40.28	40.39
50	50.38	50.52
60	60.21	60.37
70	70.09	70.27
80	79.85	80.06
90	89.58	89.82
100	97.74	97.99
110	107.05	107.32

Table 2.2: Distances measured with a tapeline and a camera system.

By comparing the two results for both average parameters it shows that overal the average of all distances fits best to the actual distance. Hence the camera parameter of 1265.10465 will be used for furter testing during the research.

2.3 Conclusions

In the previous section insights are given into autonomous operations at sea. Besides this it became clear that there is a lot to take into account in order to perform these operations. All in all, from this research, it seems feasible that the chosen tasks can be performed autonomously. However ongoing research has to be performed. This section is focusing on the following research. Recommendations will be done from which the scope for the research can be determined.

When researching autonomous operations at sea, a start has to be made by selecting a number of operations. Some challenging operations need to be performed, but for the first research the operations cannot be too advanced. Therefore four operations have been selected. The first task is the navigation, the most essential task for each vessel. Then some more challenging operations are chosen. First the approach of a stationary platform and secondly the approach of another sailing vessel. The final task will be the following of a lead vessel. These four operations will provide a natural build in operation complexity.

In order to size the research it is convenient to focus on one or a small number of sensors that will be used. It became clear that one operation requires other sensors and information than the other operation. However a camera system has the potential to be used for more purposes and in more operations. Therefore the research should focus on using a camera system for autonomous shipping, just like cameras are already used in autonomous vehicles.

There are a great number of camera sensors and configurations. In order to get the best results for the measurements with the camera system the different possibilities have to be considered. For autonomous operations a CMOS camera chip will be preferred. The main features for this decision are digital output, sampling speed and energy consumption. In order to enhance low light capabilities, a three chip sensor configuration with relative large pixels is required. Also a high resolution is preferred for beter accuracy.

The filtering of noise will be necessarry in order to improve the accuracy. Sensor fusion is probably not needed for the development of the autonomous control system. But when a number of sensors are used to obtain the full picture sensor fusion can be valuable for the final application in real vessels. With sensor fusion the most likely result is calculated from all measurements.

From the section on Matlab and simulink functionalities it became clear that the Matlab software can be used in combination with a camera system. Matlab is able to process images and provide pixel information as output. The chapter shows some functions that are provided by Matlab Simulink. However more processing is needed in order to control the model. The type of operation will require different additional input information. The output will consist of a desired speed and heading, which will be used for the thrust allocation.

The final section shows how important the placement of the camera is. In order to accurately calculate the camera parameter, the camera has to be placed with great care. When the camera is placed, roll, pitch and yaw angles should be prevented. With a roll angle the horizon will not be parallel to the centre line of the image. A zero pitch angle will make sure that the horizon will be captured on the centre line. The camera system measures the distance straight ahead. Thus when the yaw angle is zero, this is the distance to the target. When the camera is placed correctly, it is possible to calculate the required camera parameter. And finally this parameter can be used to calculate the distance to objects.

This concludes the preliminary research. A summary was made for the most relevant findings that have to be used in the main research. Finally all conclusions obtained from the preliminary research were listed.

3 System requirements

In order to develop a model system, first the system requirements have to be specified. The requirements can act as a guideline for the development but they also define when the model is finished. Hence not only functions need to be stated, but also desired accuracies have to be established. The accuracy requirements will only apply for perfect conditions. The operational limits for this system are not yet known. But near the operational limits the acccuracy will of course be influenced. The main factor for these limits will be the environmental influences.

In this chapter the requirements will be defined. All operation types have different requirements and therefore each operation will be discussed individually. First the standard navigation will be discussed. Thereafter the platform approach operations will be defined. Finally the requirements for the replenishment at sea will be defined. For these operations one or more of the sensor system functions will be performed. The functions detection, tracking and classification will be used for the sensor part of the system. Also the control part of the system will have to meet some requirements. These requirements will also be defined in this chapter.

3.1 Navigation

From the three operations, navigation is the most essential and straight forward operation. However to implement this operation into a sensor and control system it will be the most extensive and challenging operation. In order to simplify the task, first a system will be developed which will act the same for all vessels. When this system works vessel classification will be added, which will make sure that the system will avoid collisions according to the regulations[4]. For the testing of this system only the simulator can be used. Therefore all requirements only apply for simulator testing.

3.1.1 Without distinction

First the system requirements will be made for the system which will not make a distinction between different types of vessels. In order to explain the requirements in more detail figure 3.1 gives an example of a shipping situation. With this figure one can understand what type of information is needed to perform safe navigation.

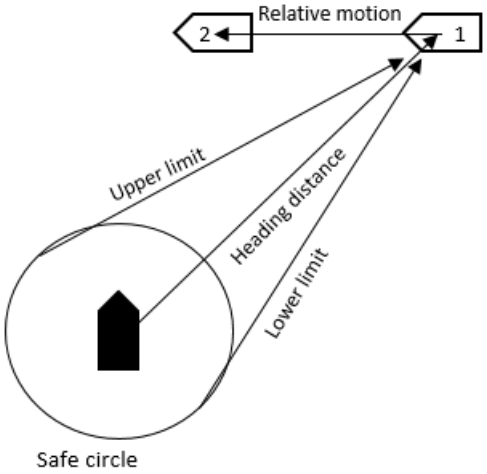

Figure 3.1: Navigation situation.

In this figure the own vessel is coloured black. The system has detected a target vessel in position 1, a little while later the target vessel is located in position 2. This movement is based on the measured heading and distance, thus this movement is relative to the own vessel. The safe circle is a predefined circle from which other vessels should keep clear in order to guarantee safe shipping. The radius of the safe circle is based on

the location and usually set by the captain. The upper and lower limits give the heading from the circle to the target vessel. If the reciprocal of the relative heading lies between the two limits, the vessel will pass through the safe circle. This has to be prevented by a course or speed change by one of the two vessels. Which vessel has to make the change is described by the regulations[4].

The camera system should be able to measure the heading and the distance to the target vessel. With a pair of these measurements, the system has to calculate the relative motion. Based on the first measurment and the set safe circle, the upper and lower limit have to be calculated. When the reciprocal of the relative motion lies outside the calculated limits, no further action has to be conducted for this target.

However, when the reciprocal of the relative motion lies within the limits further calculation has to determine whether the vessel should divert. When the target is located at the starboard side of the vessel and the passing distance is too small, the system should alter course. When the target vessel is located at the port side of the vessel, the target vessel is initially responsible for the evasive action. Only when target vessel fails to react, the system should also react to avoid the collision. In both cases a course change to starboard is required.

When the target is located whithin a few degrees in front of the vessel, other rules apply[17]. For two vessels approaching each other, both vessels are required to change course. When the vessel is overtaking the target only the own vessel is required to change course. In these cases the system should calculate if the target vessel is to pass at port side or at starboard side. When the relative motion indicates a passage at port side, the system should change course to starboard. When the passage is at the starboard side, a course change to port should be conducted.

The system should be able to calculate a sufficiently large course change in order to avoid the target vessel passing through the safe circle. Next to the course change the system should also be able to calculate how to get back on the planned track. Thus when the course change is initiated a timer should start running. When the vessel has passed, the course change is inverted and the timer is stopped. A second timer will start when the vessel has turned to sail back to the original track. When both course changes are equal, the time to get back on track is the same as the time the vessel was sailing away from the track.

3.1.2 With classification

In the collision avoidance regulations a distinction is made in vessel type[17]. Some vessels are less capable of maneuvering due to vessel type or conducted operations. Therefore the system should be able to distinguish vessel type. In the previous section, if a vessel came in from the port side no action should be conducted. In this case when some vessel types come in from port evasive action should be conducted, usually a course change to port is required.

Vessels with restricted maneuverability do not have to divert for any vessel type. These vessels look like normal vessels, but they have black shapes in the mast. These shapes depend on the type of restriction. A diamond for towing operations, a rectangle for deep draft vessels, bal-diamond-bal for genarally restricted vessels and two balls for an unmaneuverable vessel. Thus the camera system should be able to detect and distinguish these shapes in the mast.

Fishing vessels have one step less privilages, but they have right of way from all other vessels except the above mentioned types. A condition that has to be met, is that the vessel is actually fishing. The act of fishing is indicated with a diabolic shape in the mast. Thus eventhough a fishing vessel is easy to recognize, the camera system should be able to detect this diabolo.

The final privileged vessel type are the sailing vessels. It has to divert for all the above mentioned vessels, but not for engine driven vessels. However, when a sailing vessel also uses it‘s engines next to it‘s sails, the vessel is considered to be a engine driven vessel. The sailing vessel has to indicate this by a downward pointing cone. The camera system should also be able to detetct this cone.

Hence a database should be formed in order to determine the vessel type. While these shapes are not modeld in the simulator, for testing the database has to be based on recognizable vessel shapes. For fishing vessels and sailing vessels this will probably not be much of a problem. However the distinction between different types of engine driven vessels is not possible. So for this model a distinction is made between engine driven vessels, fishing vessels, sailing vessels and special operations. The last type are engine driven vessels which are more easy to distinguish, for example towing vessels and dredgers.

The model based on the requirements from the first paragraph has to be expanded with the database. The system should recognize the vessel type of port side contacts. If the vessel is one of the special types, the system should also calculate a course change for port side contacts.

3.2 Platform approach

In this section the system requirements for the platform approach operation are being stated. The requirements will be different for the small scale test compared to the simulator tests. The requirements for both test cases will be discussed in the following two paragraphs. Figure 3.2 shows a real life platform approach which could be automated.

Figure 3.2: A platform supply vessel loading at a platform.

3.2.1 Simulator test

In the simulator no direct feedback loop will be used. The system will calculate speed and heading changes, which will be forwarded to the simulator operator. The system will use the video feed to calculate a heading and distance to the platform. These will be the inputs for the model.

During the approach the system should calculate small course changes, in order to maintain a straight approach to the platform. As the distance is reducing, the vessel speed should be decreased for a smooth approach. For some approaches the vessel should keep a specified distance clear of the platform and in this case the system should stop the vessel at that distance and then maintain position. For example when a crane is to load and unload cargo from platform to the vessel. For other applications the vessel could be required to gently touch the platform and then maintain position. This could be the case when a personel transfer has to be performed.

For both tasks accurate station keeping performance is required. This accuracy has to be ensured by the controll system in the model. In these simulator tests the time to relay the heading and speed changes has to be taken into account. Therefore the operation has to be performed at relatively low speed. For example when the controll system is directly connected to the actuators, the vessel will start reacting as soon as the

system has calculated the new settings. However in this case the system calculated new settings and will present them on the screen. Then someone has to read the new settings and give the order to the helmsman before the ship will start to react.

3.2.2 Small scale test

The benefit of the small scale test is the closed loop, which results in a fully autonomous vessel. In this case the vessel will react instantly to an offset, which ensures better testing of the developed system. From the video feed the distance and heading offsets are calculated. The controll system calculates new actuator settings, which will be adopted by the vessel. Eventually the vessel should perform the approach fully autonomously. The working principle should however be exactly the same as described for the simulator system in the previous paragraph. Because of the closed loop the relay delay will not be a problem in this case. Hence the approach speed does not have to be limmited.

3.3 Replenishment at sea

Replenishment at sea is a military operation by which at least two vessels exchange fuel and goods. These two vessels will have to sail in close proximity of each other in order to establish the connection. The receiving vessel will make the approach towards the tanker. Because the distances are so small, the margin for errors is also very small. Figure 3.3 shows a replenishment operation performed by the Royal Dutch Navy. For testing only the approach will be tested and not the final station keeping. This is because the target vessel will run off from the side of the picture when the vessels are coming closer, while the available webcam has a limited viewing angle.

Figure 3.3: Replenishment at sea by the Royal Dutch Navy.

The receiving vessel will be positioned behind the target vessel. When the operation commences the speed will be increased and the required heading is calculated. Form the desired lateral distance and the measured actual distance to the vessel, the heading in which the target should be located is calculated. By comparing this heading with the actual heading it is determined what the course change should be. The process of measuring heading and distance is performed constantly in order to make sure the required lateral distance will be obtained. When the vessels are getting to close for sensor measurements the lateral distance will be maintained visually until the vessel has reached the assigned station. During station keeping the distance is checked by a cable at the bow of the vessel. As mentioned before testing will take until the approach is getting to close for accurate sensor measurments.

3.3.1 Simulator test

The ship handling simulator is a very good way to test this operation, while the operation can be simulated realisticly. This operation is very similar to the platform approach operation. The main difference is that the target is moving in this case compared to the stationary platform. Therefore in this case the controll system should be able to understand that the target is moving. With this information it should regulate an overspeed in order to establish the approach. Finally the system should match the target speed when the station is reached. Again this process goes via multiple communication steps, hence the relatively slow reaction time has to be taken into account.

3.3.2 Small scale test

The replenishment approach will also be tested with two small scale vessels. Again the principles stay the same as before. However in this case the system can be tested on it‘s full autonomous capabilities, but the operations remain the same and the requirements remain the same. The only differences are the scale and that the system now has a closed loop.

3.4 Follow the leader

The final operation that will be tested is a typical naval excersize of follow the leader. A leader will be assigned and one or more vessels will follow in it‘s wake at a designated distance. An image of what this operation looks like is presented in figure 3.4. Usually the largest or least maneuverable vessel is assigned as leader. This operation is in some ways similar to the replenishment operation, as a station has to be kept relative to a moving target. Only for the replenishment operation, the target has to maintain heading and speed. But in this operation the leader is free to change both speed and heading. The following vessels will have to react to these changes.

Figure 3.4: US Navy performing a follow the leader excersize.

This operation will only be tested with the use of small scale vessels. In this way the movement of the leader can be controlled better and the reaction of the follower can also be monitored more easily. First off all the system should be able to keep position right behind the leader, in his wake. Also the distance should be regulated in order to keep position even if the leader is changing speed. Finally when the leader is changing course, the system should be able to follow this change and eventually again take position behind the leader at the required distance.

4 Offline model

The main goal for this research was to develop a system which is capable of performing naval operations autonomously. A good way to begin modeling is to start by devoloping an offline model. An offline model is a closed loop system in which the vessel motion is predicted through the equations of motion. With an accurate offline model the controll system can be tuned for real testing. This can reduce the time spent on testing signifficantly. An offline model can also aid in obtaining a better understanding of the model.

4.1 Theoretical model

In the first half of this chapter the full offline model will be discussed. A more in depth analysis of the different subsystems will be provided. The full offline model can be found in appendix A, were it is placed because of the large size. The analysis will start at the right with the settings. Then the clockwise route through the subsystems will be taken, because this is also the order in which the signals travel.

4.1.1 Block: Settings

The first block in the model is the settings block. In this block the initial conditions can be set. Fifteen parameters, devided in five groups, can be changed in order to set different conditions. The fifteen parameters together make up the eight output parameters of this block. The first settings that can be changed are the operational actuators, figure 4.1 shows how the actuators can be controlled.

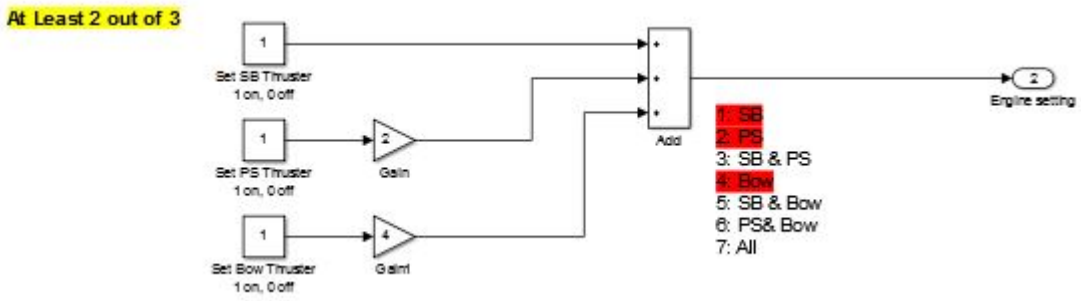

Figure 4.1: Actuator settings controll.

The model is based on a three actuator configuration, with a port and a starboard stern thruster and a bow thruster. Hence the three input boxes. Each box represents an actuator. Value one represents a working actuator and value zero represents a faulty actuator. The output is a single engine setting parameter. Each actuator was assigned a multiplier value. The sum of the three values indicates which actuators are available. This system can be compared to a binary counter, were each index is worth double the value of the previous index. Only one actuator is allowed the fail each simulation, because otherwise the vessel can not be controlled. The result of the summation indicates the engine mode that is simulated. In engine mode three only the stern thrusters work. Engine mode five has a working starboard side thruster and a bow thruster. In engine mode six the port side thruster and the bow thruster are operational. Finally in mode seven all thrusters are available.

The next group of input parameters is to set the initial position and heading of the vessel. In this group also the availability of the heading sensor can be set, in the same way as for the actuators. When the sensor is not working the initial heading will be changed to zero. The value will be used later in the model for the vessel controlls, which will be explained at a later stage. The setting for the initial position can be found in figure 4.2.

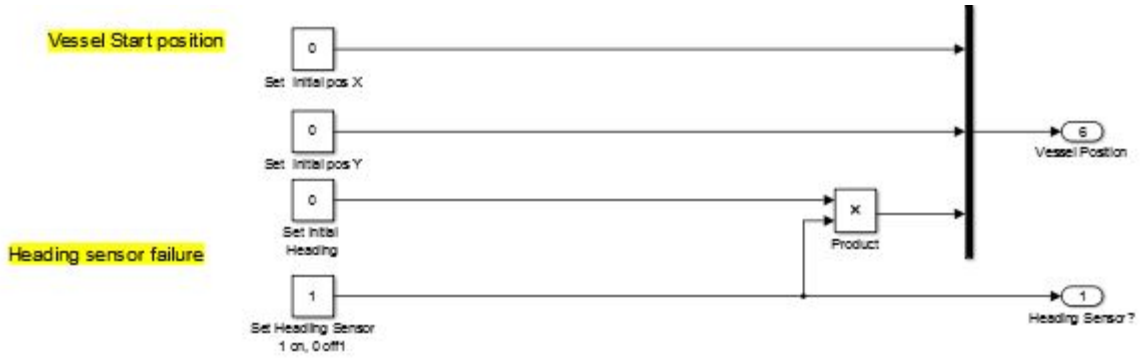

Figure 4.2: Initial vessel position settings.

Just as for the own vessel, also the initial position and heading for the target vessel has to be set. An extra parameter that has to be set for the target vessel is the target speed. The target speed and heading can not be changed during the simulation. In figure 4.3 the settings for the target vessel are presented.

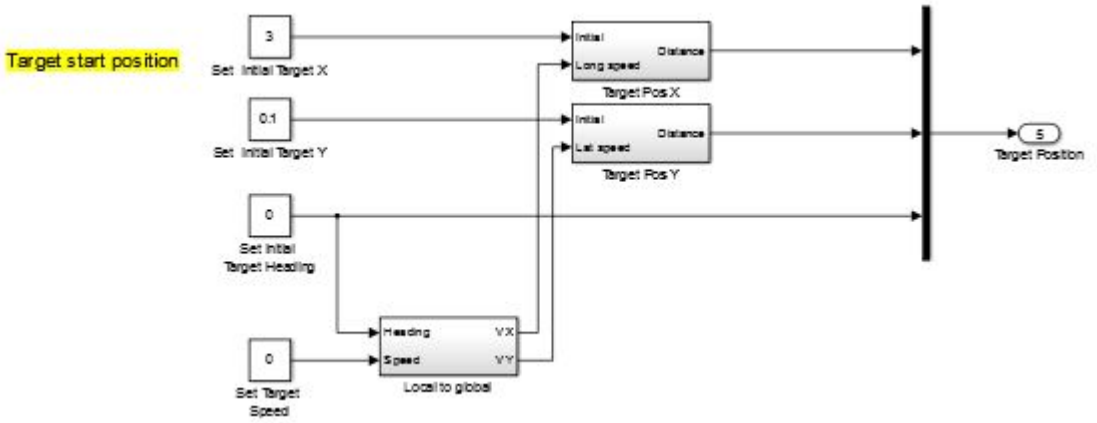

Figure 4.3: Initial target position settings.

Where for the own vessel the position settings are only used once as an initial position. For the target vessel the position is constantly updated. For the position update the target speed is used. But in order to do so, first the local speed has to be converted into global speed in x and y direction. Equation 4.1 shows the formula used for this computation.

$$\begin{bmatrix} V_x \\ V_y \end{bmatrix} = \begin{bmatrix} cos(Heading) \\ sin(Heading) \end{bmatrix} * Speed \tag{4.1}$$

In each itteration, for both directions, the new target position is calculated. For each time step the translation is calculated and the covered distance is added to the position from the previous itteration. In this way the target position is continuously updated.

The next part of the settings is to determine the approach values. In other words the values represent the relative location to the target vessel in which the own vessel needs to take station. The RAS (Replenishment At Sea) distance indicates the lateral distance between both vessels. The approach distance indicates the longitudinal distance between both vessels. At the end of the simulation the vessel should be exactly located at this position relative to the target vessel. Figure 4.4 shows these settings.

Figure 4.4: Approach values.

The final settings that can be done previous to the simulation are the environmental influences. Figure 4.5 presents the setting through which wind and current can be switched on and off. Again the indicators work in the same manner as for the actuators and sensor.

Figure 4.5: Environmental influences.

This concludes the changeable settings for the offline model. By changing multiple settings different operations can be set. For example when the target speed and the RAS distance are zero a platform approach is done. However when the target speed is set and the RAS distance is not zero, a replenishment approach can be simulated.

4.1.2 Block: Offset

The next block that is encountered in the offline model is the block where the offsets are calculated, the full model is presented in appendix B. For this block six inputs are used in order to calculate the three offsets. The first two are distance offset in longitudinal and lateral directions locally. The third offset is the heading offset in degrees. This block is based on four parts to calculate all the offsets. The first part is the longitudinal offset. This is also the most simple offset to calculate. The distance offset is composed of the difference between the distance and the approach distance from the settings. The next part is to calculate the heading offset. Figure 4.6 shows how this is modeled.

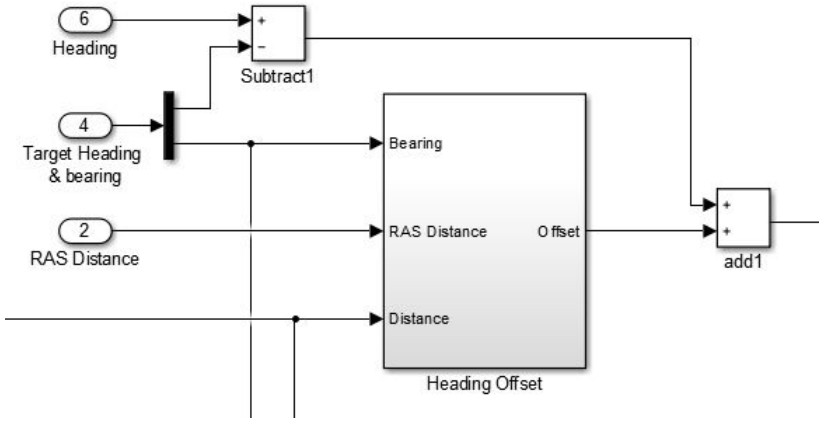

Figure 4.6: Model to calculate the heading offset.

This figure shows that the heading offset is calculated in two parts. The first part is in order to get exactly behind the target vessel with the same heading. This is done by substracting the target heading from the vessel heading. The second part is only added when de RAS distance is larger than zero. During a RAS approach small course changes are used to correct the lateral offset. First the theoratical bearing to the target vessel is calculated from the distance and RAS distance. Then this value is compared to the actual bearing to produce the offset. The difference between both values is the heading offset. Equation 4.2 shows how this is done.

$$Offset = atan\left(\frac{RASdistance}{Distance}\right) - Bearing \tag{4.2}$$

The heading offset is then used in the third part, together with the distance and bearing, to calculate the lateral offset. In figure 4.7 the method to calculate the lateral offset is presented.

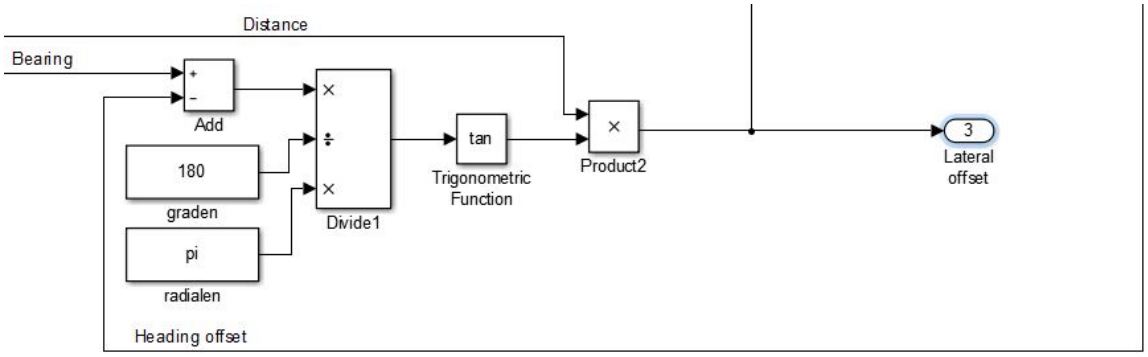

Figure 4.7: Model to calculate the lateral offset.

First the bearing and heading offset are used to check if a lateral offset is present. When the bearing is different from the heading offset, there has to be a lateral offset. Then with the distance it is calculated how large the offset is. The fourth and final part to calculate the offsets is only applicable when the bow thruster fails. The model for this part can be found in figure 4.8.

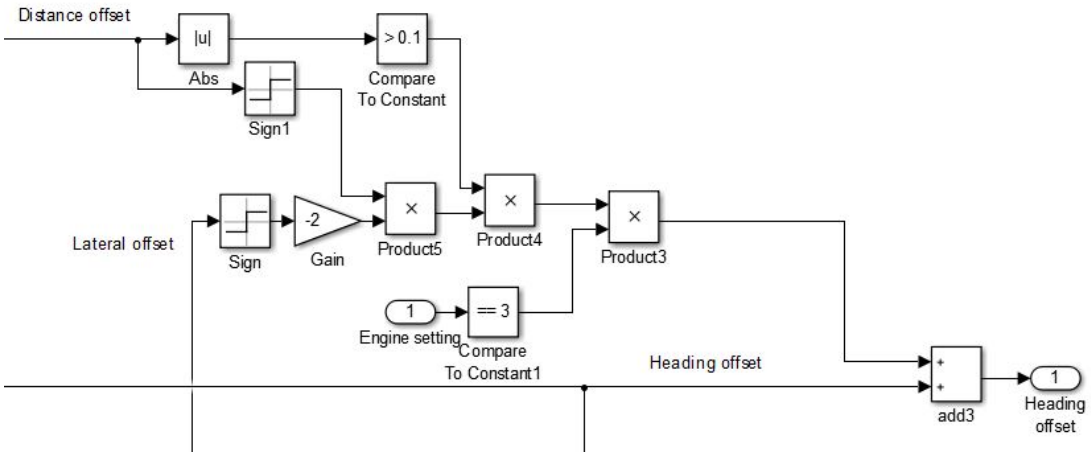

Figure 4.8: Extra heading part when the bow thruster fails.

When the bow thruster fails, the vessel will not be able to translate sideways. Therefore this fourth part will be used to compensate the lateral offset by a change in heading. Hence first of all with the engine setting parameter the check is done if the bow thruster is operational. When the bow thruster is operational this fourth part will always be zero. The only way to reduce the lateral offset with a change in heading, also requires that a longitudinal distance has to be covered. Therefore the check is done if the distance offset is

sufficiently large. When this is not the case the heading will not change as well. Finally when a lateral offset occurs, the course will be changed two degrees. This means that three percent of the covered longitudinal distance is also covered laterally.

4.1.3 Block: PID Controller

One of the most important blocks for the offline model is the PID controller block. This block takes the offsets for the three parameters and gives for each parameter a relative controll output. When the offset is zero, the output will also be zero. When the offset is large the output will be one, which is equal to maximum thrust or moment. Figure 4.9 shows how this block is divided in each direction. In figure 4.10 for longitudinal direction the full controll system is presented.

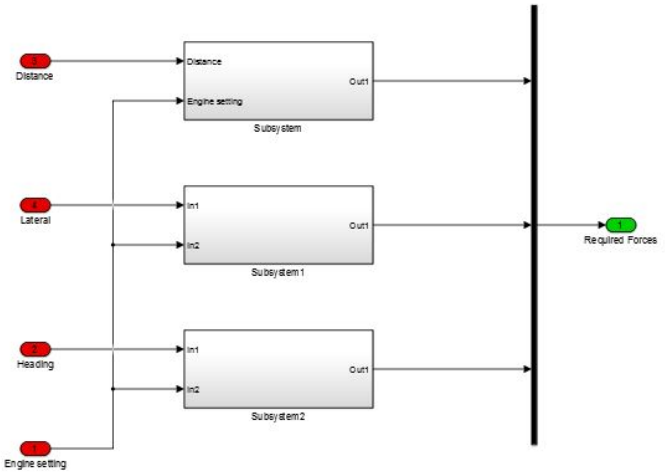

Figure 4.9: Contents of the PID controll block.

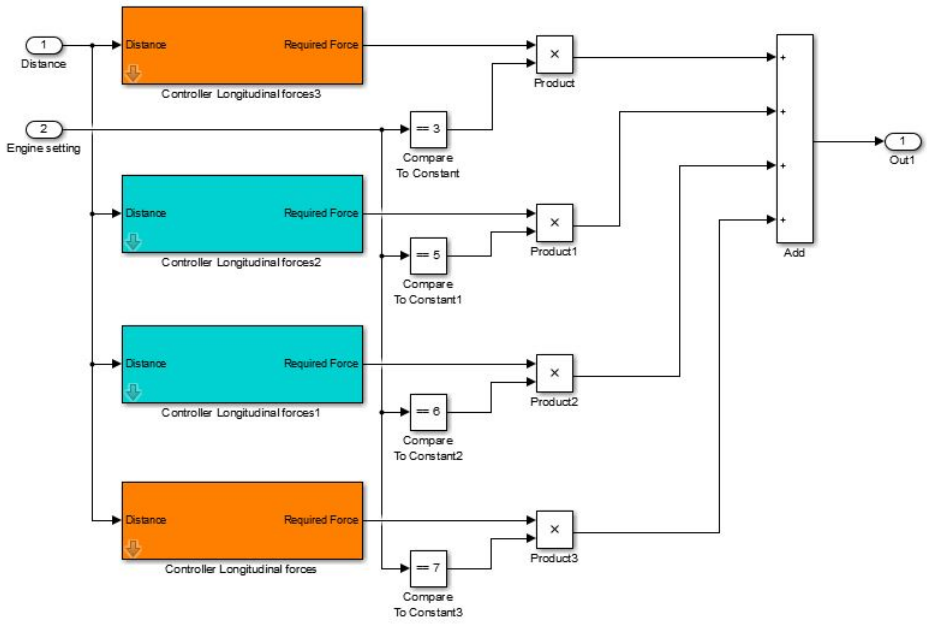

Figure 4.10: Single parameter PID controller.

Normally each direction only needs a single controller. However in this case each parameter has four controllers. The expectation is that when an actuator fails the settings need to be different in order to obtain accurate controll. For each of the four possible actuator settings a separate controller is used that only can produce an output when the corresponding actuator setting is present. Why some controllers have different colours is discussed with the results in the second part of this chapter. How the settings can be changed is presented in figure 4.11.

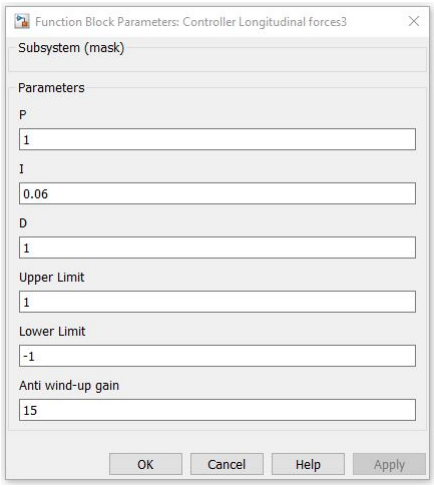

Figure 4.11: PID settings input.

In this figure the six changeable settings for one controller is shown. For each of the twelve controllers this looks the same. Now the influence of each setting will be discussed. In the second part where the results will be discussed. The actual settings for each controller will be explained.

The three most important settings for a PID controller ar the P, I and the D settings[18], just as the name implies. First of all the P setting, which stands for the Proportional gain. This parameter will result in a positive output for a positive offset and vice versa. A larger number will cause the offset to reduce more quickly. But as a negative result it will take longer to slow down which results in a large overshoot. The second parmeter is the I for Integral gain. This parameter uses the integral of the offset. This parameter will influence the controller by accelerating the output when the offset is reduced to slow. In order to cope with constantly changing environments this parameter is neceserry. In order to follow a moving target, or to cope with current and wind this parameter is required. However a large value will destabalize the controller. The third and final parameter is the Derivative gain from the D. This parameter uses the derivative of the offset. The output will be reduced or reversed when the offset is closing in on zero.

The final three parameters are influencing the working principle of the controller. The upper and lower limit are used to make sure that the maximum actuator thrust cannot be exceded. When the maximum output is known this can be transformed to maximum thrust. But when there would not be a limit the actuator could be overloaded. The anti wind-up gain is used to shut down the integrator action when the actuator is saturated. This is done to not only cut off the output signal when it is to large, but also to reduce the signal. Because when the offset is not reduced signifficantly the integrator controll will keep increasing exponentially.

4.1.4 Block: Thrust allocation

From the PID controller three values between minus one and one are passed through to the thrust allocation block. The three values represent longitudinal, lateral and rotational relative forces. In this block this is converted to actuator rotational speeds. In order to move in one direction multiple actuators need to cooperate. Hence the forces need to be distributed over all actuators in the right ratio. Figure 4.12 shows that also in this case the thrust allocation is devided into groups representing the four engine settings.

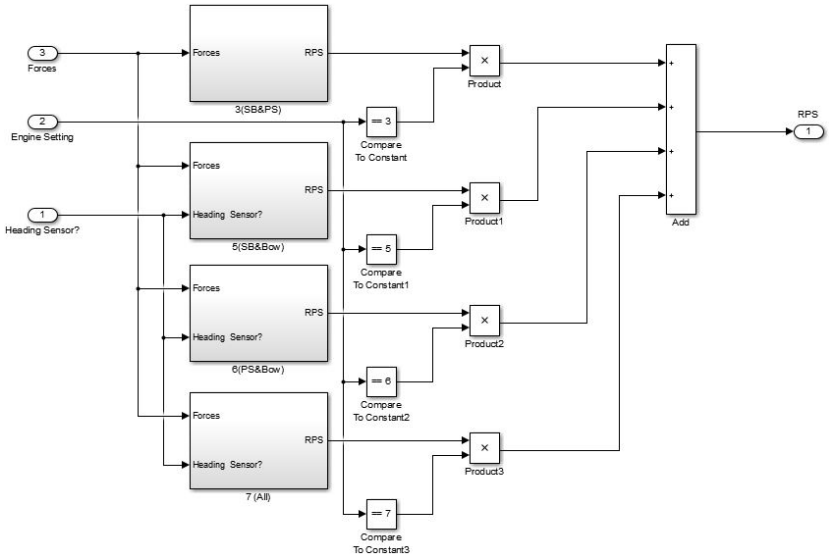

Figure 4.12: Overall thrust allocation.

Just as with the PID controller, the thrust allocation block is only used when the corresponding engine setting applies. When the heading sensor fails, the thrust needs to be distributed differently. Therefore in three of the four groups this parameter is also used. The contents of each of the four allocation blocks is relatively large and therefore these models can be found in appendix C in figures C.1, C.2 and C.3.

First the thrust allocation model for all thrusters will be discussed as this is the base for the other three models. The model of this setting is presented in figure C.3. The first inputs gives the three thrust values from the PID controller. The second input is the indicator for the heading sensor. The first path in the allocation is for the longitudinal direction. This path splits in two directions for the port and starboard side thruster. The second part is for lateral thrust. Hence this path splits in three ways for all actuators. The gain values are selected in such a way that the rotational moment for the stern thrusters and the bow thruster cancel out each other. Only the lateral thrust from the bowthruster remains. In order to cancel out the moments the distances from actuator to the centre of motion are used. The look up table is used to make sure that the stern thrusters do not turn when the bow thruster is not turning because for a small force the bow thruster cannot operate. The third part is for the moment to change heading. This is done by the stern thrusters in order to only have the moment and no translations because both thrusters have equal but opposite thrust. The lookup tables transform the forces in actuator rotational speed. Finally when the heading sensor fails, the thrust from the bow thruster is increased. With a failing sensor the system is not able to make a distinction between lateral offset and heading offset. By increasing the bow thruster value the lateral motion will also cause a rotation in order to make sure that both offsets are covered.

The second thrust allocation is when the bow thruster fails. This model can be found in figure C.1. First of all the bow thruster cannot be used. Therefore a gain of zero is used. Hence lateral movement is not possible. The way of overcoming lateral offset was explained in the part where the offsets are covered. The longitudinal motion and rotation are exactly the same as for the configuration with all thrusters.

The final two models will be discussed at once through the model from figure C.2. The difference between those two models is only which thruster has to be used and which thruster is zero. In the case of the figure only port side thruster and bow thruster is working. Longitudinal motion can only be performed through one thruster. The output is set to zero because the model cannot cope with a missing output. For lateral movement only one thruster and the bow thruster can be used. To cancel the moment the gain was doubled. Heading change will in this case be done with the bow thruster. The missing thruster will cause that by using one or both thrusters, the vessel will never only move in the desired direction. But the controll system will have to cope with the unwanted motions.

4.1.5 Block: RPS to thrust

The next step in the offline model is to calculate the thrust and moment from actuator speed. In order to do this first one has to know in what direction the actuator is influencing the motion. The starboard and portside thruster will cause a longitudinal thrust and a motion, while they are not placed in line with the centre of motion. The bow thruster will result in a lateral thrust and a moment. The three moments add up to the resulting moment. Both stern thrusters add up to the resulting longitudinal thrust.

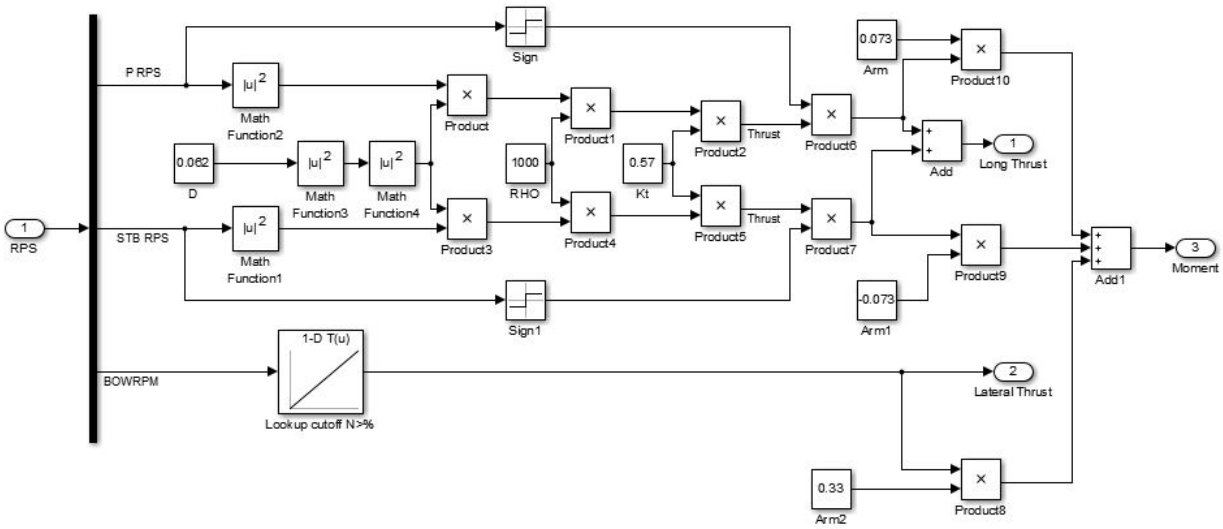

Figure 4.13: Model for transforming actuator speed into thrust and moment.

The figure shows that for both stern thrusters the same calculation is performed. This calculation is based on the formula presented in equation 4.3[19].

$$T = n_p^2 * D^4 * \rho * K_T \tag{4.3}$$

From this equation the thrust is composed of four terms. First of all the propeller speed, in rotations per second, is squared. Secondly the propeller diameter to the power four. This was measured for the Tito Neri tug at the university. The third part is the fresh water density as it is used in the flume tank. Finally the thrust coefficient which was already available from the mechatronics course[20]. For the bow thruster no RPM could be calculated. Therfore the look up table changes the relative speed to a corresponding thrust. Finally for each thruster the moment is calculated. The moment is calculated by multiplying the thrust with the perpendicular distance from the thruster to the centre of motion.

4.1.6 Block: Environment

In order to make a realistic offline model the influences of wind and current need to be taken into account. For both wind and current two directions, longitudinal and lateral, will be used separately, because a random number is generated for the force. This can be done separately. Due to this approach it is not necessary to transfer these forces from global to local. Firgure 4.14 shows how wind and current are included in the model.

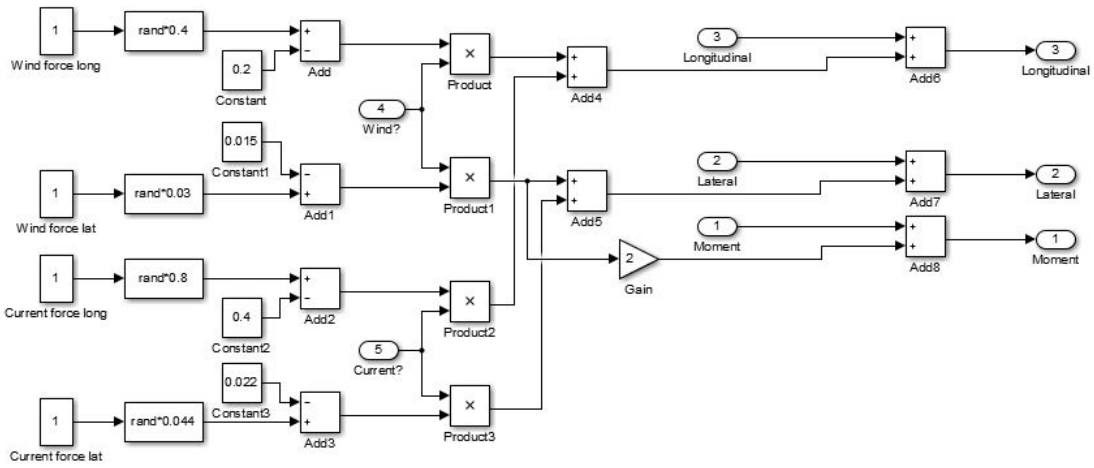

Figure 4.14: Model for adding wind and current influences.

First of all for each of the four values a random number is generated at the beginning of each simulation. Then half of the maximum possible value is substracted in order to enable positive and negative influences. The two inputs ensure that this random force is only used when the wind or the current are present. The current only causes translations of the vessel. But the wind will also cause a rotation if the vessel has a large structure at the front or at the aft. In our case the superstructure is located at the front of the vessel. Finally the random generated forces and moments are added to the previous calculated thrust and moment.

4.1.7 Block: Thrust to speed and heading

The next part of the offline model is used to calculate the longitudinal and lateral speed as well as the heading. The thrust and moment are transformed into the speed and heading with the use of the equations of motion[2]. Figure 4.15 shows the model for the three equations of motion.

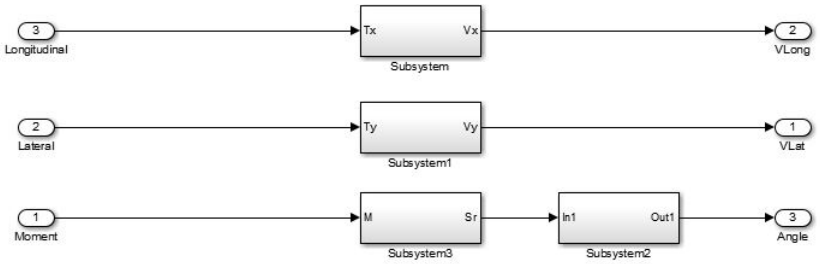

Figure 4.15: Model for calculating the speed from the thrust.

The first three subsystems contain the models for the equation of motion in the three directions. The extra subsystem for the heading is used to transform the heading from radians to degrees. The equations of motion for longitudinal direction and lateral direction only differ in values for some constants. Therefore only longitudinal direction is discussed. Because for the rotation the model is somewhat different. This one will also be discussed. The model for longitudinal direction is presented in figure 4.16. The model for the rotation is in figure 4.17.

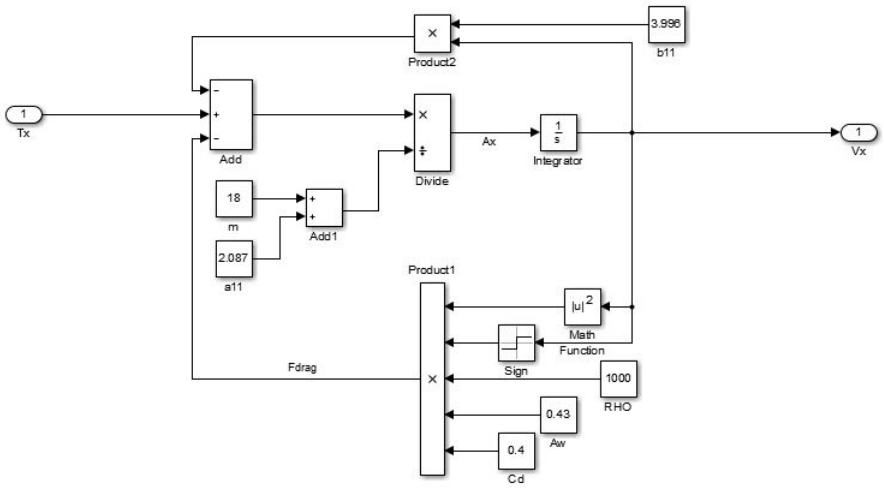

Figure 4.16: Equation of motion for longitudinal direction.

The standard equation of motion on which this model is based will be calculated with equation 4.4. The drag force in the equation of motion can be calculated with the formula presented in equation 4.5.

$$a + \frac{b_1}{m + a_1} * v = \frac{1}{m + a_1} * (T_x - F_{Drag}) \tag{4.4}$$

$$F_{Drag} = c_D * \rho * A_w * v^2 \tag{4.5}$$

These two equations are combined in order to form the model from the previous figure. The first part of the equation of moment consists of the acceleration a, damping b_1, mass m, added mass a_1 and speed v. The mass and added mass also come back in the second part of the equation together with the longitudinal thrust and drag froce. The drag force is calculated with the drag coefficient c_D, fresh water density ρ, wetted area A_w and the speed squared. These values were also taken from the mechatronics course[20]. Next the equation of motion for the rotation will be discussed.

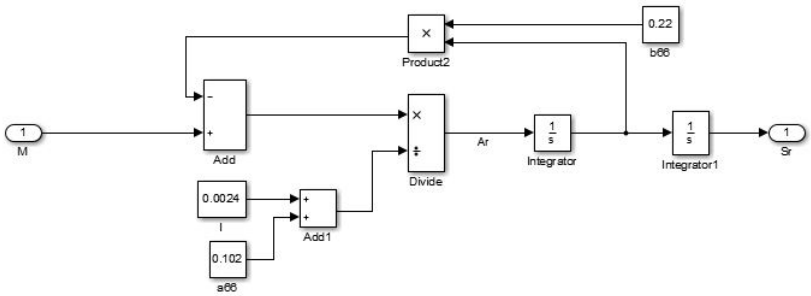

Figure 4.17: Equation of motion for the rotation.

The difference is that for the rotation the mass moment of inertia is used instead of the mass. The drag force is neglected due to relative low speeds and small movements. An extra integrator is added in order to calculate the heading from angular velocity. This model is also based on two equations. Equation 4.6 gives the equation of motion for the rotation and equation 4.7 calculates the heading.

$$\alpha + \frac{b_6}{I + a_6} * \omega = \frac{1}{I + a_1} * (\tau) \tag{4.6}$$

$$\omega = \dot{\theta} \tag{4.7}$$

4.1.8 Block: Local speed to global position

In order to calculate distance and bearing between the two vessels both vessel positions are required to be in the same reference system. Therefore the transformation is done from local to global reference system. In the local system the origin lies in the centre of gravity with the x-axis straight to the front of the vessel and the y-axis perpendicular on the x-axis. So when the vessel is moving and changing course, the axes system moves with the vessel. However, the global origin an axes orientation will always be stationary. Figure 4.18 shows the model that uses the local speeds and heading to calculate the global position. Equations 4.8 and 4.9 are used to develop the model.

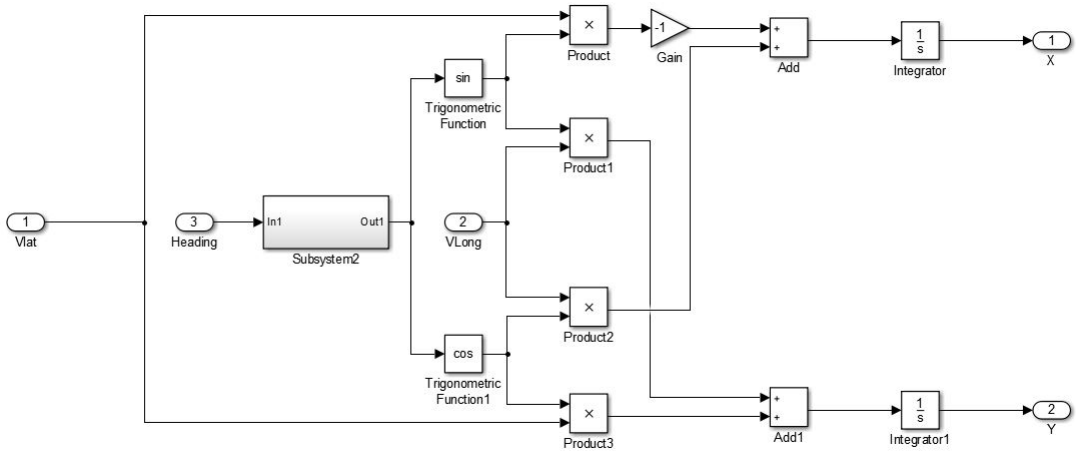

Figure 4.18: Model to transform local speeds to global position.

$$\begin{bmatrix} X \\ Y \end{bmatrix} = \begin{bmatrix} cos(Heading) & -sin(Heading) \\ sin(Heading) & cos(Heading) \end{bmatrix} \times \begin{bmatrix} VLong \\ Vlat \end{bmatrix} \tag{4.8}$$

$$\begin{aligned} Vx &= \dot{X} \\ Vy &= \dot{Y} \end{aligned} \tag{4.9}$$

First of all the subsystem at the heading is placed here to transform the heading from degrees back to radians. Next the heading is used to calculate the four parts of the matrix from equation 4.8. Also with the minus at the sine for the X coordinate. Thereafter two terms are combined to form the speed in x direction. The other two are used for the speed in y direction. Finally the integrators are used to calculate both coordinates according to equation 4.9.

4.1.9 Block: Current position

The next block for the offline model is the current position block. This is a simple block that takes into account the initial position as set in the settings block previous to the simulation. The only thing this block does is passing the initial position when the time is zero. After that when the time is larger than zero the actual position will be fed through as it was calculated in the previous block. This model is shown in figure 4.19.

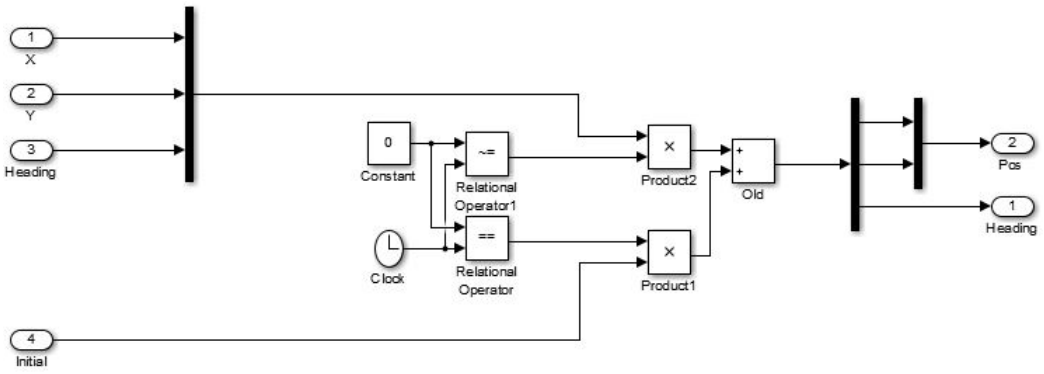

Figure 4.19: Model that takes initial conditions into account.

4.1.10 Block: To camera inputs

This offline model is developed in order to test the camera system without the actual hardware. Therefore this block is used to calculate the distance and bearing as they would have been calculated by the camera system. As an extra feature the target heading is also an output from this block. This block calculates the distance between the positions of both vessels. The block also calculates the heading from one position to the other. Figure 4.20 gives a representation of how this is done. Equations 4.10 and 4.11 show the formulas, on which the model is based, to calculate distance and bearing.

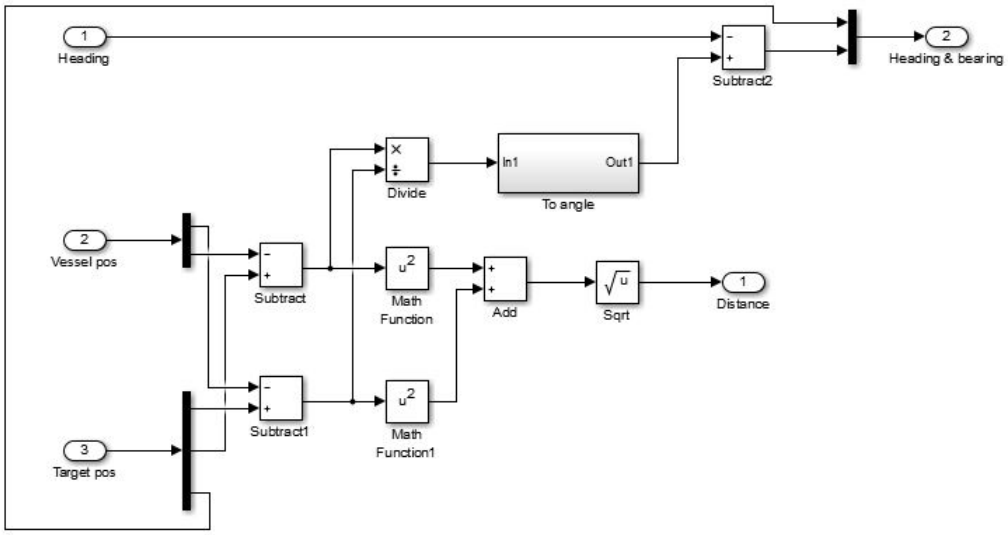

Figure 4.20: Model to calculate variables as they would be measured by the camera system.

$$D = \sqrt{(x_2 - x_1)^2 + (y_2 - y_1)^2} \tag{4.10}$$

$$Bearing = atan\left(\frac{(y_2 - y_1)}{(x_2 - x_1)}\right) - Heading \tag{4.11}$$

The distance between two points can be considered as the hypotenuse of an right-angled triangle. The difference in x-coordinates and the distance between both y-coordinates make up the other two sides of the triangle. To calculate the distance the theorem of Pythagoras is used as shown in equation 4.10. The

heading from one point to the other is then the angle between the hypotenuse and the difference between the two x coordinates as in equation 4.11 is presented. The subsystem is again used to transform the heading from radians to degrees. Finally to calculate the bearing in the local reference system the vessel heading is substracted from the global heading.

4.1.11 Offline model for LCF

In the ship handling simulator a model of the air defence and comd frigate (LCF) of the Royal Dutch Navy is used. In order to get the appropriate behaviour in the simulator some of the control settings may have to be different. Hence the offline model is changed in order to simulate the LCF. In this section the differences between the previous discussed offline model and the model for the LCF are discussed. Later in the results section the control settings are investigated.

First of all the engine configuration from the frigate needs to be discussed. The LCF does not have a bow thruster. The two stern propellers cannot be rotated, but two ruthers are placed behind the propellers. For this model the rotation of the ruthers is not used. Therefore the frigate can be modeled by using the engine setting 3, from the offline model, with only the two stern thrusters available.

The thrust allocation uses look up tables to change the relative engine speed into real rotational speed. However the 1200 rotations per minute for the Tito Neri tug are much more than the 230 rotations for the frigate. Therefore a new look up table is used, with the same ratio, but with lower speeds.

The block RPS to thrust uses particular vessel parameters. The Dutch Navy is not keen on publishing these parameters, but these parameters have been used by Schulten in his thesis[21]. The main parameters used in this block that were obtained from the thesis were propeller diameter, thrust coefficient and propeller placement. The propeller diameter is 4.95 meter and the thrust coefficient is 0.15. Both propellers are placed 5.2 meter from the centreline. In this block the final parameter that was changed is the water density, from 1000 to 1025 kg/m^3 for salty water.

The final part which contains changes are the subsystems from the thrust to speed and heading block where the equations of motion are used. The mass of the frigate is 6050 tons. An approximation for the wetted area can be calculated with the use of equation 4.12[22]. The added mass, damping, drag coefficient and mass moment of inertia are obtained by experiment. The offline model was executed with a large offset in order to obtain maximum thrust. The parameters were changed in order to match vessel characteristics for the frigate. For example maximum speeds of 29 knots and 7.5 degrees per second.

$$A_w = 0.75 * L(B + T) \tag{4.12}$$

4.2 Modeling results

In the first part of this chapter the offline model was fully discussed. Now the results from the simulations will be discussed. First of all the tuning process will be explained, which also indicates the effect of each tuning parameter. Then the results for the four engine settings and the LCF model will be presented. With the engine settings the system performance can be assessed in the case that one of the thrusters is failing. The model for the LCF is used as a step up to the simulator models, while in the simulator a model of the LCF is used. The main reason to use these offline models is to check how the models for autonomous operations will work. In this case when the model is not working as expected it can be observed very quickly. The model can then be changed and a new test can comence immediately. This will safe a lot of time in the development process. The camera measurements are only calculated, but the offline model is replacing the actual camera and vessel. The test with the offline model show how the control system tuning is performed. It also shows the tuning results that will be used for the simulator and small scale tests.

4.2.1 PID Tuning

The block that mainly determines the vessel response is the PID controller. The respons depends on the values for the regulator parameters. The three main parameters are the proportional, integral and derivative gains. In order to develop a system with a stable response the three control parameters need to be tuned. When the tuning commences, the first parameter that will be set is the proportional gain. The other two parameters first remain zero. Figure 4.21 illustrates the influence of the proportional gain.

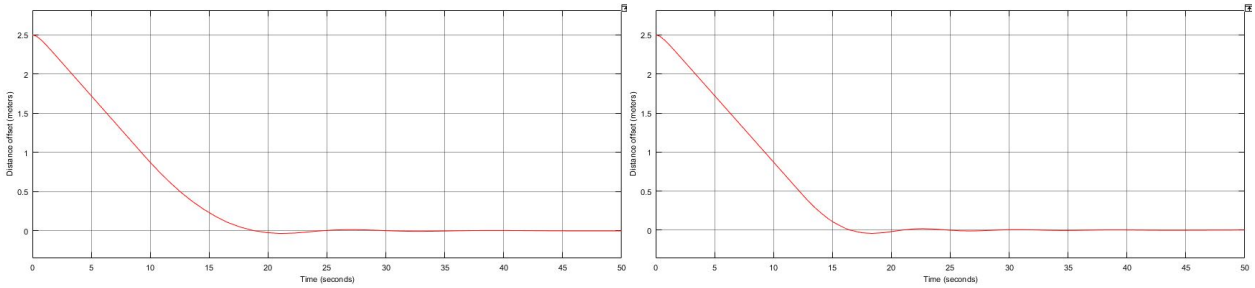

(a) P = 1. (b) P = 2.

Figure 4.21: Plots to show the influence of the P regulator.

The first graph shows a proportional gain of one. In the second graph a proportional gain of two was used. A positive effect of an increased value is that the response will be faster. This can be seen in the figure where the second graph reaches the zero offset line faster. However a large value also causes an increased overshoot. An overshoot is the maximum error after the first zero crossing has occured. As a result of this overshoot it also takes longer to settle on a constant value. In the end a compromise has to be found in order to obtain a response that is fast enough with an acceptable overshoot and settling time. Another way to reduce the negative effects, is to use the integral and derivative actions.

After the proportional gain is set, usually the derivative gain is set next. The derivative gain is used to slow down the response when the offset is closing in on zero. The derivative action also results in a reduced overshoot. So by using this action a larger proportional gain can be used with reduced negative effects. First figure 4.22 shows the influence of the derivative gain. In this case only the derivative gain was set. The other two parameters were again set to zero.

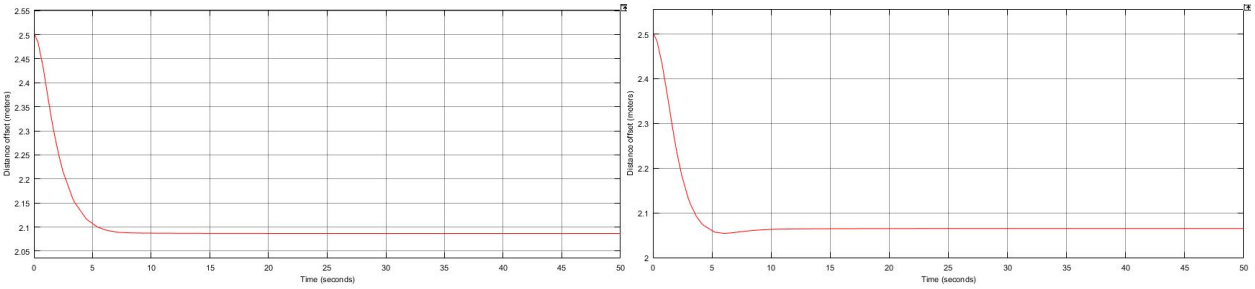

(a) D = 1. (b) D = 2.

Figure 4.22: Plots to show the influence of the D regulator.

The first thing that shows from this figure is that the derivative gain controller is not able to overcome the offset. The larger derivative value from the second graph has a faster respons and a more abrupt brake. Both graphs show that when the signal is approaching the zero offset fast, the derivative action will stop the movement. In the end this figure shows the importance of combining multiple actions.

The final action is introduced by the integral gain. This controller will accelerate the signal when the offset is not reduced signifficantly. When the offset remains too large the integral action will increase the response even more in order to reduce the offset. The integral action will also assist to overcome constant disturbances like currents and wind for example. Figure 4.23 shows the effect of a controller which only uses the integral action.

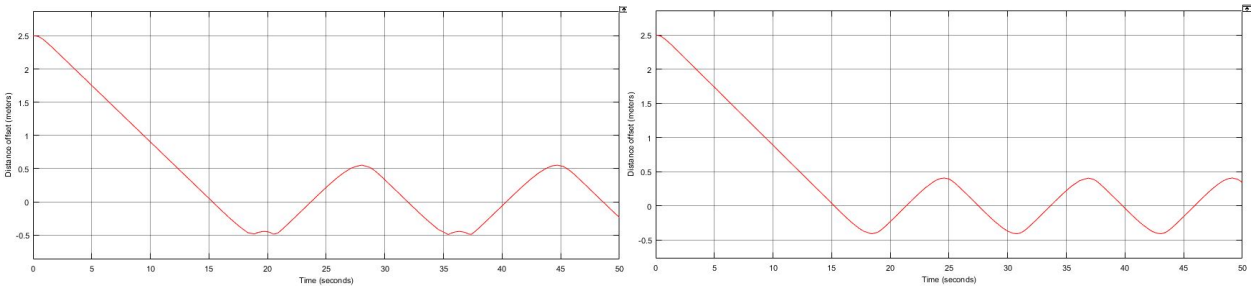

(a) I = 1. (b) I = 2.

Figure 4.23: Plots to show the influence of the I regulator.

These graphs immediately show that the integral action is not able to reach a steady state. It will however oscillate around the zero offset line. Steady state is not reached because the integral action only will act when an offset is present for a longer period. However by increasing the integral action the amplitude of the oscillation will reduce. The larger value also results in a somewhat faster response, but the differences are very small in this case.

The three previous figures show the importance of developing a control system that combines these three actions. When a fast response is required and an overshoot is not unwanted a normally damped system is a good option. Figure 4.24 shows a normally damped signal.

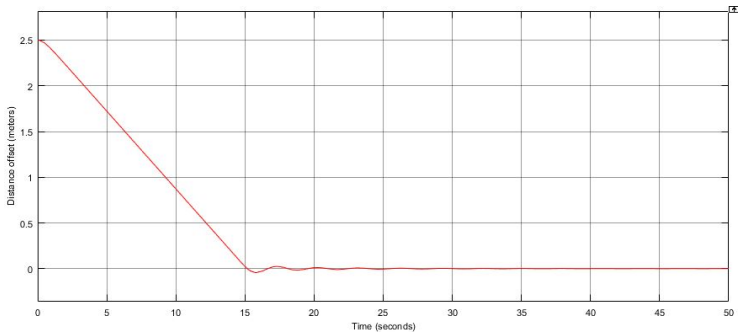

Figure 4.24: Normally damped signal.

This figure shows that the normally damped system has an overshoot. Due to the oscillation at the end it will take some time to reach the steady state. When the oscillation is unwanted, but still a relatively fast response is required a single peak overshoot damping can be used. The single peak overshoot signal is presented in figure 4.25.

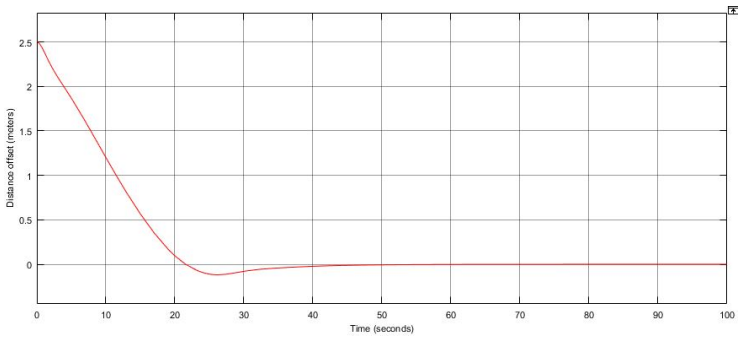

Figure 4.25: Signal with a peak overshoot.

By choosing for a response with a single peak overshoot the compromise for a slower response has to be made. Also the settling time will be larger, but the unwanted oscillations are avoided. When even the slightest overshoot is unwanted a critically damped control can be used. A critically damped signal is presented in figure 4.26.

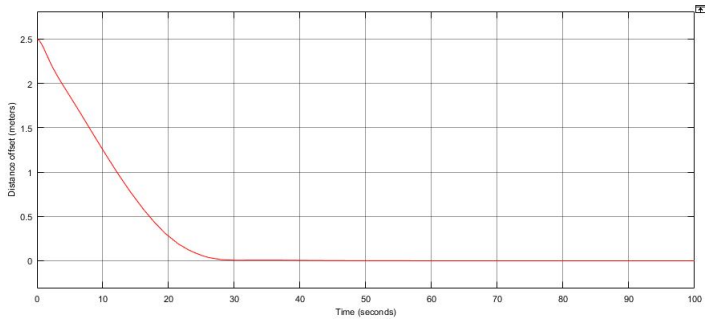

Figure 4.26: Critically damped signal.

Compared to the other two responses, the critically damped system has the slowest response. However the unwanted overshoot and oscillation are both avoided. An extra positive effect is that the critically damped signal reaches the steady state quite fast compared to the other two. For the marine applications a critically damped system will be desired.

By avoiding the oscillations engine loads can be reduced, because the engines do not have to follow these direction changes. When the single peak overshoot response is considered it will take quite some time to reach a steady state from the overshoot. Even when this overshoot is relatively small. However for a vessel this slow speed is not possible. Therefore the control system should be tuned in order to obtain the desired response. Tuning is done by changing the parameters until the proper response is obtained.

4.2.2 Engine mode 7, all actuators

The first mode for wich the PID controller will be tuned is the standard setting where all actuators are operational. First of all the longitudinal offset will be tuned. While only the stern thrusters are used for the longitudinal offset it should be possible to establish a tuning result which is critically damped. After changing the PID parameters a critically damped response is obtained with the following control parameter. The proportional gain is equal to one, the integral gain equals 0.08 and the derivative gain equals 0.9. The system response with these values is presented in figure 4.27.

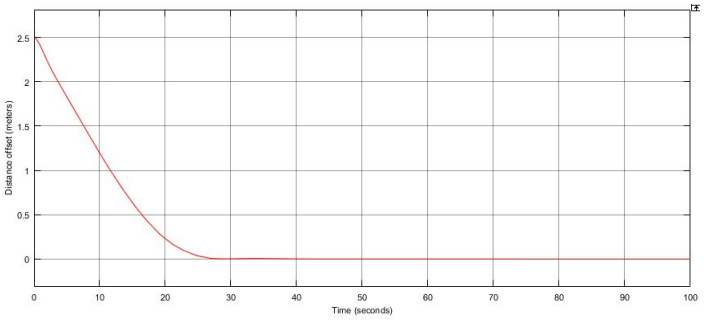

Figure 4.27: The controlled longitudinal offset.

The figure shows that these values for the control parameters result in a critically damped system. This value for the proportional gain is optimal because by decreasing the parameter an overshoot will occur. However by increasing the value the settling time will significantly increase. Also by decreasing the integral gain the settling time will be increased. An overshoot will also be caused by increasing the integral gain. An reduction of the derivative gain will again cause an overshoot. Finally an increase of the derivative gain will destabilize the system. These control parameters result in the control system transfer function presented in equation 4.13. From this transfer function the Bode plot and the Nyquist plot are calculated. These plots are presented in figure 4.28. The input for this transfer function will be the longitudinal offset. The output will be the relative forward thrust. In this case an output of one will mean maximum forward thrust, where minus one will mean full reversed thrust. So the control system transfer function describes the response to a longitudinal offset.

$$TF = \frac{(1.9S^2 + 1.08S + 0.08)}{(S^2 + S)} \tag{4.13}$$

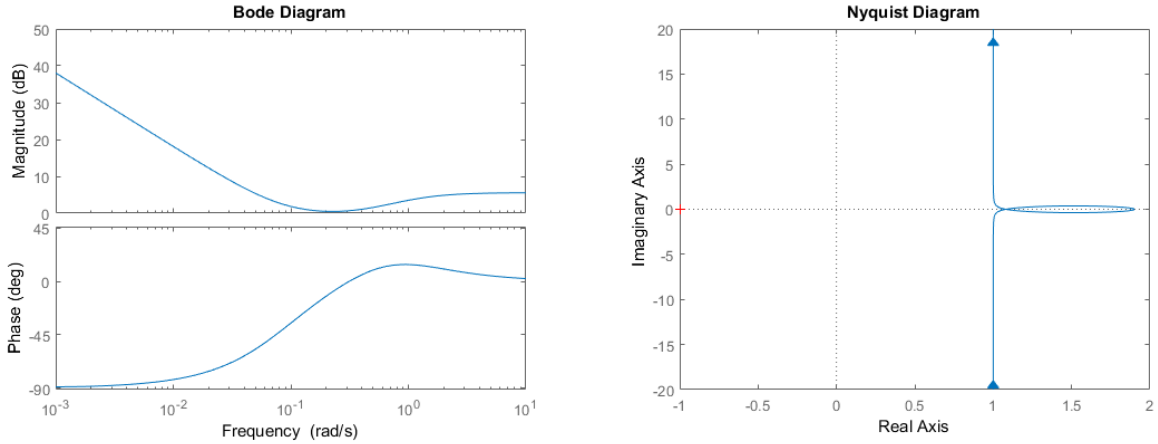

(a) Bode plot.

(b) Nyquist plot.

Figure 4.28: Plots that shows the Bode and Nyquist plots for longitudinal control.

The Bode plot shows that this system behaves as an PI compensation system for low frequencies. However for high frequencies the derivative action increases the magnitude and reduces the phase. Where a PI compensation results in a phase of zero degrees for high frequencies. This system also reduces to zero for high frequencies. This system helps to reduce steady state errors. While at zero frequency this system has an infinite gain. Earlier the system response was described as critically damped. However the Bode plot shows that the system is over damped. An over damped system reacts slower to an offset than a critically damped system. Thus a critically damped system was desired, but an over damped system is also sufficient when

the critical control parameters cannot be found.

The Nyquist stability is calculated by the number of unstable roots. For stability it is desired that the number of unstable roots is zero. When the Nyquist plot circles around minus one clockwise there will be an unstable root. A counter clockwise rotation adds in stability. If poles are located in the right hand side of the plot the system will be destabilized. However this system does not meet any of these requirements. Another way to calculate the stability of a system is with the sensitivity function. this function is shown in equation 4.14.

$$S \triangleq \frac{1}{1 + DG} \tag{4.14}$$

In the equation for the sensitivity function DG is the distance from the unstability point perpendicular to the Nyquist plot. The unstability point is located at minus one, thus in this case the distance is approximately 2. Therefore the sensitivity is 0.333. High values for the sensitivity function imply an unstable system. From the previous criteria as well as from the sensitivity function the system proves to be stable.

Next the tuning of the heading controller will be discussed. Also in this case only both stern thrusters will be used. The best result that has occurred during tuning was not exactly critically damped, but it is very close. In this case the tuning is a PD controller with values of 1.5 and 4 for proportional and derivative gains respectively. Figure 4.29 shows the tuning result.

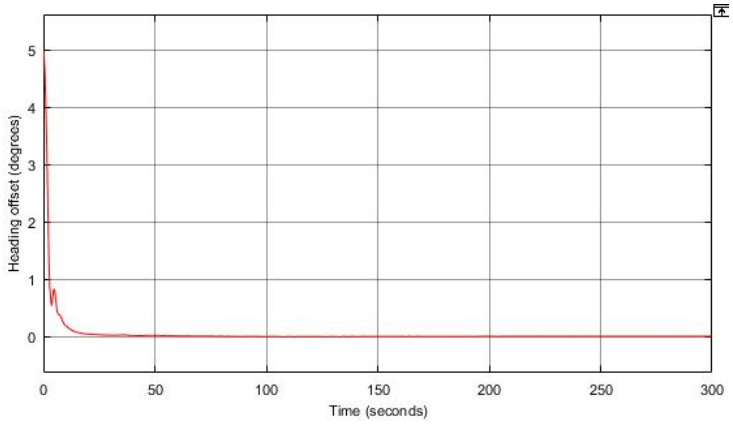

Figure 4.29: Controlled heading offset.

During the approach of the zero offset, the derivative gain causes a small disturbance. However after this disturbance the response is critically damped. By changing the parameters an effort was done to remove this disturbance, but without any positive result. A decrease of the proportional gain results in a longer time before steady state is reached. However an increased value causes a significant overshoot with some oscillations before a steady state is reached. The integral gain is not used because even a small value will destabilize the response and cause a massive increase in settling time. A decrease of the derivative gain will increase the disturbance. However an increase of the derivative gain will increase the settling time. Therefore the choice was made for these PD values. Again these control parameters are influencing the control system transfer function, which can be found in equation 4.15. Also this transfer function results in Bode and Nyquist plots, presented in figure 4.30. This control system transfer function describes the system response to a heading offset. As an input the heading offset is used. A relative yawing moment will be the output for this function.

$$TF = \frac{(5.5S + 1.5)}{(S + 1)} \tag{4.15}$$

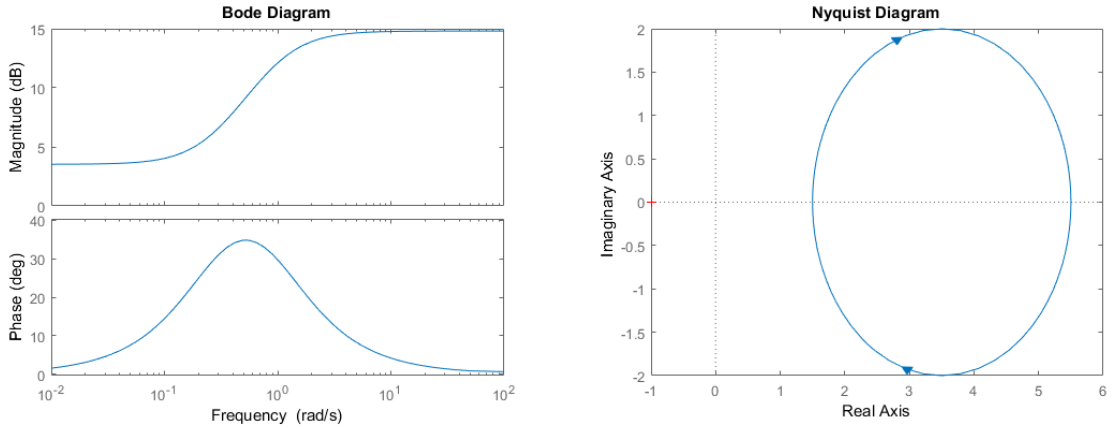

(a) Bode plot.

(b) Nyquist plot.

Figure 4.30: Plots that shows the Bode and Nyquist plots for heading control.

From the Bode plot a different response is observed. This was also expected while the transfer function is significantly different. This Bode plot does not have an infinite gain. Therefore the steady state error will not be corrected as fast. But that is probably due to the fast turning capabilities of the vessel. The Bode plot shows that the system is close to be critically damped, but only phase response does not comply.

Also this time the Nyquist plot does not circle minus one and no poles are located at the right side. With the sensitivity function in equation 4.14 was calculated. The value for sensitivity is 0.278 with a distance of 2.6. The result from the sensitivity is a little smaller this time, thus the heading control will be slightly more stable than the longitudinal control. Also according to all criteria this system will behave stably.

The final tuning for this setting is the tuning of the lateral offset. Now the stern thrusters and the bow thruster will co-operate in order to counteract the rotating moment. A critically damped system was not obtained because the optimal values for the stern thrusters are different from the optimal value for the bow thruster. The best result was obtained with a proportional value of 5, an integral value of 0.12 and a derivative value of 8. Figure 4.31 shows the tuning result.

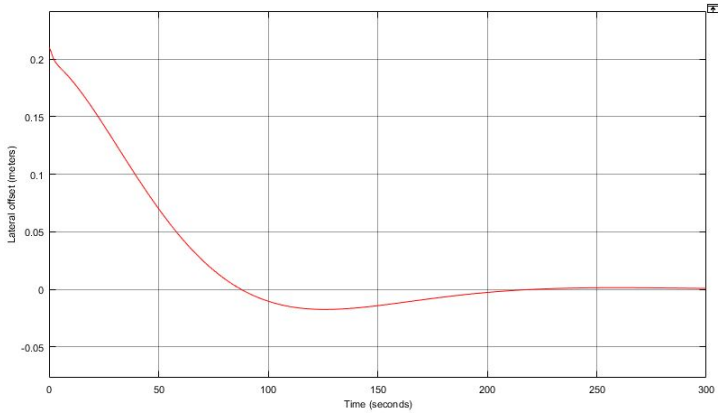

Figure 4.31: Lateral offset controlled.

After tuning the result is a system with a single peak overshoot as can be seen from the figure. The overshoot is below 10 percent an therefore it was accepted for this purpose. A reduced proportional gain does not influence the response speed, however it causes multiple overshoots which are also larger. By increasing the proportional gain the response is slowed down. Reducing the integral gain also slows down the response,

but by increasing the integral gain the overshoot is significantly increased. A lower value for the derivative gain will cause a faster response at the cost of a larger overshoot. Finally the increase of derivative gain destabilizes the first part of the response, therefore increasing the settling time. The control system transfer function from these control parameters is presented in equation 4.16. Figure 4.32 shows the Bode and Nyquist plots for the lateral control system. In oreder to calculate relative lateral thrust this transfer function uses lateral offset. The control system transfer function describes the response to a lateral offset.

$$TF = \frac{(13S^2 + 5.12S + 0.12)}{(S^2 + S)} \tag{4.16}$$

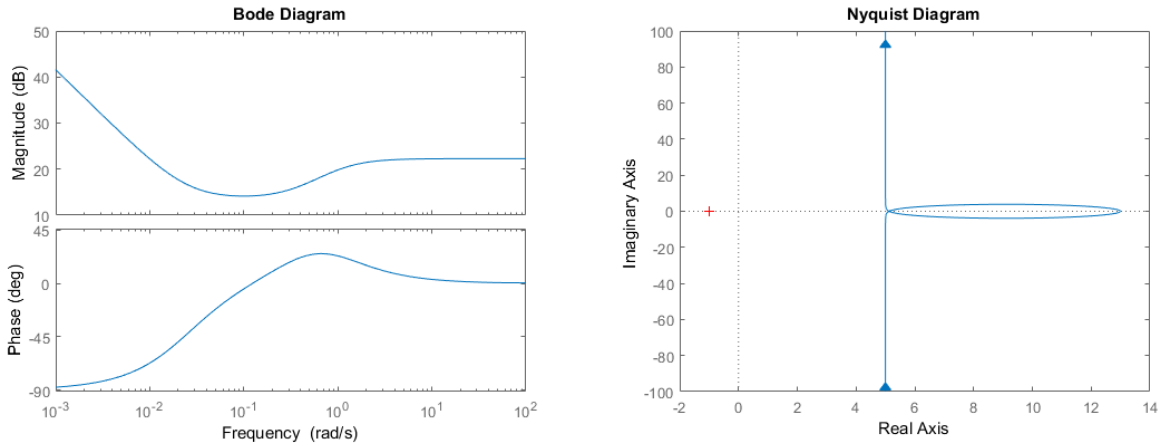

(a) Bode plot.

(b) Nyquist plot.

Figure 4.32: Plots that shows the Bode and Nyquist plots for lateral control.

This control system shows a similar transfer function as was obtained from the longitudinal control system. The difference in the Bode plot between both systems lies in the size of the peaks. A larger negative peak for the magnitude and a larger positive peak for the phase. These larger peaks are caused by larger control values in the transfer function. Again the bode plot shows that the lateral control will be more likely be over damped then critically damped.

The Nyquist plot for the lateral control shows that the circle is longer and wider. But also this time minus one will not be circled and also no poles are present in the right plane. The sensitivity from the sensitivity function is calculated at 0.143 with a distance of approximately 6. Therefore both criteria show that the final control system for lateral control is also stable. According to the sensitivity function this system is even more stable then the previous two.

By the tuning of the PID parameters for all three offsets a response was obtained which is acceptable for further model testing. These values will be used in the small scale tests with the Tito Neri tug. With a correct offline model these responses should be the same for the scale test, if no other disturbances will be influencing the vessel.

These tests show the importance of the heading sensor in this model. Without a heading sensor the system is not able to make a distinction between the heading offset and the lateral offset. Because when the system calculates the bearing offset from the video feed, only the relative offset can be measured. So in order to control the vessel the thrust allocation will react for both offsets. This is done by increasing the gain for the bow thruster in lateral motion. In this case the stern thrusters will not fully compensate for the rotation. The assumption was that by accounting for both offsets, eventually a steady state would be reached close to the desired position. The results for the distance and the bearing are presented in figure 4.33

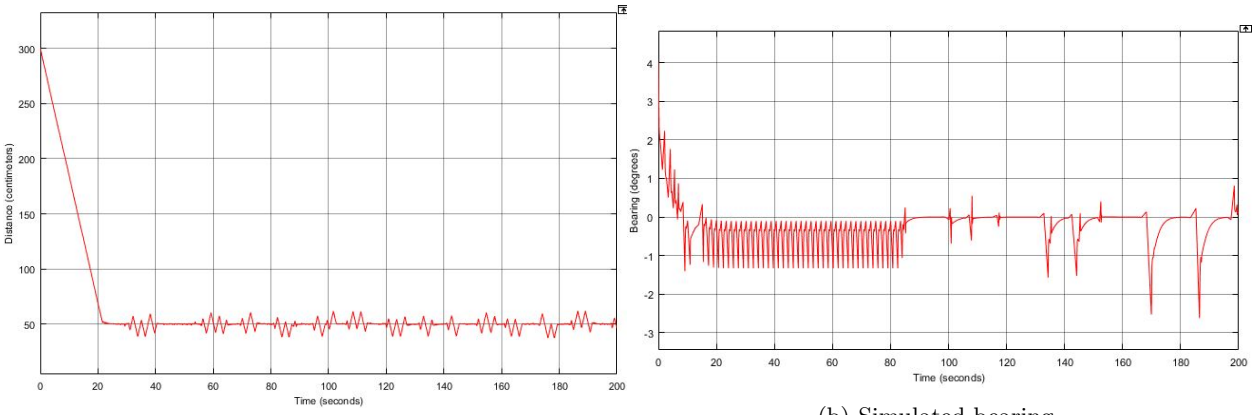

(a) Simulated distance.

(b) Simulated bearing.

Figure 4.33: Plots that show the distance and bearing for a simulation without a heading sensor.

First the result of the bearing measurement will be discussed, which can be found in figure 4.33b. Initially the bearing is set to 4 degrees. In the begining of the simulation is reducing quite normally, but very soon the system starts oscillating. the magnitude of the offset is reduced, but the system remains unstable. Even when the offset is almost fully reduced to zero, it is not able to remain steady. The unsteady behaviour for the bearing control also causes disturbances in the control for the distance, as can be seen in figure 4.33a. Therefore the choice was made to add a heading sensor to the offline model. The heading sensor resulted in the ability to distinguish heading offset and lateral offset. Individually these two offsets can be controlled very well, as was proved previoussly in this chapter. After this proof the choice was made also to use a heading sensor on the scale model.

4.2.3 Engine mode 3, stern thrusters

The next engine setting which will be discussed is the setting number three. In this case only starboard and port side thrusters can be used. First the thrust allocation models for this mode and the fully operational mode, from figures C.1 and C.3, will be compared. These models show that both configurations use the stern thrusters for longitudinal movement and rotation. Therefore the vessel behaviour will also be the same for both engine modes if the PID control values will be kept constant. Hence figure 4.27 shows the vessel behaviour in longitudinal direction and figure 4.29 shows the behaviour when the heading is controlled.

However in this engine mode lateral motion is not directly possible. Therefore as indicated in figure 4.8 the heading offset is changed in order to reduce the lateral offset. When the lateral offset is zero or when the distance offset is zero the heading controll will transform back to the original state. For the lateral control the heading control values were not changed. Figure 4.34 indicates how the lateral offset is changing during this operation.

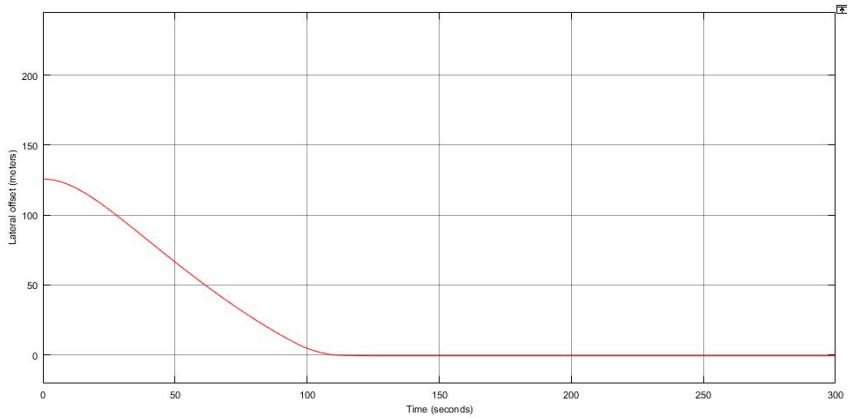

Figure 4.34: Lateral offset controlled without bow thruster.

This figure indicates that the heading control PID settings actually result in a critically damped lateral control. When there is a lateral offset and a longitudinal offset an extra heading offset is added. This means that first the heading will change three degrees. When one of both offsets reaches zero the heading is changed back to zero again. Figure 4.35 shows the actual heading during the operation. Figure 4.36 presents the distance to the target vessel during the operation.

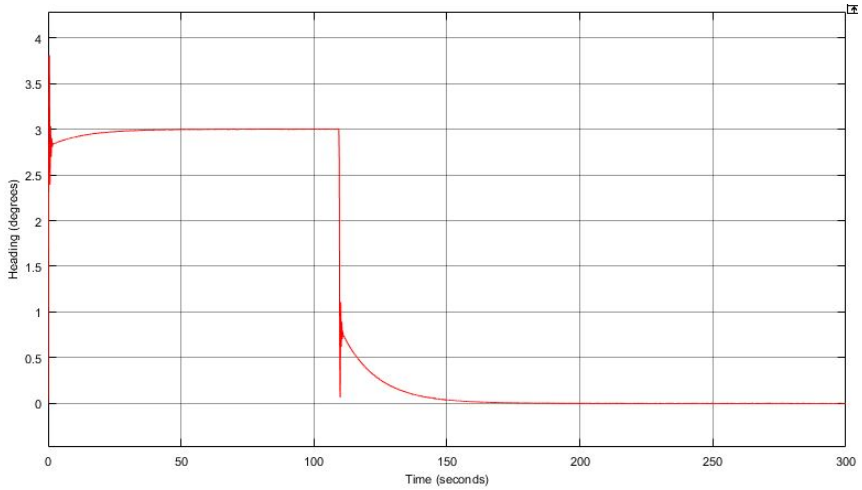

Figure 4.35: Heading during lateral control.

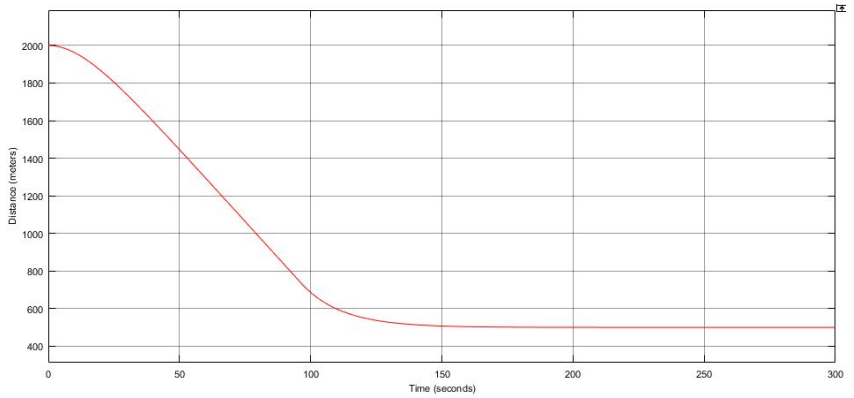

Figure 4.36: Distance during lateral control.

The abrubt change in heading offset causes a peak response at the start and when the heading is turned back. Besides that the first figure shows that the heading is changed three degrees in order to reduce the lateral offset. When the offset is gone the heading is indeed changed back to zero. The second figure shows that the control works as long as there is a longitudinal offset.

4.2.4 Engine modes 5 and 6, failing stern thruster

The final engine mode that will be tested is engine mode 6, which uses port side thruster and bow thruster. The model was tested by only introducing a longitudinal offset, just like it was done for the previous engine settings. The response of the distance offset control is presented in figure 4.37.

The thrust allocation model from C.2 shows that the combination of these thrusters will not directly be able to overcome an offset in any direction directly, but the hope was that the control system would reduce the offset and eventually all offset would become zero, maybe taking more time than the other operations. However when evaluating the results it shows that it is not possible to control the vessel in this way. When allowing thruster rotation these engine modes can stably control the vessel. However thruster rotation was not used for the scope of this research.

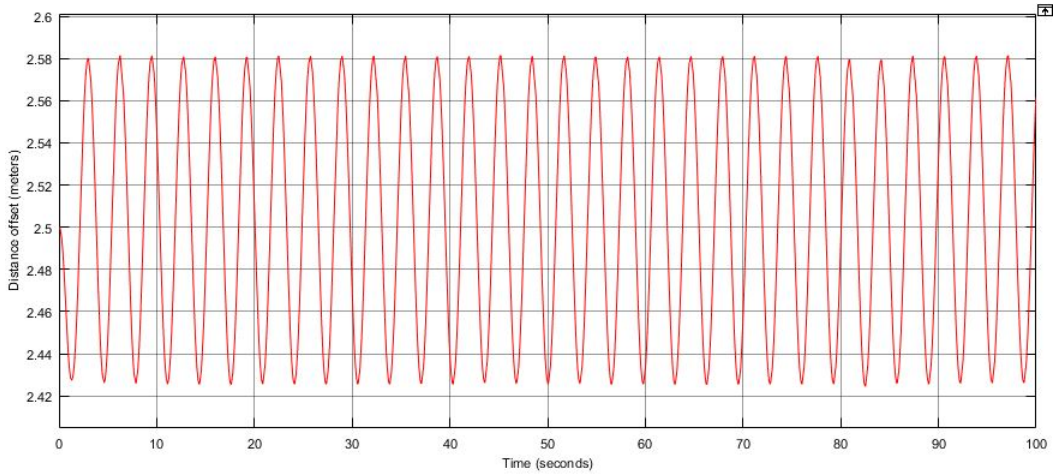

Figure 4.37: Distance control for engine mode 5.

The figure shows that the distance offset is oscillating around the original offset value, overall it is slightly reducing the offset. This response raises the question how the heading and lateral offsets are responding. Figure 4.38 shows the heading offset and figure 4.39 shows the response for the lateral offset.

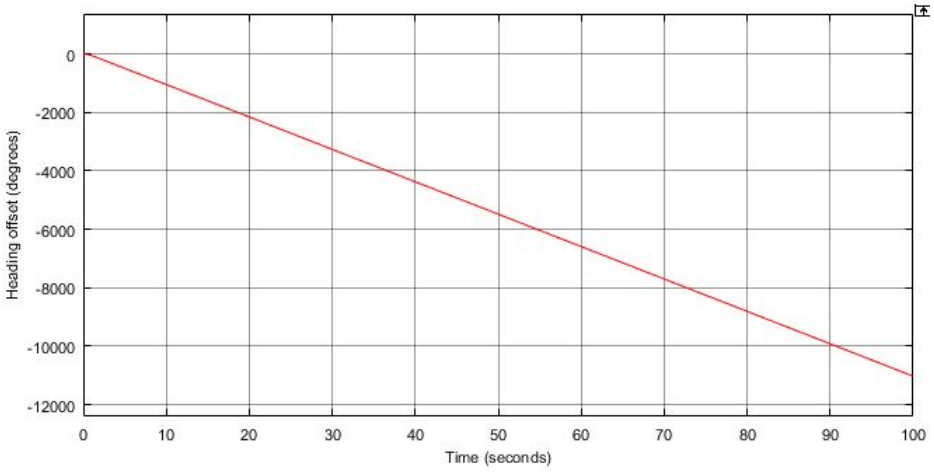

Figure 4.38: Heading response.

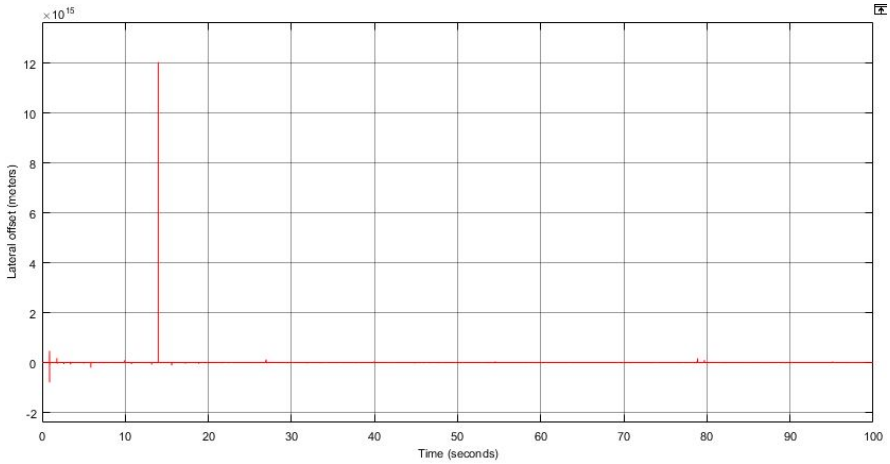

Figure 4.39: Lateral response.

The first figure, for the heading, shows that the heading is continuously decreasing. This means that the vessel is just turning in circles. Because the model does not compensate for the crossing from 360 to 0 degrees the heading value is just growing. In normal operation only small heading offset and changes will occur and therefore it is more easy to have the crossing from positive to negative. The line in the figure appears thicker than in all other figures, which indicates a fast oscillation arround a steadily decreasing value.

The final figure shows the lateral offset response. This figure proves that it is just not posssible to control the vessel with this mode of operation. The peaks are of the magintude 15, which is just not possible in such a short period of time. Also the offset appears to be constant, but also this line is thicker. By removing the large peaks an oscillation was found with the magnitude of 12. Which is also not feasible.

These three figures show that for this model it is not possible to operate when one stern thruster is not operational. An offset in one direction results in fast oscillations in all directions. The initial offset will not reduce. The other offsets will grow impossibly large. Therefore engine modes 5 and 6 will not be used for further research.

4.2.5 LCF model

In order to test the control system for the LCF some changes were made to the offline model, as was discussed in the first half of this chapter. This frigate does not have a bow thruster so the operational mode is the same as engine mode 3 for the Tito Neri tug. Therefore the first tests for the frigate were done with the same control values as were used for engine mode 3.

The results for this test showed that despite the vessel dimensions and configuration differences the control system parameters cause the same response. Figures 4.36, 4.35 and 4.34 also show the response for the LCF. This means that no further tuning is needed and that the same PID control parameters can be used for testing in the simulator.

5 Simulator Testing

In the previous chapter all ins and outs of the offline model were discussed. In this chapter parts of the offline model were taken to make models suitable for testing in the ship handling simulater at the Royal Dutch Naval Academy. The main difference for these models is that a camera is added, therefore the loop will no longer be closed. The models for the simulator operations start with the camera. From the feed, bearing and distance will be calculated. Just like in the offline model these will be the inputs for the offset calculation block. These models then use PID control and thrust allocation. The generated outputs will be required RPM or required heading change. This is were the model will end. All other tasks from the offline model will be taken care off by the camera. All models for the simulator operations are placed in appendix D.

In this chapter three operations play a central roll. These three operations are platform approach, RAS approach and collision avoidance. The complexity of the model increases steadily in this order. For all operations first the specifics of the simulink model will be discussed, thereafter the test results will be presented. The fourth part is based on finding the operational limits of this camera system. The influence of sea state, precipitation, fog and light are investigated.

In order to make sure these tests are repeatable first the test setting will be explained. When the same set up is used, it does not matter in what simulator the tests will be conducted. The only things that need to be checked when using a different simulator is the observer position. First of all the observer height. The observer height needs to match the camera height in the model in order to obtain an accurate measurement. The observer position needs to be on the centre line of the vessel, but can be shifted to the front of the vessel. The position was shifted to the front in order to remove the cannon and the jack staff from the image. Figure 5.1 will show the general setup in the simulator.

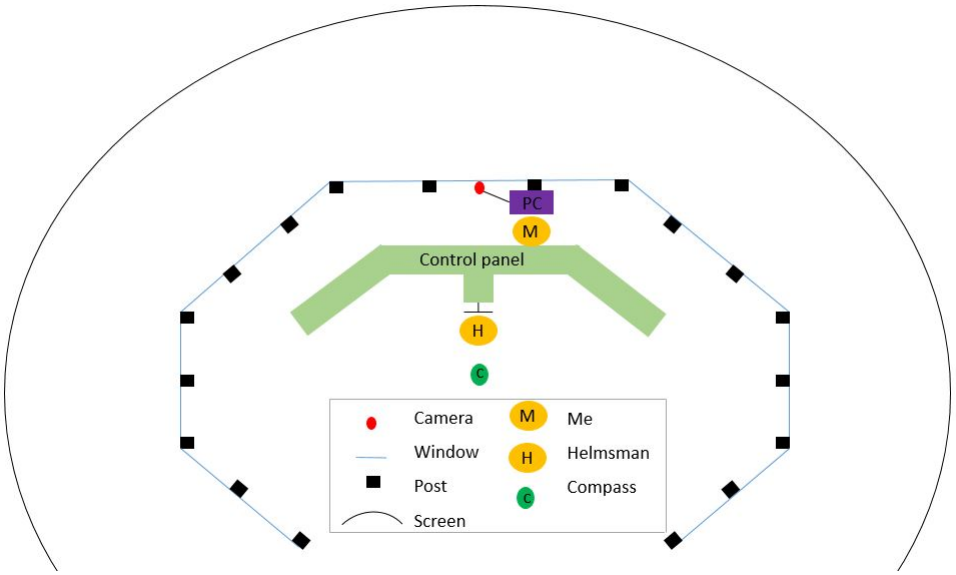

Figure 5.1: Test set up for simulator testing.

The figure shows the test set up in the ship handling simulator at the Royal Netherlands Naval Academy. The only component of which the placement is critical, is the camera. The camera has to be placed exactly in the centre of the central window. The placement of the computer can be wherever the cable and simulator lay out allow. The computer shows setting changes on the screen, which have to be repeated to the helmsman. Therefore the person with the computer should also be located as close to the helmsman as possible. This is to improve the communication between these people.

5.1 Platform approach

The first operation is the platform approach operation. This is the most straight forward operation, which is also the reason that it was the first operation. During the approach the system should adjust the heading in order to perform a straight approach. The control system should also slow down and stop the vessel at the required approach distance. Figure 5.2 shows the intendent movement for this task.

Figure 5.2: Platform approach operation.

This figure shows that a small vessel is approaching a relative large stationary platform. The heading should be controlled in order to approach the centre of the platform. The vessel should be controlled in such a way that the vessel is stopped at the specified approach distance. Now first the model that should be able to perform this operation will be discussed.

5.1.1 Simulink model for platform approach

For the platform approach operation a simulink model was developed which takes the camera feed and produces a heading and speed control. The full model can be found in appendix D, figure D.1. This model shows some new functions, for this model, not discussed in chapters 2 or 4. These functions will now be explained. The new functions are the red coloured to multimedia file block, the histogram equalization block and the large subsystem. PID control and thrust allocation are for this application combined in the PID controller block.

First of all the to multimedia block is used to save the video feed in a file so that the video can be used for processing afterwards. The block is coloured in order to remember to change the name after each test. This has to be done to save all tests otherwise the new test would overwrite the old one.

The new simulink function that is used in simulator testing is histogram equalization. This is a standard functionality that enhances the contrast in the intensity image. With the set up of this block the number of bins can be changed. The number of bins indicates the number of gray tones that are allowed in the image. The darkest pixels of the intensity image are transformed to black. At a discontinuity the lightest pixles are transformed to white. All gray tones between black and white are then divided over the specified number of bins minus the two for black and white. Every bin will contain an equal ammount of pixels, 3037 pixels for an HD image. This method enhances the contrast, because the intensity range of the image is increased. Figure 5.3 shows the influence of this function. Figure 5.3a presents the standard intensity image as it enters the block. The second figure, figure 5.3b, shows the output of the histogram block with 256 bins. For this image besides black and white 254 tones of gray are used. The images immediately show that the platform is better distinquishable from the back ground.

(a) Intensity image before histogram eqalization. (b) Intensity image after histogram equalization.

Figure 5.3: Images to show what the histogram equalization block does.

The final new block is the subsystem. This system is introduced in order to obtain a better distance measurment. First test in the simulator showed that the distance measurements were unstable. This subsystem will be able to produce a more steady measurement and hopefully also more accurate. First figure 5.4 shows the result of the distance measurement without this subsystem. The histogram equalization bin number is 256 for this measurement. The measurement is the result of the first two minutes of the platform approach.

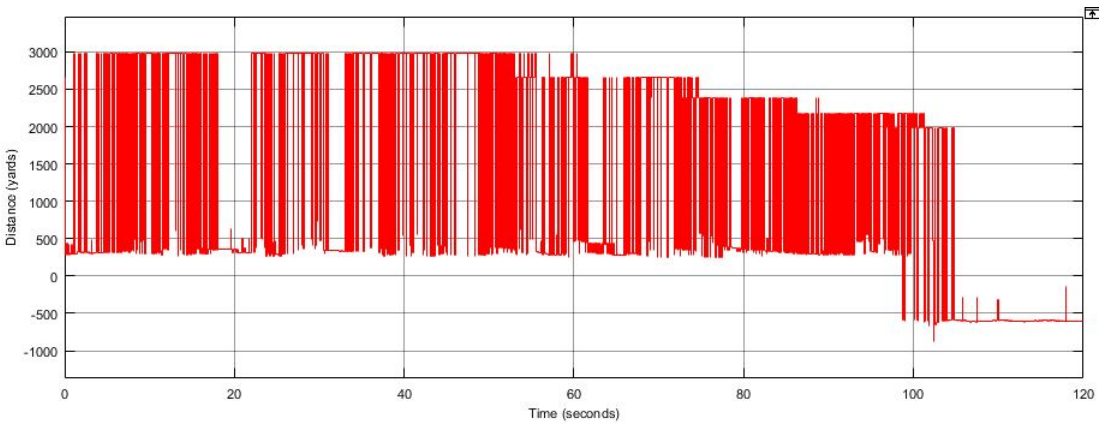

Figure 5.4: Distance measurment with 256 bins histogram equalization.

This figure shows that the distance measurement is constantly fluctuating between the correct value which at the start should be 3000 yards, and a value around 300 yards. It is obvious that with this measurement a control system is not able to operate. Therefore the subsystem was developed. The system consists of multple lines that perform the same operation, but with a different number of bins in the histogram equalization. One line is presented in figure 5.5.

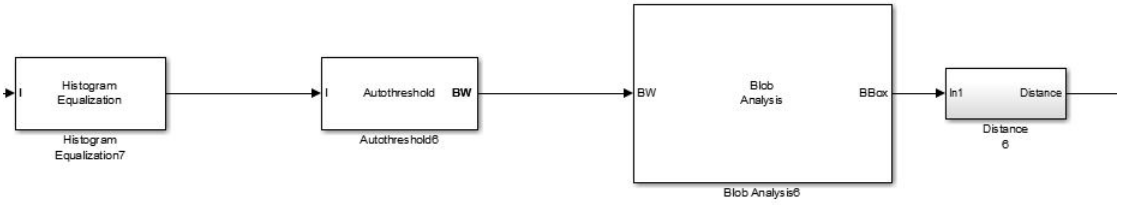

Figure 5.5: Single histogram equalization path.

Each line consist of a histogram equalization block with a different number of bins. The next blocks on the line are the standard blocks that were used for the distance measurement, autothreshold, blob analysis and the distance calculation block[3]. The lines are brought together in a block that determines the maximum value. The maximum value is also the correct measurement. While targets for which the lowest point lies above the horizon are discarded. Targets close to the horizon are the furthest away, usually the correct target. Close taregt usually come from valse target in the waves. Waves can only be observed close to the own vessel and not at the target vessel. Because of these reasons the maximum value from all lines will be the target.

Next the number of lines and the number of bins have to be set in order to obtain the best measurement. From the histogram equalization block it became clear that the number of bins for this block follow fromula 2^n, the default value was 256 bins which is used for the first model. The first application of the subsystem uses three lines with 64, 128 and 256 bins. The distance measurement result for this model is presented in figure 5.6.

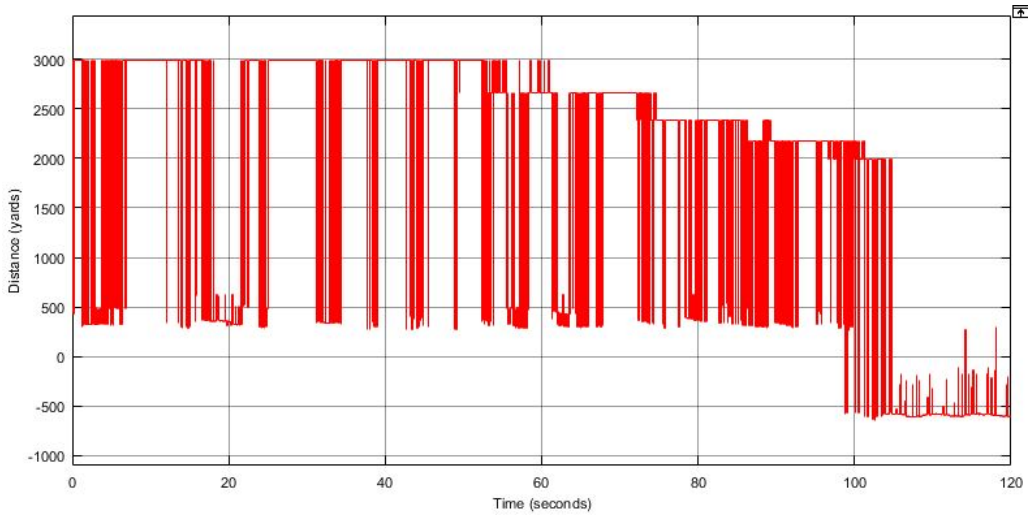

Figure 5.6: Distance measurement with three histogram equalization paths.

This figure shows a better measurement, but still a lot of fluctuations are present. Also at the end faulty measurements are done. Measurement values below zero should not be possible. In order to improve this more lines will have to be inserted in the model. Before this is done first influence of the bin number is investigated, in order to find better values. Figure 5.7 shows the difference between 8 bins and 2048 bins.

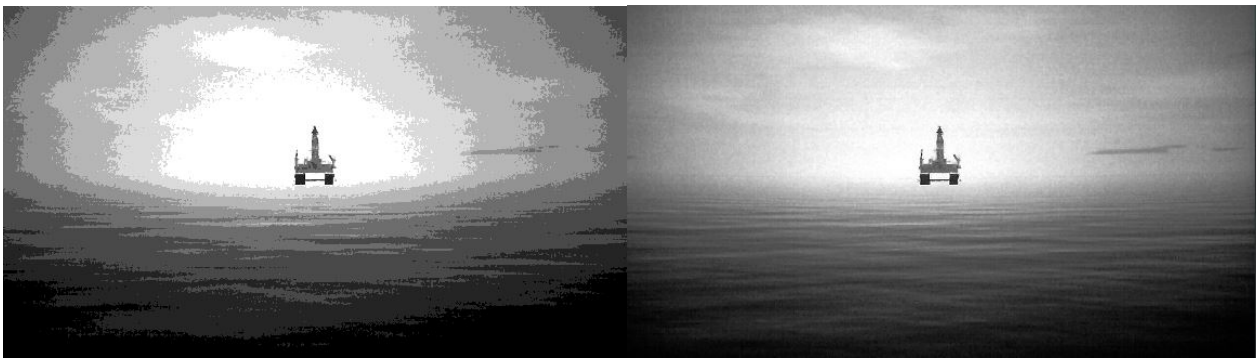

(a) Intensity image from 8 bins. (b) Intensity image from 2048 bins.

Figure 5.7: Images to show differnece between two numbers of bins.

When comparing these images it shows that with 8 bins the contrast between background is larger, but details will be lost. When using 2048 bins most details are kept and still extra contrast is obtained from the original image. Because the first image, figure 5.7a, only has 8 bins it is possible to count the bins. The image shows that between black and white six different gray tones are present as expected.

Next the choice was made to use all 9 lines starting with 8 bins and finishing with 2048 bins. By increasing the number of lines and increasing the span from the number of bins this system should have an improved distance measurement compared to the model with three lines. The measurement results are presented in figure 5.8.

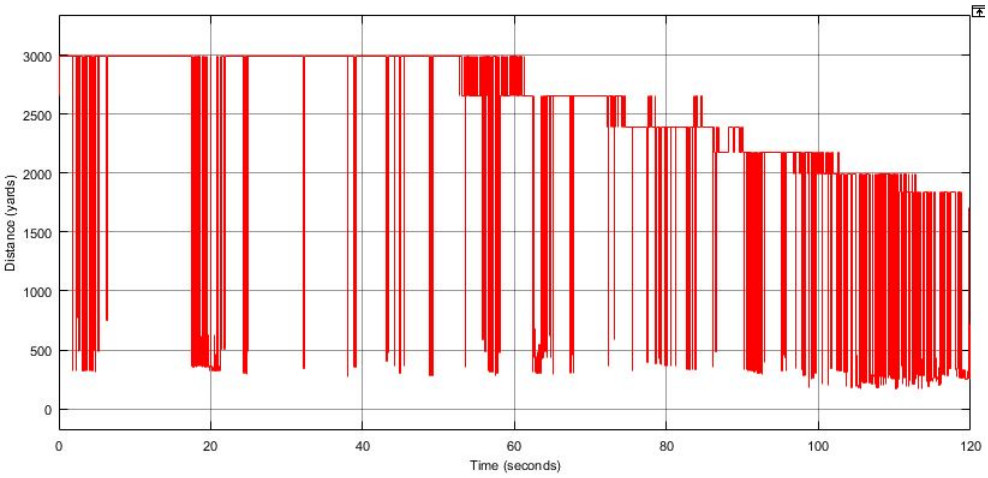

Figure 5.8: Distance measurement with nine histogram equalization paths.

This image shows that again an improvent was obtained. This system has less fluctuations compared to the model with three lines and also the negative distance at the end of the simulation is gone. However the measurement is still fluctuating too much. Because the overall measurement now is more accurate this signal will be filtered in order to remove the large fluctuations. Maybe when adding even more histogram equalization blocks with different bin numbers and also numbers between existing values all fluctuations could be removed. But the model is slowed down when adding too much of these blocks. The filter will make sure that the signal remains constant when the new value differs too much from the previous value. A vessel can simply not sail a few thousand yards in less than a second. Figure 5.9 shows the distance measurement with the filter.

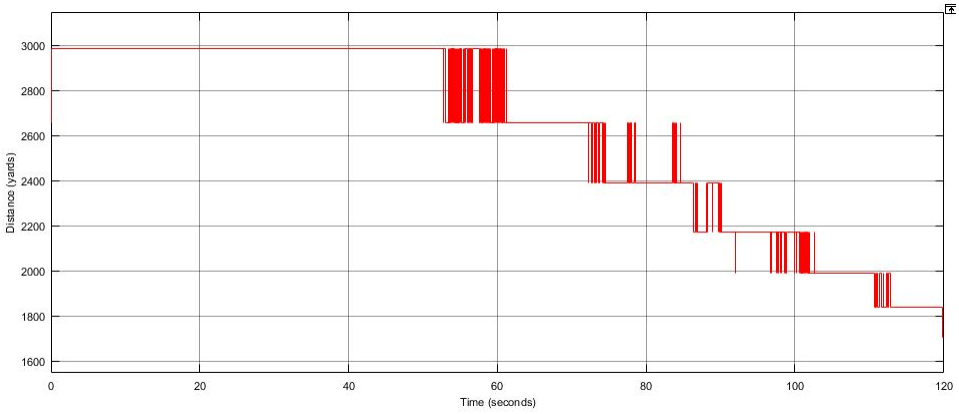

Figure 5.9: Distance measurement with nine histogram equalization paths and a filter.

This figure shows that the distance measurement finally produces a steady output with realistic values. The small fluctuations at the transfer from one distance to the next is because of the camera resolution. When using equation 2.4 with the calculated camera parameter and a observer height of 18.9 yards, the eight pixel from the centre results in a distance of 2988.8 yards. When the vessel is getting closer, the ninth pixel results in a distance of 2656.7 yards. The relation is linear; twice the number of pixels results in half the distance. This means that the 16th pixel calculates the distance at 1494.4 yards. When the lowest point of the target is switching between two pixels this fluctuation occurs. Each step in the image indicates that the lowest point is captured at the next pixel. Now the maximum detectable distance, at the first pixel from the centre, is 23910 yards. A single step closer results in a distance of 11955 yards. Theoratically the smallest distance which could be measured at the last pixel will be 66.4 yards in this setting.

Figure 5.9 also shows the accuracy of this measurement system. For example when the eight pixel captures the lowest point of the vessel, the system indicates a distance of 2988.8 yards. However due to the accuracy the actual distance might be somewhere between 3202.3 and 2822.75 yards. A way to increase the accuracy and to reduce the fluctuations is to use a camera with a much higher resolution. More pixels will reduce the step size compared to the other camera at the same distance. With a smaller step size the system is beter able to identify the exact pixel, therefore reducing the fluctuations. Another effect from the increased resolution is that the maximum detectable range will increase. The vessel is lost when to litle pixels make up the vessel in the image. With an increased resolution more pixels are used for the image of the vessel.

The method of using multiple lines of histogram equalization is not suitable for the heading measurement, because no maximum or minimum number will indicate that this should be the accurte heading. The heading can be positive as well as negative and will not have to be close to the centreline of the picture. Therefore only one histogram equalization block is used with the default value of 256 bins.

As mentioned before the final new feature of this model is that the thrust allocation is implemented in the PID controller. The reason for this is that the thrust does not have to be divided over multiple thrusters. The only parameters needed is the RPM for both propellers and the required heading change in degrees. Therefore the look up table that is used to calculate the vessel specific RPM is used after the PID control. The relative speed from the controller is than transformed into an RPM value which is compatible for the vessel. In the case of the frigate when the PID controller sets a maximum relative speed with an output value of one the look up table will output 230 RPM.

5.1.2 Testing of platform approach

Now the simulink model for this operation is properly adjusted the tests can be conducted. At the start of the test the vessel will be placed at 3000 yards from the platform. Then the vesssel will approach the platform until 500 yards. The platform will remain stationary and for the maximum vessel speed 10 knots is set. During the operation the model will indicate heading changes, but small changes will not be done. This is in order to stabilize the video feed. Figure 5.10 shows the start and end point of the approach.

(a) Start position. (b) End position.

Figure 5.10: Images indicating start and end of the platform approach operation.

Next the results of this approach will be presented. The total simulation from start to end took almost 17 minutes. First of all the distance from the vessel to the platform will be presented. This distance is shown in figure 5.11.

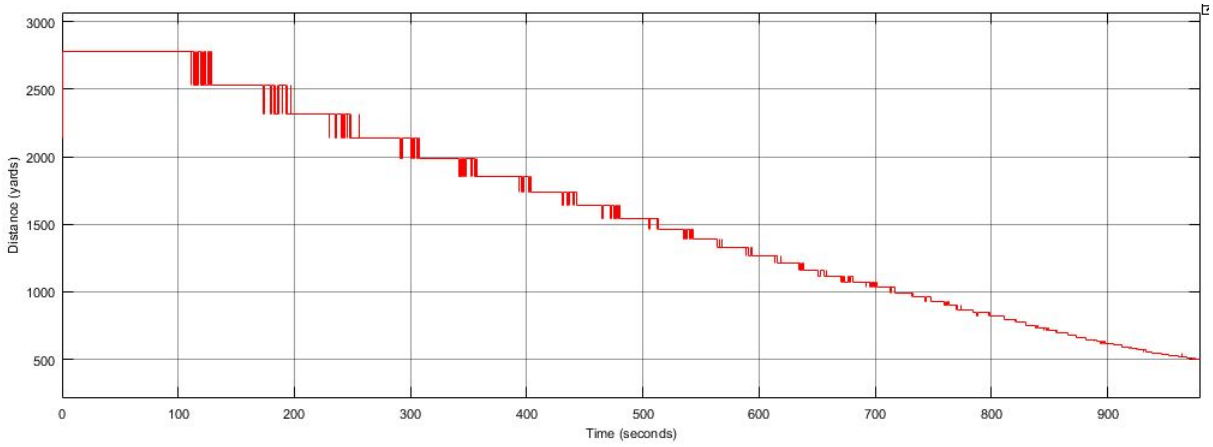

Figure 5.11: Distance measurement during the platform approach operation.

the first thing this figure indicates is that the multiple histogram equalization lines in combination with the filter works for this approach. Still some fluctuations occur when shifting from one pixel to the next, but this effect reduces as the vessel gets closer. During the final minutes of the approach a more smooth output is generated as the indicated distance between two consecutive pixels is reduced significantly. For example at 500 yards distance, the difference between two pixels is only ten yards. The figure also shows that the vessel slows down in the end. A trend line through these values would show a small parabolic curve. The speed output from the model during the operation is the next interesting parameter. The speed is presented in figure 5.12.

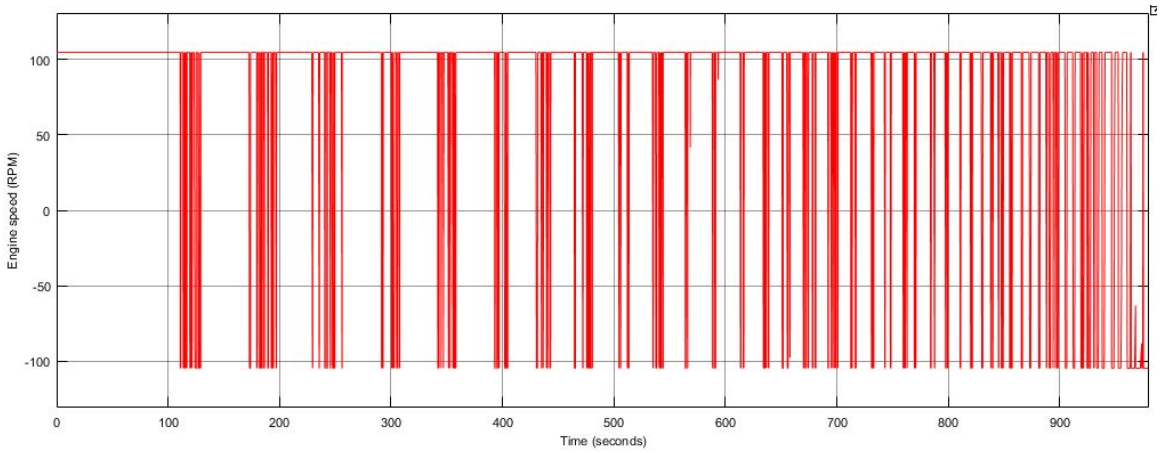

Figure 5.12: Engine speed indicator during the operation.

This figure clearly shows the derivative action from the control system. Each step between two pixels the model calculates a very high speed. Hence the derivative action tries to slow down the vessel in order to limit the overshoot. Therefore the engine speed indicator asks for reversed thrust. However soon after this step response the model settles back at full speed ahead. In the end of the simulation close to the end position the figure indicates a reversed thrust with small peaks to positive thrust. Also in this case a better camera resolution will reduce these fluctuations and that will result in a better response and a better control system. The final parameter is the heading change indicator. Figure 5.13 shows the requested heading change during the operation.

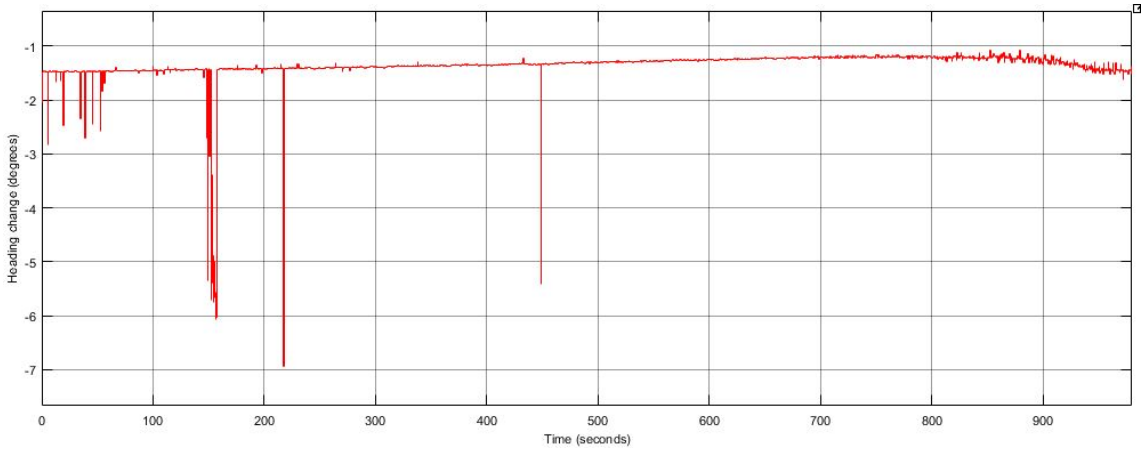

Figure 5.13: Requested heading change during the operation.

In the figure the heading change is constantly between minus one and minus two degrees. This indicates a requested heading change to port side. As mentioned before the choice was made not to react to these small offsets. The peaks that indicate larger offset come from the fact that for the heading change no filtered solution could be made like for the distance. The used histogram equalization block with 256 bins in these cases captures a false target. Finally after about 850 seconds when the thrust is reversed the figure shows a more significant course change. This is a normal phenomenon for a vessel. Due to the reversed thrust the water flow on the rudder is slowed down. When the water flow at the rudder stops, the vessel will no longer be able to keep heading.

All in all this model is able to measure heading and distance quite well. Also the control of vessel speed and heading is possible. However a better camera with much higher resolution is required for a more accurate measurement and control.

5.2 RAS approach

The promissing results from the platform approach operation give hope to take the next step by increasing the operation complexity. Instead of approaching straight on a stationary platform the approach will be performed next to a moving vessel. Just like navies do when replenishing at sea. Therefore the replenishment at sea operation will be the next operation to be tested in the simulator. Figure 5.14 shows the intendet approach in the simulator.

Figure 5.14: Replenishment at sea approach as performed in the simulator.

5.2.1 Simulink model for RAS approach

For the RAS operation the simulink model from the platform approach was slightly adjusted. The full model for the RAS operation can be found in figure D.2. This model also uses histogram equalization and the subsystem with the multiple lines of histogram equalization. The only differences lay in the offset calculation block. First of all the distance offset. This will be equal to the actual offset, because the final position should be when the two vessels sail next to each other at the specified distance. The model is not capable of following the vessel until that point while the camera has a much smaller viewing angle. Therefore when the system is not able to see the target no further heading changes are done. In the simulator the distance between both vessels is measured when the vessels sail past each other. Next the heading offset is calculated. Figure 5.15 presents the model for this calculation.

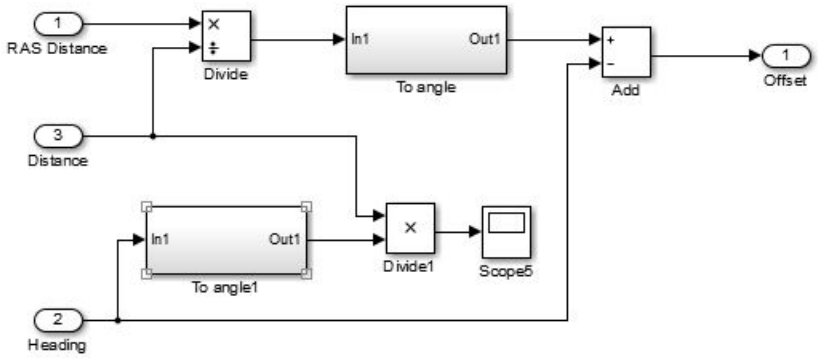

Figure 5.15: Model to calculate the heading offset.

First of all the specified RAS distance, 50 yards for this test, and the actual distance are used to calculate the bearing in which the target should be located at this point. The to angle block is used to calculate the heading and transform it from radians to degrees. Then the actual bearing is substracted in order to find the offset. The second to angle block does the opposite. It takes the heading and transforms it to radians and then takes the tangent. This value is then multiplied with the actual distance in order to calculate the lateral distance at that point. Also for this model thrust allocation is performed with a look up table in the PID controller.

5.2.2 Testing of RAS approach

With the changes to the model the RAS approach can now be tested. This operation starts with a distance from the vessel to the target of 2000 yards. The operation ends when the target vessel disappears in the noise at the edges of the image. The target vessel is sailing a constant speed of 10 knots. During the approach the maximum vessel speed was set to 15 knots. The lateral approach distance was set to 50 yards. During the test it was discovered that in the heading offset calculation the minus should be at the expected bearing and not at the actual bearing. Therefore the heading change from this model directs the vessel in the opposite direction. The mistake was observed during the test, but first when analysing the result the origin of the mistake was discovered. Therefore the tets was not repeated for a correct model. In the results a sudden heading change can be observed, which was performed when the mistake was observed. The start and end position of this test can be observed in figure 5.16.

(a) Start position. (b) End position.

Figure 5.16: Images indicating start and end of the RAS approach operation.

The image of the start position, figure 5.16a, shows that a vessel at 2000 yards seems very small when compared to the platform from figure 5.10a. This also indicates that it is much more difficult for the algorithm to detect these vessels. Figure 5.16b shows the end position of this test. The image still clearly shows the vessel. However the image processing is not able to distinghuish the vessel anymore while the vessel gets close to the edge of the image. This can be illustrated by figure 5.17.

Figure 5.17: Binary image from the end of the simulation.

The vessel is now getting covered by the noise at the edge of the image. Hence no clear distance measurement can be obtained. Next the results for this approach will be discussed. Starting with the distance to the target vessel in figure 5.18 and the lateral distance to the target vessel in figure 5.19.

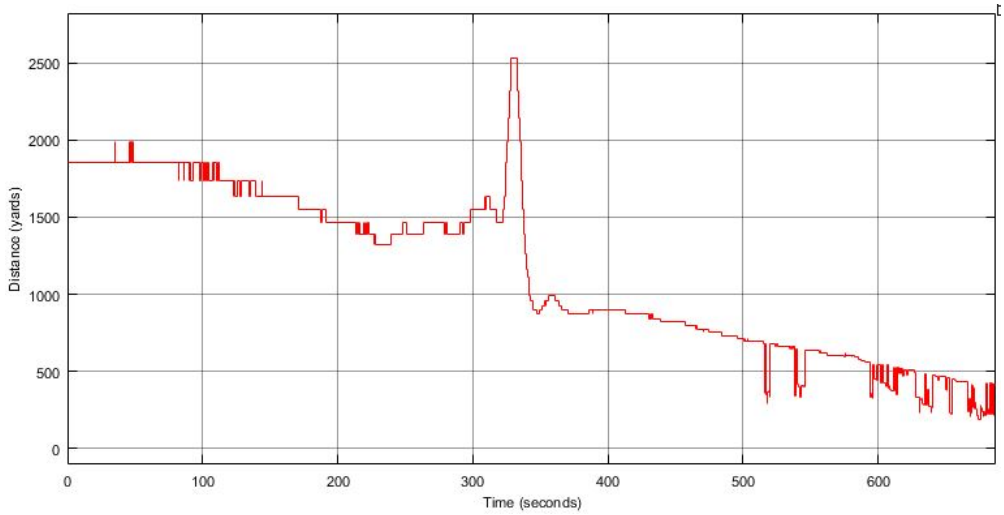

Figure 5.18: Distance measurement during the RAS approach.

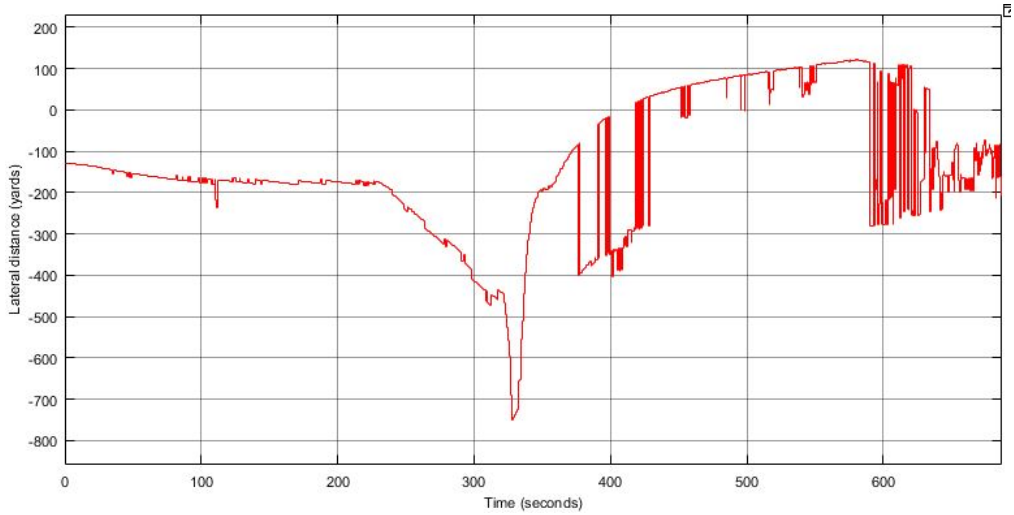

Figure 5.19: Lateral distance during the RAS approach.

First of all the peaks at 330 seconds are caused by the relatively large heading change due to the wrong offset calculation. The first figure shows that except during the course change the system is well capable of measuring the distance. The first drop in the second figure is due to the initiating of the course change, the second drop is due to the end of the course change. Both figures show disturbances at the end of the simulation. These are present because the vessel is disappearing at the edge. Figure 5.20 shows the output of the speed control for this operation.

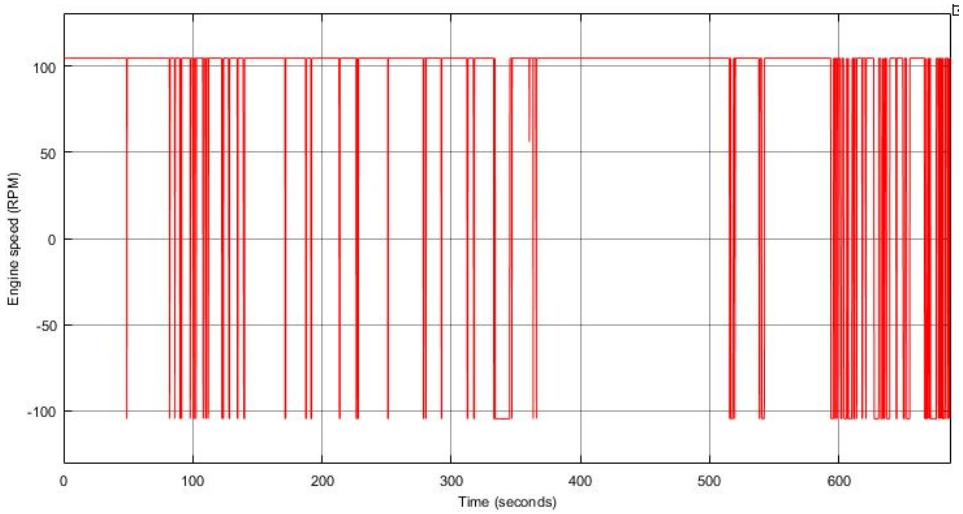

Figure 5.20: Engine speed requested during the operation.

First of all this figure shows less fluctuations compared to figure 5.12 for the platform approach. The main reason for this is that the distance is reducing more slowly. The target is also moving, which results in a reduced overspeed. It is notable that in the first period after the heading change no fluctuations are present even when the distance is still reducing. Finally figure 5.21 shows the requested heading change during the operation.

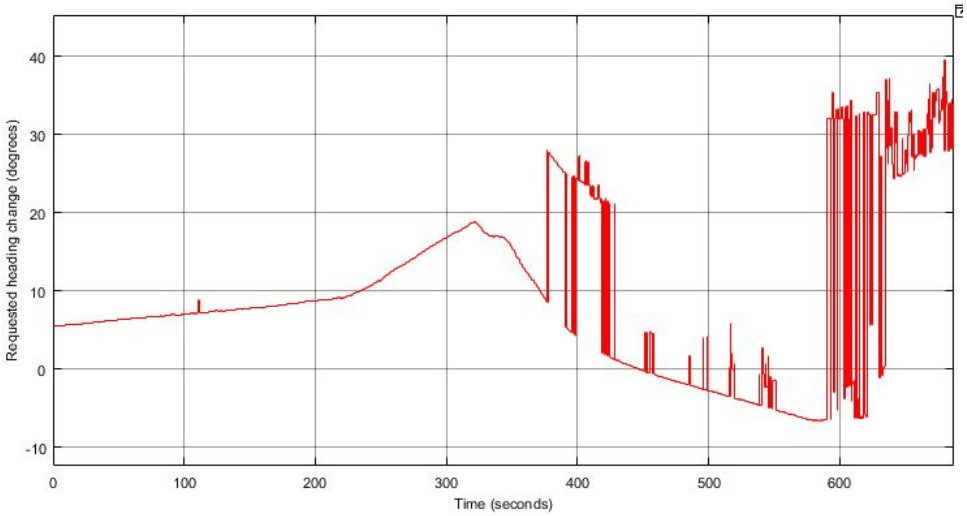

Figure 5.21: Requested heading change during the RAS approach.

Initially the heading was not changed in order to enable the system to settle. After the course change at 200 seconds the requested change is even increasing which indicated that the change should be in the opposite direction. This was soon corrected as can be seen by the reduction of the requested change. When the vessel reaches the requested heading end the rotation is terminated a rolling motion occurs which explains the disturbances. Just before the 600 seconds mark the final usable value was available. A requested heading change is indicated by the figure. This is in compliance with the measurement from figure 5.19 which indicates an offset of 100 yards. The indicated lateral distance was 50 yards which explains the requested changes. Finally the approach distance at the end of the simulation was measured in the simulator system which also indicated a lateral distance of 100 yards.

All in all these results show that this model is capable of performing the approach for a replenishment operation. The first thing that should be changed is the minus in the offset calculation which prevents a turn in the wrong direction and the resulting large heading change. Also a camera with a better resolution and a larger viewing angle, preferably 360 degrees, will improve the capabilities of this system.

5.3 Collision avoidance

The final operation that will be tested in the simulator is the collision avoidance operation. For this operation the vessel has to detect an upcomming collision and divert according to the regulations[4]. The model used for this operation is somewhat more complex than the models for the previous operations. But first the intendet movement will be explained by figure 5.22.

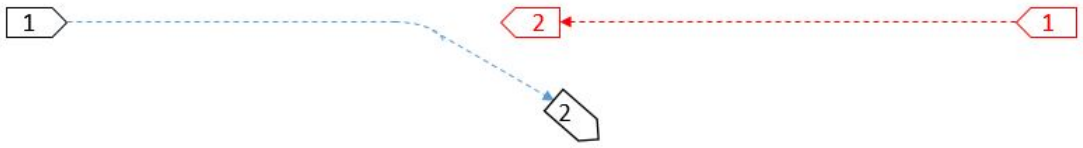

Figure 5.22: Collision avoidance test in the simulator.

The image shows that two vessels are approaching each other head on. Normally both vessels are required to take avoiding action, but to test the system the target vessel will not change course. Due to the limited viewing angle of the camera a head on approach was the only collision situation that could be tested. The first part of this paragraph will be used to explain the new model for collision avoidance. Thereafter the results from the test will be discussed.

5.3.1 Simulink model for collision avoidance

First of all the model starts with the same block as used in the previous two operations. The full model for the collision avoidance operation is divided into two sections that are presented in appendix D, in figures D.3 and D.4. The new features for this model start after the subsystems that calculate the heading and the distance.

This model calculates the relative heading of the target vessel. Then the model checks if this heading will pass through the safe circle of the own vessel. In order to calculate the relative heading the initial position and the current position of the target vessel are used. Because the camera system is only able to measure relative distance and heading the system can only calculate the relative motion of the target vessel. The first block for this model is the initial detection block which safes the initial target specifics. Figure 5.23 shows the internal details for this block.

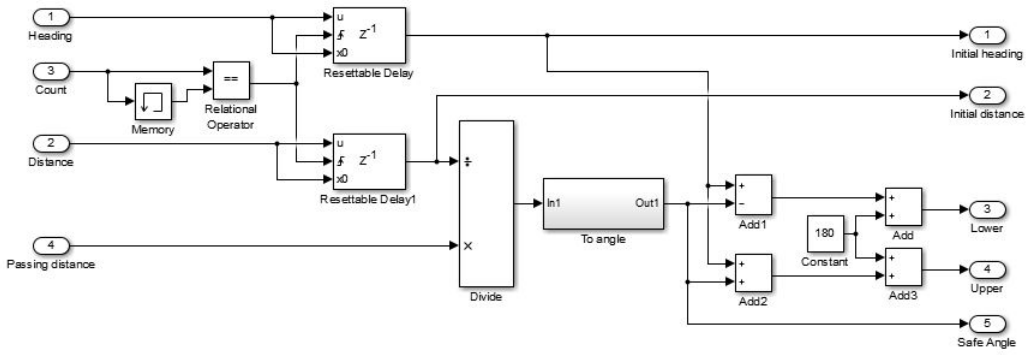

Figure 5.23: Model showing how the initial values are saved.

This model uses the calculated heading and distance as well as the count of blobs directly from the blob analysis block and the safe passing distance which is set to 500 yards for this test. Then the heading and distance to the target are safed when the count changes the bocks will reset. Next these values are used with the safe passing distance to calculate an upper and lower limit for the safe circle as wel as the safe angle. Figure 5.24 will help to understand these calculations.

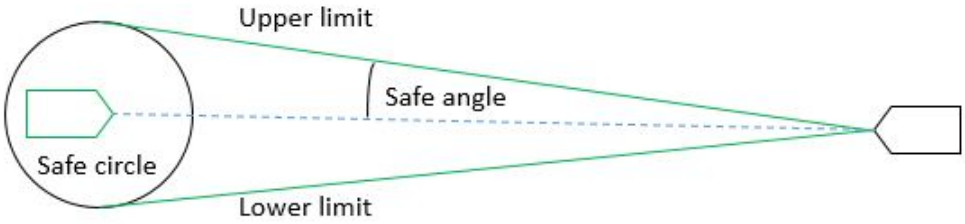

Figure 5.24: Illustration to explain the safe circle.

In the illustration the green vessel is the own vessel and the black vessel is the target vessel. The circle is drawn arround the bow as the camera is also placed at the fron of the vessel. The radius of this circle is the safe passing distance which can be set previous to the simulation. First the safe angle is calculated. This is done by placing the radius at the target vessel and then calculating the angle in the right-angled triangle. Then this angle is added to the target bearing for the upper limit and deducted for the lower limit. Because these limits are from the own vessel to the target vessel 180 degrees are added in order to get the limits from the target vessel. Later in the model these limits are compared to the relative motion. When the relative heading lies within these limits there will be a risk of a collision. The safe angle is used to determine the magnitude of the evasive action.

According to the regulations a vessel has the obligation to divert for vessels at the starboard side. The vessel is then required to change course to starboard[17]. When two vessels are approaching each other head on both vessels are obliged to react, but a course change to port side is allowed. When a vessel is overtaking another vessel only the overtaking vessel has to divert. The next part of the model is used to invert the direction when for a target, which is located right in front of the vessel, a course change to port side is more logical. This model can be found in figure 5.25.

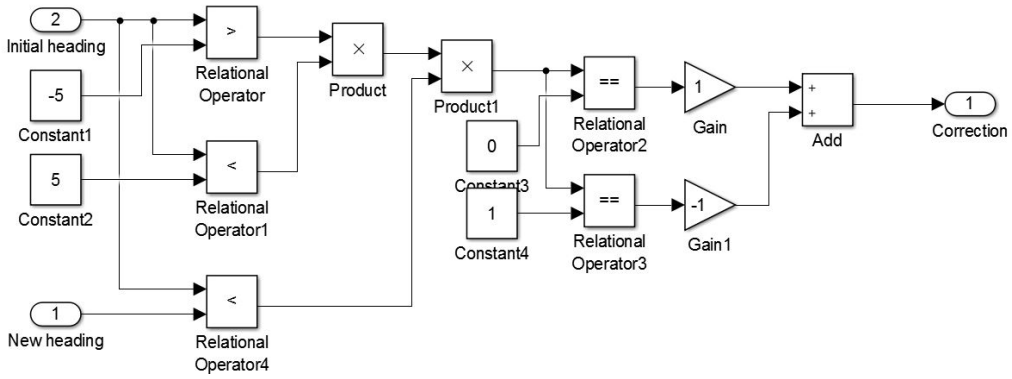

Figure 5.25: Model to change direction during a head on approach.

First of all this model checks if the target is located in front of the vessel. A vessel is considered in front when the bearing is smaller than 5 degrees to either side. Then the initial heading and the current heading are compared. When the initial heading is smaller than the new heading the target vessel will pass at starboard side. When the initial heading is larger then the new heading the target vessel is passing at port side. For head on approaches usually vessels will change course in order to increase the passing distance at the side at wich the other vessel is already passing. So when the initial heading is smaller, the direction of the change has to be inverted. So if all three relational operators have an output of the value one the target will pass at starboard side and thus the heading needs to be diverted to port side. If one of the operators outputs a zero no course change is required or a change to starboard is obliged. Therefore in this case the direction will not be inverted.

The next blocks that will be discussed are the four coordinate calculation blocks. Each block is the same. The only difference is the trigonometric function according to the direction. Therefore only one of these block will be presented, the model can be found in figure 5.26.

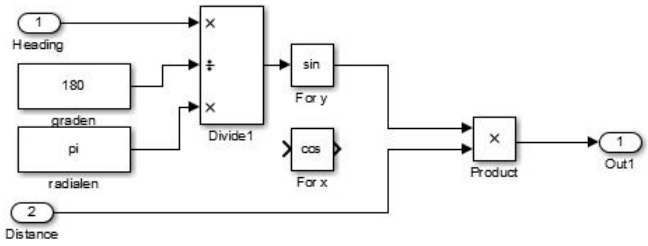

Figure 5.26: Model that shows how the coordinates are calculated.

This simple model calculates the coordinates from the bearing and the distance. The X-coordinate and the Y-coordinate are calculated for the initial measurements and the current measurement. First the model transforms the heading from degrees to radians. Then from this value the sine is taken for the Y-coordinate and the cosine is taken for the X-coordinate. When these values are multiplied with the distance the result will be the coordinate in that specific direction. These positions are then combined in order to calculate the relative heading The formula used for this is the same as the first part from equation 4.11. This result is then used in the model to calculate the relative heading which is presented in figure5.27.

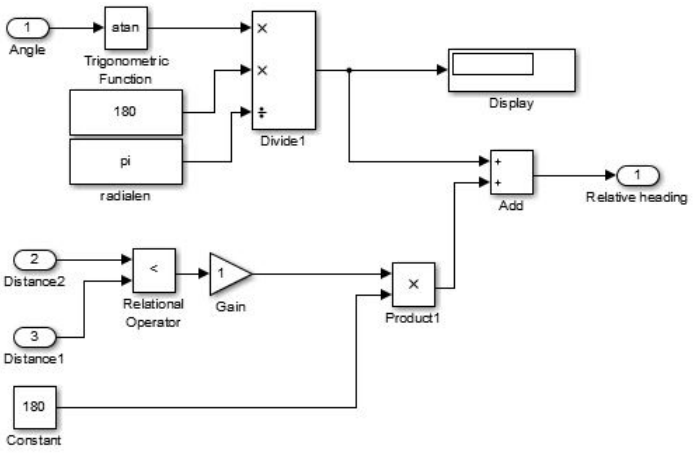

Figure 5.27: Model to calculate the relative target heading.

First of all, after the positions were divided, this model takes the inverted tangent. Thereafter this value is transformed from radians to degrees. The model is not able to make a distinction into the four quadrants. Therefore when the target vessel is closing in on the vessel a value of 180 degrees is added to the relative heading. This is done to make a distinction between the first and third quadrant. When the vessel is moving in the second or fourth quadrant relative to the vessel there will be no risk. The next block, shown in figure 5.28, will check if the situation is safe.

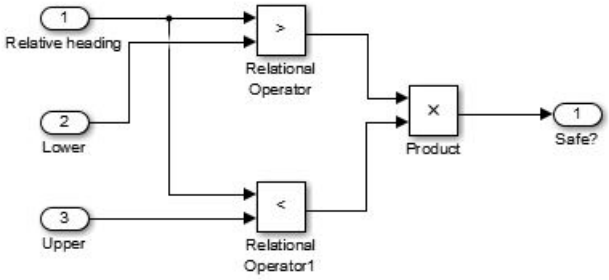

Figure 5.28: Model that checks if the approach is safe.

As metioned earlier the upper and lower limits can be used to determine whether the situation is save. This is also the reason that the limits are taken from the target vessel to the edges of the safe circle. If the relative heading lies within the two limits the target vessel will pass through the safe circle, resulting in an unsafe situation. When both relational operators indicate a value one the approach is unsafe and the model will output a value of one. A value of zero will be outputted when the situation is safe. The next model will check if the vessel is obliged to take evasive actions, figure 5.29 shows this model.

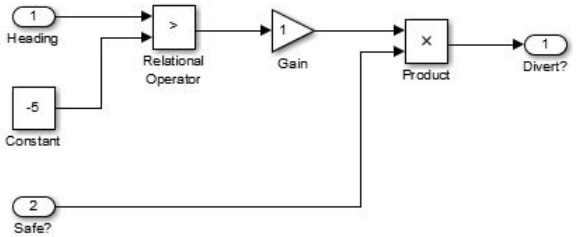

Figure 5.29: Model to check if the vessel is required to take action.

In the beginning of this section it was explained that a vessel has to divert when it encounters vessel at starboard or straight ahead. It was also mentioned that a bearing of five degrees was considered to be ahead. Therefore this model checks if the bearing is larger than minus five degrees. When this is the case, the vessel is obliged to take action. However when the situation is safe it is not necessary to divert. Therefore the safe indicator is multiplied with the relational operator. This means that the vessel only has to divert when both the relational operator and the safe parameter are equal to one. An output value of one means that the vessel has to divert. The final block will calculate the magnitude of the course change. The model that represents this is shown in figure 5.30.

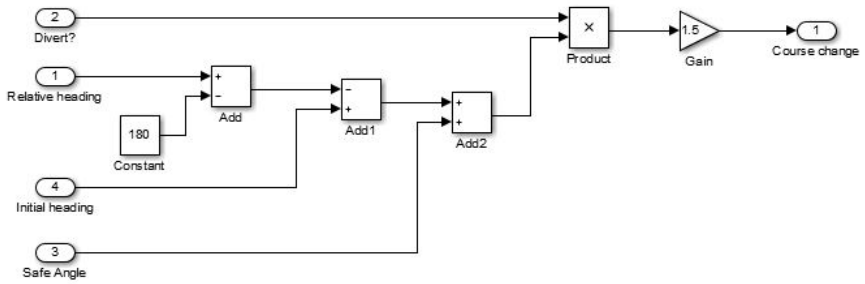

Figure 5.30: Model to initiate avoiding action.

First of all the relative heading of the target vessel is rotated again with 180 degrees in order to calculate the difference to the initial bearing. For example when the situation of figure 5.24 is considered. When the vessel diverts the safe angle in degrees to starboard, the relative motion of the target vessel will make it move along the upper limit. Therefore increasing the passing distance to the safe distance, hence the safe angle is added to this difference. The difference from relative heading and initial heading results in the fact that the vessel will always move accros one of the limits. However this model assumes an instant course change, but in reality the vessel will take some time to divert. Therefore the required course change is increased by 50 percent.

Finally after this block the output is multiplied by the head on approach indicator in order to divert to port side when this is required. This factor was already used to change the bearing from positive to negative or vice versa. That was done in order to calculate the appropriate course change, but in the wrong direction. By again multiplying at the end the course will be changed to port. When this would not be done twice the course changes to port would be too large. For example when the vessel is passing at half the safe distance at starboard side only a course change of half the safe angle to port side is required. However the model would calculate a course change of one and a half time the safe angle to starboard. When this value is inverted the passing distance would be twice the safe passing distance. Which will result in lost distance and time during the transit.

5.3.2 Testing of collision avoidance

With the model explained in the first part a test in the simulator was conducted. Due to the limited viewing angle of the camera a head on approach was chosen. The initial starting distance was 6000 yards and both vessels were sailing with 10 knots towards each other. The safe passing distance was set to 500 yards. Just like with the previous test, the start and end positions will be presented. Figure 5.31 will show the operation.

(a) Start position. (b) End position.

Figure 5.31: Images indicating start and end of the Collision avoidance operation.

The first image, figure 5.31a, shows the start position. The image shows that the target vessel is relatively small. Hence the system could have troubles to initially detect the target. However when both vessels come closer the system should be able to detect and calculate a sufficiently large evasive action. The measurements were ended when the target vessel got out of the image, but the simulation was still running in order to determine the closest point of approach. The vessel runs relatively quick from the edge of the image, when the turn to starboard was performed.

Now that the simulator test for collision avoidance is clear, the results can be discussed. The presentation of the results will start with the figure presenting the distance to the target. This figure is presented in figure 5.32.

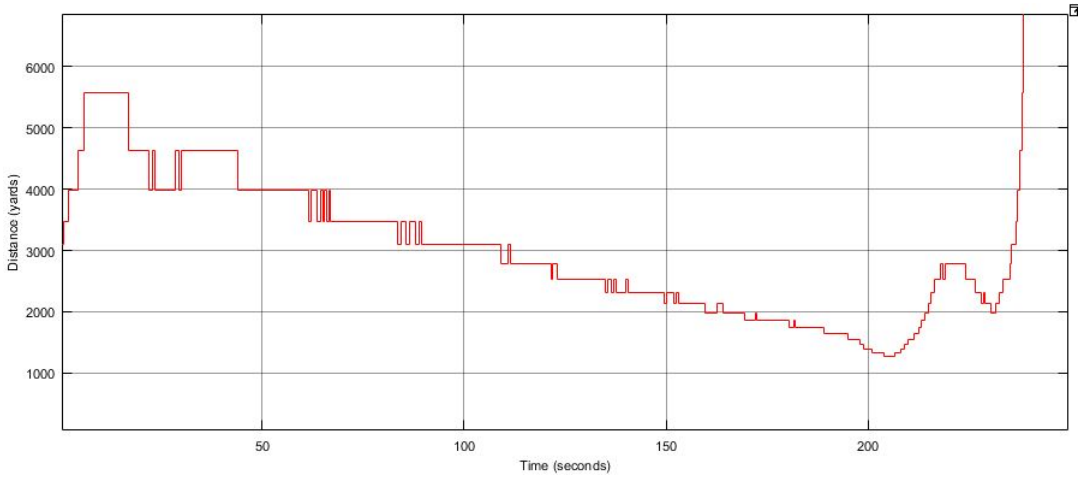

Figure 5.32: Distance measurement during the Collision avoidance test.

As expected, the figure indicates that at the start of the simulation that the system is not able to detect the target. However after ten seconds the vessel was first detected, but a steady measurement was obtained from 40 seconds. This figure also show the fluctuations when transfering from one pixel to the next. At the end of the simulation the system loses the target, but that is due to the turn. Hence until 200 seconds the distence is assumed to be measured correctly. Figure 5.33 shows the upper and lower limits throughout the entire simulation.

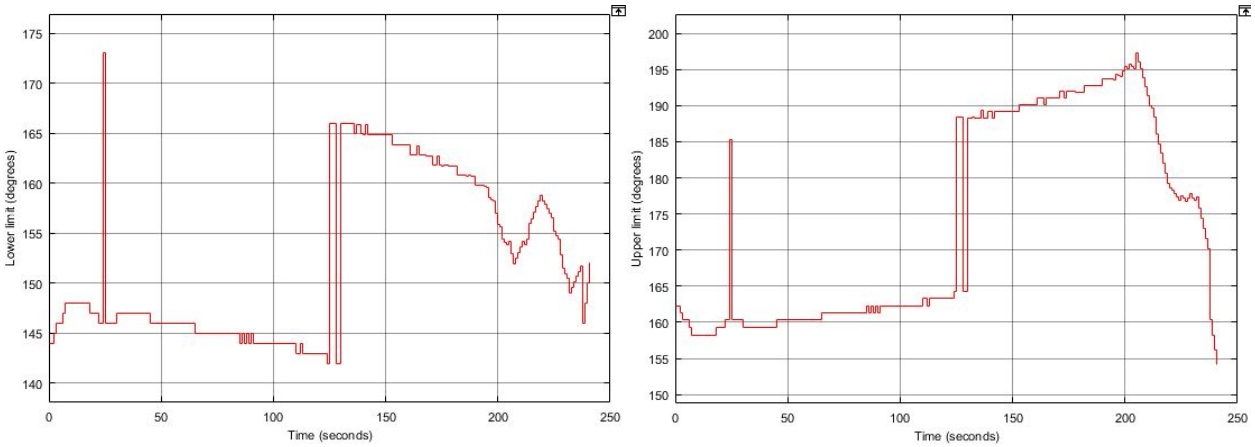

(a) Lower limit.

(b) upper limit.

Figure 5.33: Images showing the limits of the save approach.

These images show some small fluctuations, but overall the system is able to produce a stable value for the upper and lower limits. The second figure also shows that after 200 seconds, when the course is changed, the limits also change fast. The upper limit reduces, while due to the course change to starboard the relative heading will increase. To see if this is also the case, figure 5.34 shows the relative heading.

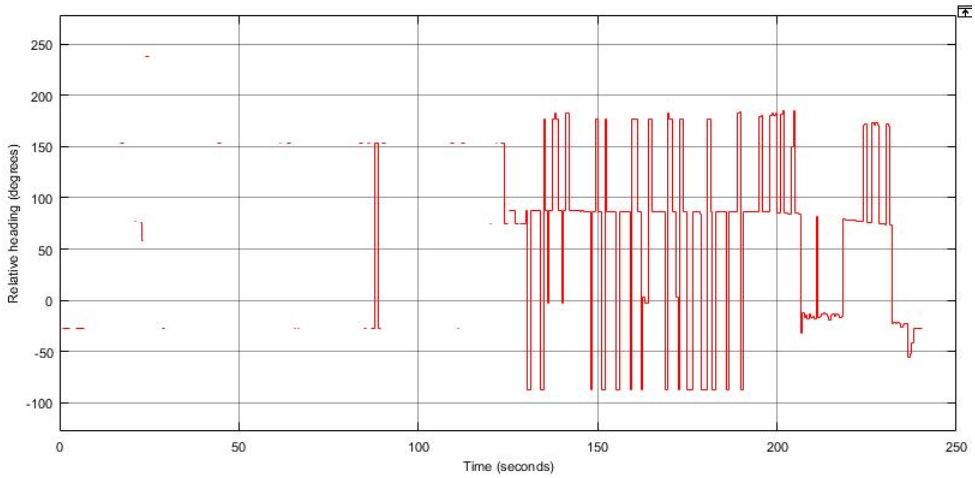

Figure 5.34: Relative heading of the target.

This image shows that during the first half of the simulation, the system is not able to calculate a steady relative heading. This can be caused that due to the large distance, the initial condition is constantly reset. Therefore no relative heading can be calculated between two points. The figure shows large fluctuations after the model is able to calculate the heading. However a heading of minus 100 equals a heading of almost 260. Which would imply much smaller fluctuations and a steady measurement. Around 200 seconds the model is able to produce a steady output of about 180 degrees. This value lies between the limits at this point which are 166 and 196. These values would imply a course change of about 20 degrees, after the factor to overcome the delay is used. In order to check this value figure 5.35 will present the indicated course change during the simulation.

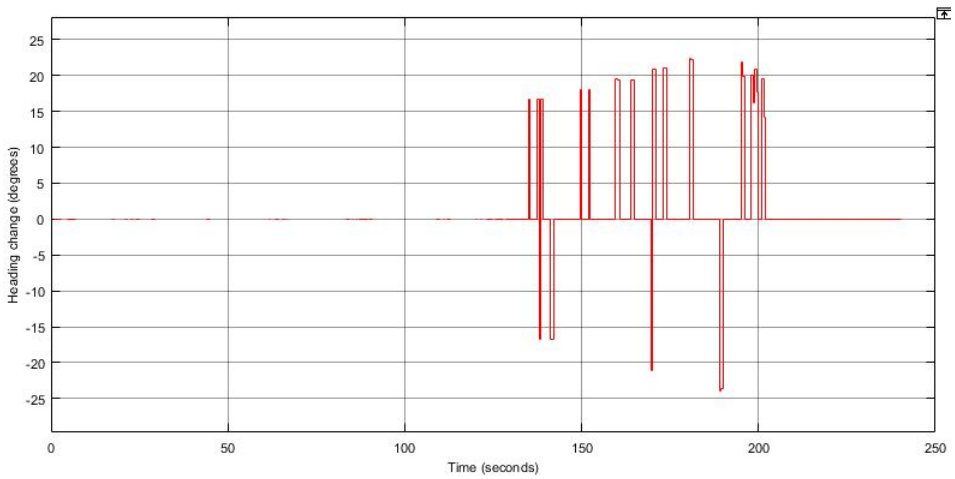

Figure 5.35: Indicated heading change during the operation.

While no relative heading was calculated, also no course change could be calculated. After halfway through the simulation the model was able to sometimes calculate a change, but still no steady figure. After 200 seconds the model produces a somewhat more steady output, which is 20 degrees as was expected. After the simulation the closest point of approach was measured at a litle over 300 yards. This can be explained from this figure. When the model is able to calculate the course change, it shows that the peaks are steadily growing. However when the stable output is generated the peak is smaller than before. But when the course change is performed later, a larger change is needed in order to keep the same passing distance. Therefore when at a later point a smaller change is done, the passing distance will also be too small. Therefore the first nine peaks can be assumed to be correct, but unfortunately too unstable.

Why the model produces a stable value at the wrong magnitude is not clear, but at least the model is able to react to a dangerous situation. These results also show that the model is capable of calculating the distance and also quite good able to determine the safe passing limits. At large distances the detection is too unstable to safe and keep the initial conditions, but at smaller distances this is possible. Finally the model is able to calculate an appropriate course change, but not stably.

5.4 Operational limits

The final tests that were done in the simulation were done in order to determine the operational limits of the system. For this one has to think of the environmental conditions for which the system still is able to produce a stable measurement. The conditions tested were seastate, fog, precipitation and light. The model used for these tests is a simple model which only gives the measured distance as an output. The subsystem calculating the distance will be the final block of this model.

5.4.1 Seastate

The first condition that is tested is the seastate. Both longitudinal incoming waves as lateral incoming waves are simulated. While longitudinal waves cause a pitching moment where lateral incoming waves cause roll and sometimes yaw. Initially the target vessel is placed at 2000 yards distance. Then the distance is reduced in order to investigate at what distance the measurement becomes unstable. While the camera is only able to detect waves close to the vessel, the minimal measurable distance will increase with increasing wave height. At a calm and level sea the system is able to detect vessels from 500 yards onwards. The first test was done with a seastate of 1 meter in head waves. Figure 5.36 shows the end point of the simulation and the measured distance.

(a) End point of the simulation.

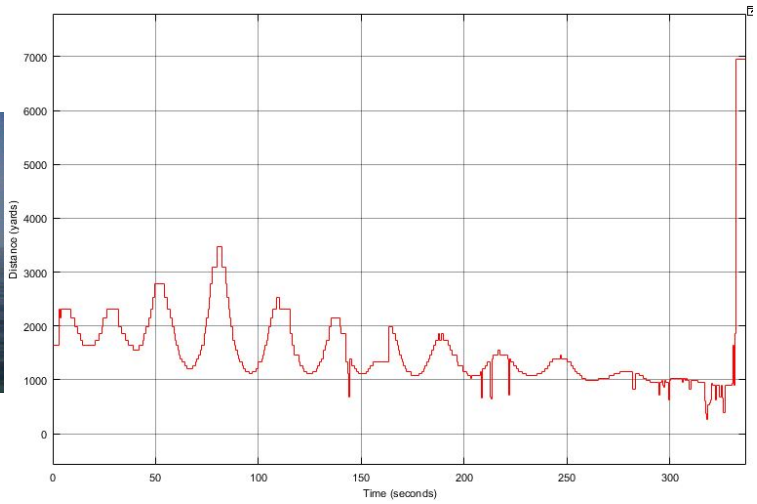

(b) Distance measurement during the simulation.

Figure 5.36: Images showing the end point and distance measurement for head waves of 1 meter.

The first thing the picture on the right shows is the presence of waves when compared to all other pictures from the simulation. When looking at the measured distance in the right of the figure, the presence of oscillations is the first thing that is noticed. These are caused by the pitching of the vessel which sometimes cause a too large distance and sometimes a too small distance. The middle between two peaks can be considered as the correct measurement. As the distance is reduced it is expected that the oscillations will reduce, which is also true after 100 seconds. The increasing peaks at the start are caused by a small heading change in order to get the target right in front of the camera. The increased peak at the end is the result of the fact that the system has lost the target. Overall this graph shows that the sytem is able to detect the vessel until about 900 yards, which is confirmed by a measurement from the simulator itself. Next the starting distance was reduced in order to speed up the testing proces. The next seastate that was tested was 1.5 meter, which is presented in figure 5.37.

(a) End point of the simulation.

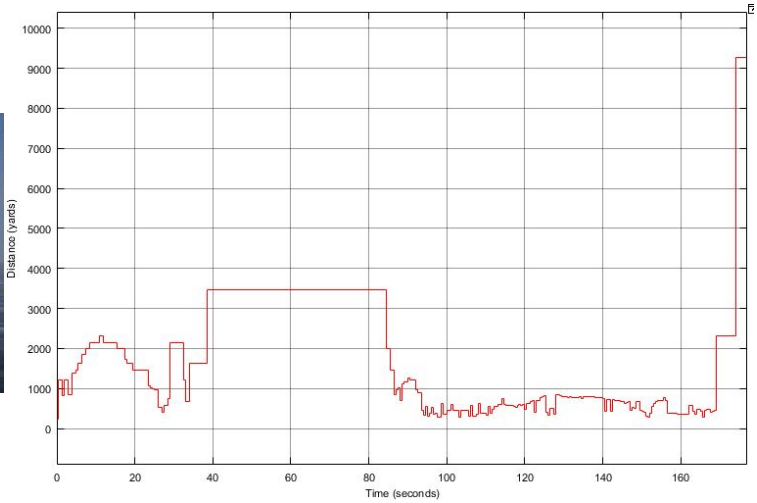

(b) Distance measurement during the simulation.

Figure 5.37: Images showing the end point and distance measurement for head waves of 1.5 meter.

The image on the left shows that the waves were increased for this test. The first thing that is noticed from the graph on the right is that the system is not able to detect the vessel for about 40 seconds. This was during a course change to get the target vessel in front of the vessel again. Thereafter the system was able to

detect the target, but the displayed values are too small. When the target was lost, the simulator indicated a distance of 1000 yards, were the system indicates 600 yards. Hence the target is detectable from 1000 yards onwards, but for some reason the values are incorrect. However the next test will be for a seatsate of 2 meter, which figure 5.38 is showing.

(a) End point of the simulation.

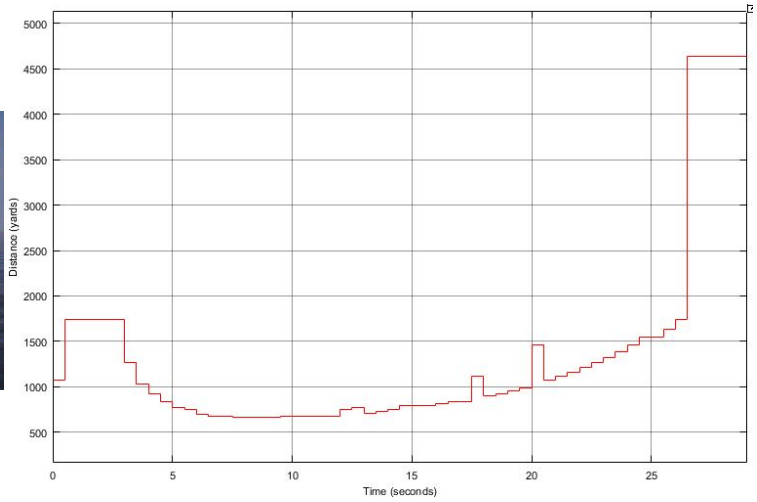

(b) Distance measurement during the simulation.

Figure 5.38: Images showing the end point and distance measurement for head waves of 2 meter.

The test at the seastate of 2 meter is relatively short, but after 20 seconds the system was no longer able to detect the target. This time the measurement was not restored like with the previous test. However the simulator indicated a distance of 1200 yards when the target was lost. The final test voor head waves was done for a seastate of 2.5 meter. Figure 5.39 presents these results.

(a) End point of the simulation.

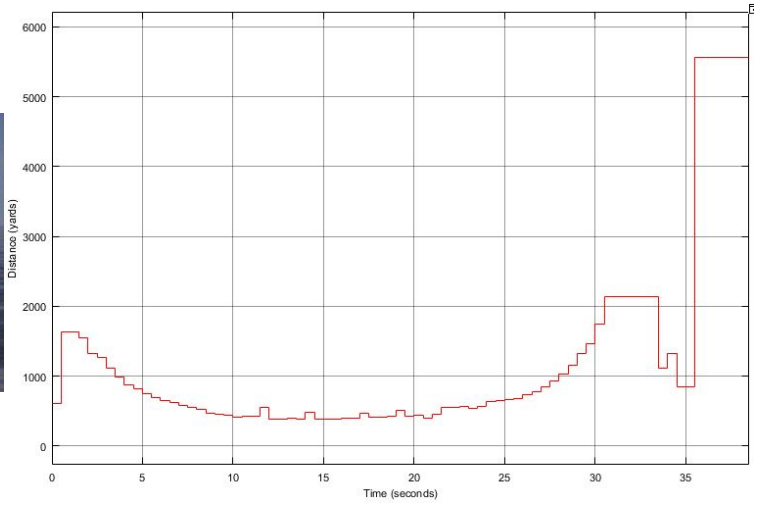

(b) Distance measurement during the simulation.

Figure 5.39: Images showing the end point and distance measurement for head waves of 2.5 meter.

The image of the test shows significantly increased waves for this seastate. However the system is able to detect the target for a longer period. The distance measured by the simulator is however larger in this case. At smaller distances than 1350 yards the system is not able to detect a target. This concludes the test for head waves. Now lateral incoming waves will be tested, starting with a seastate of 0.5 meter. For which the result is presented in figure 5.40.

(a) End point of the simulation.

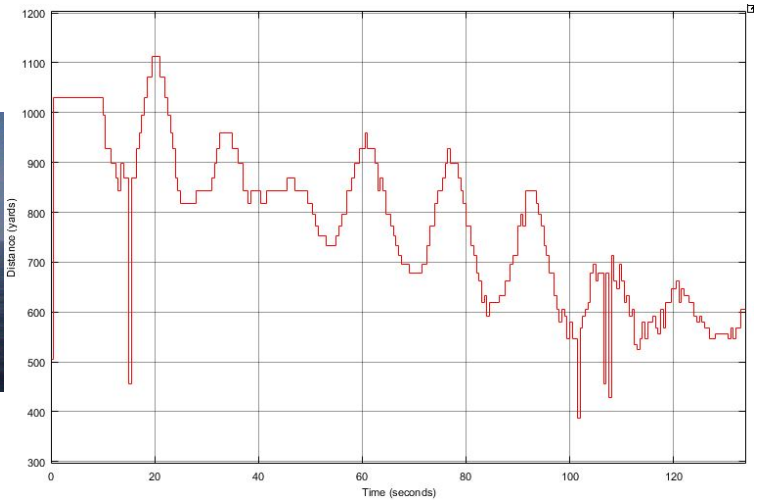

(b) Distance measurement during the simulation.

Figure 5.40: Images showing the end point and distance measurement for lateral waves of 0.5 meter.

The graph at the right of the figure again shows an oscillation. Due to the roll no steady measurement can be done, but the mean will approach the true value quite accurate. At the end of the simulation the simulator produced a distance of 600 yards, which comes quite close to the measured mean. The wave height is again increased to 1 meter. Figure 5.41 presents the results for this test.

(a) End point of the simulation.

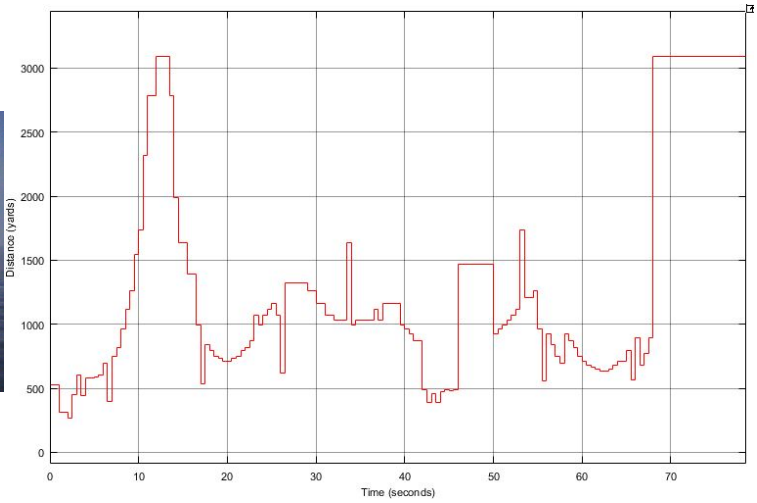

(b) Distance measurement during the simulation.

Figure 5.41: Images showing the end point and distance measurement for lateral waves of 1 meter.

The image also indicates a small increase in wave height. From the measured distance it is clear that no stable measurement can be taken. When the target is fully lost at 70 seconds the simulator measures a distance of 1000 yards. This value is approached by the system, but no valuable distance measurement could be done. For the next step the seastate is increased to 1.5 meter. In figure 5.42 the results of this test will be presented.

(a) End point of the simulation.

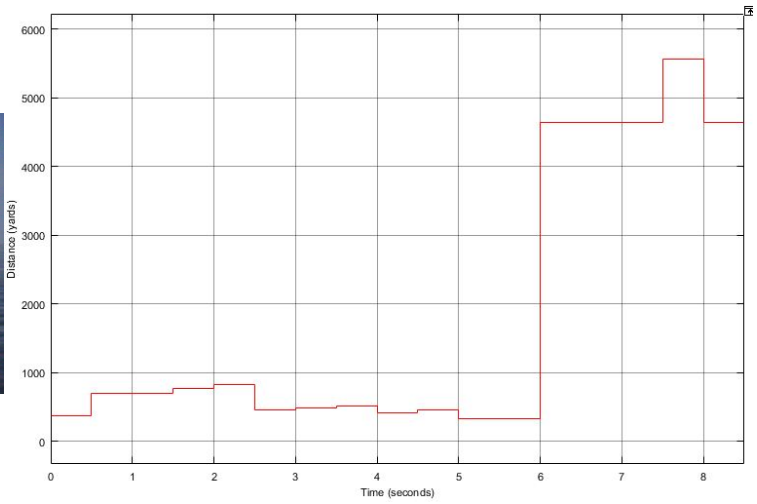

(b) Distance measurement during the simulation.

Figure 5.42: Images showing the end point and distance measurement for lateral waves of 1.5 meter.

From the image a white line can be seen, which indicates the wave peaks. This line clearly shows the wave direction, which is perpendicular to the direction of travel. The graph shows that the system is not able to take an accurate measurement from the target vessel. Therefore the minimal detectable distance is also 1500 yards at which the simulation started. Finally the sea state is increased once more, but a similar result is expected. Figure 5.43 shows the results for a seastate of 2 meters.

(a) End point of the simulation.

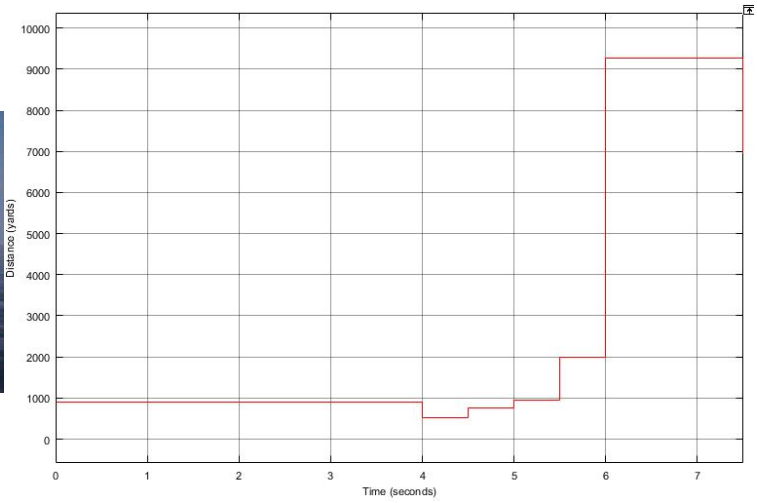

(b) Distance measurement during the simulation.

Figure 5.43: Images showing the end point and distance measurement for lateral waves of 2 meter.

From the image, the roll of the vessel can be observed. the rolling motion was caused by the incoming waves. The measurement of the distance indeed produces the same result as before. Meaning that the minimal detectable distance will be more than 1500 yards. The tests were not started at a larger distance, because at these distances the system needed to be closer in order to get an accurate measurement. By improving the camera resolution and stabalizing the camera mount with a gyro, the distance measurements can be improved. Then the only limiting condition is when the target vessel is lost in the noise caused by the waves. Finally the results for the seastate tests are summarized in table 5.1.

Seastate (meter)	Detectable distance (Yards)	
	Head waves	**Lateral waves**
0.5	500	500
1	900	1000
1.5	1000	1500
2	1200	1500+
2.5	1350	-

Table 5.1: Operational limits for seastate.

5.4.2 Fog

The next environmental condition that is simulated and tested is fog. Fog can reduce the contrast between the target vessel and the back ground. For these tests the target vessel is set at 500 yards. The own vessel is kept stationary and the target vessel will sail away. At one point the system will loose the target. This will then be the maximum detectable distance in fog.

Fog can be modeled in the simulator by setting a maximum visibility. For the first test the visibility is set to 5000 yards. In clear weather the maximum visibility can be as much as 30000 yards. Figure 5.44 shows the end position of the target vessel on the left and the distance measurement at the right.

(a) End point of the simulation.

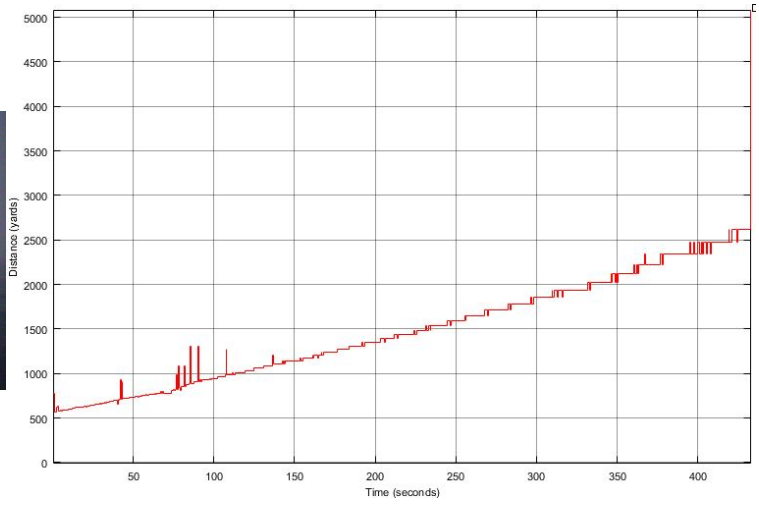

(b) Distance measurement during the simulation.

Figure 5.44: Images showing the end point and distance measurement for the fog test with 5000 yards visibility.

First of all the image shows that the target vessel already is fading away in the back ground. The wake of the vessel is almost completely disappearing. From the graph on the right a clear distance measurement is visible. Some small fluctuations are present during a change of heading of the own vessel, but overal the system gives a good result. At the end when the target is lost the system outputs an extremely large value. However the system is able to measure the distance until 2500 yards. For the next test the visibility is reduced to 4000 yards. The results for this test are presented in figure 5.45.

(a) End point of the simulation.

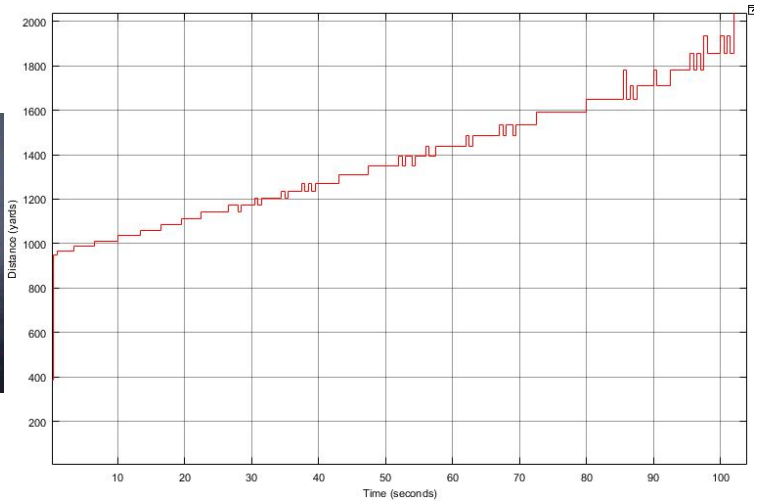

(b) Distance measurement during the simulation.

Figure 5.45: Images showing the end point and distance measurement for the fog test with 4000 yards visibility.

When comparing this image to the image from the previous test, it already shows that this time the target was lost on a closer distance. While the vessel is printed larger in this image. However the back ground appears more dense, which is expected with a lower visibility. Also with this test the system is able to obtain a stable measurement for the distance until the value shoots up. But until 2000 yards the system is able to track the target. For the final test with fog the visibility is set to 3000 yards. In figure 5.46 the results can be found.

(a) End point of the simulation.

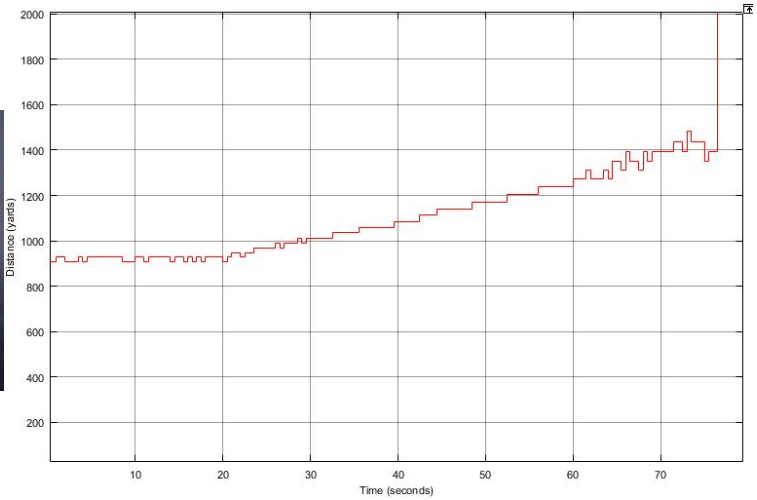

(b) Distance measurement during the simulation.

Figure 5.46: Images showing the end point and distance measurement for the fog test with 3000 yards visibility.

Also in this image the vessel appears larger and thus closer, as well as an even more dense back ground. Again for the final test the system is capable of tracking the vessel steadily, however the target was lost at 1500 yards. From these three test a relation between the visibility and the maximum detectable distance was obtained. The maximum detectable distance is about half of the visibility.

5.4.3 Precipitation

Next to fog also rain can have a negative influence on the contrast between the target and the back ground. In the simulator rain can only be turned on and of, but also a visibility range can be set. The later will only introduce fog as an extra feature. Therefore only one test with rain was done. For this test a frigate was placed at 1500 yards, but the distance was not changed. Figure 5.47 shows the results for this test.

(a) End point of the simulation.

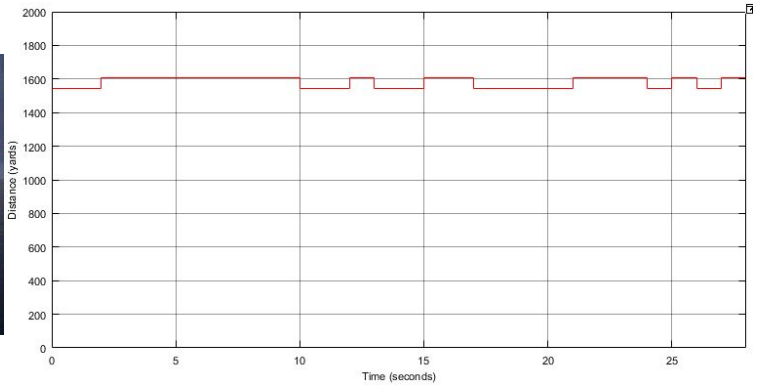

(b) Distance measurement during the simulation.

Figure 5.47: Images showing the end point and distance measurement for the fog test with 3000 yards visibility.

First of all the image shows no clear difficulties with the contrast, only some vertical lines are detected from the falling rain. Also the distance is accurately measured with only a very small fluctuation. This fluctuation however can be caused because the lowest point of the vessel is oscillating between two pixels. This test shows that rain has no negative influence on the performance of the system. Only when combining rain and fog a reduced performance can occur.

5.4.4 Light

Another important feature is the lighting condition, because when it is dark no distinction can be made between the target and the back ground. Therefore in this section the capability of the system will be tested around the time of sunset. The simulated test date was the fourte of May. This day sunset was at 2030 in time zone bravo[23]. Hence the first test was conducted exactly at sunset. Figure 5.48 shows the results of the test at 2030 B.

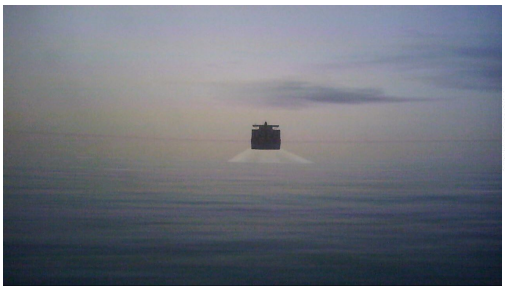

(a) Image from simulation at 2030.

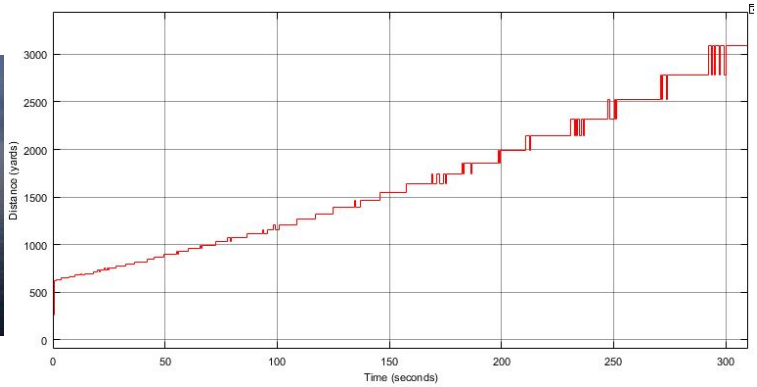

(b) Distance measurement from simulation at 2030.

Figure 5.48: Images showing the test and the distance measurement at 2030.

The image shows that dispite there is less light the contrast between the vessel and the back ground actually increases. Therefore the system is able to measure the distance even beter, which also can be concluded from

the graph showing the measured distance. The graph shows a smooth measurement, which is only oscillating when switching to the next pixel. In order to find the maximum operating window the next test was done half an hour later at 2100 B. The results for this test are presented in figure 5.49.

(a) Image from simulation at 2100.

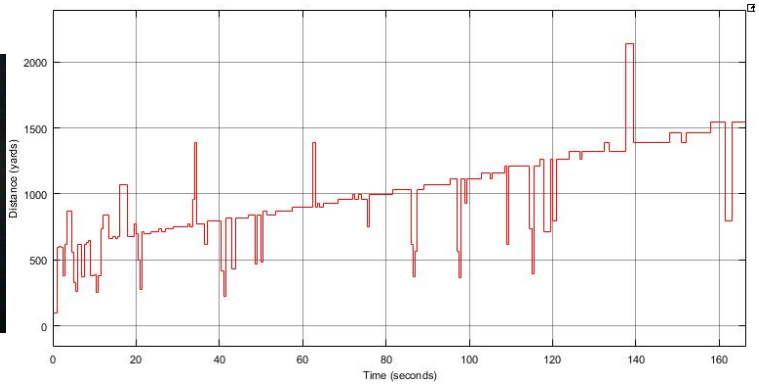

(b) Distance measurement from simulation at 2100.

Figure 5.49: Images showing the test and the distance measurement at 2100.

From the image the assumption can be made that it will be difficult to measure the distance as the contrast is now reduced again. However the target vessel is still clearly visisble. The graph that presents the distance also shows that the system sometimes has difficulties to accurately track the target. But all in all the system is still able to measure the distance quite well. Because this test is already much more dark than the previous, the choice was made to do the next test at 2115 B. There will be no figure showing this test, while there is no visibility at this time. When looking closely during this operation still a slight contour of the target vessel can be observed, but this is to weak to be detected by the system. Hence the conclusion is made that the system is able to operate until half an hour after sunset. The other way around it is also true that the system will be operational from half an hour before sunrise onwards.

5.4.5 Limits

From the test on the environmental conditions informational graphs can be made that show the operational limits for the different conditions. First of all a graph was made that shows the range in which the vessel can be detected. For normal operations the system is able to detect a vessel from 500 yards until 3000 yards, outside this range the measurements become too unstable. Figure 5.50 shows the graph for detectable range and images for certian conditions.

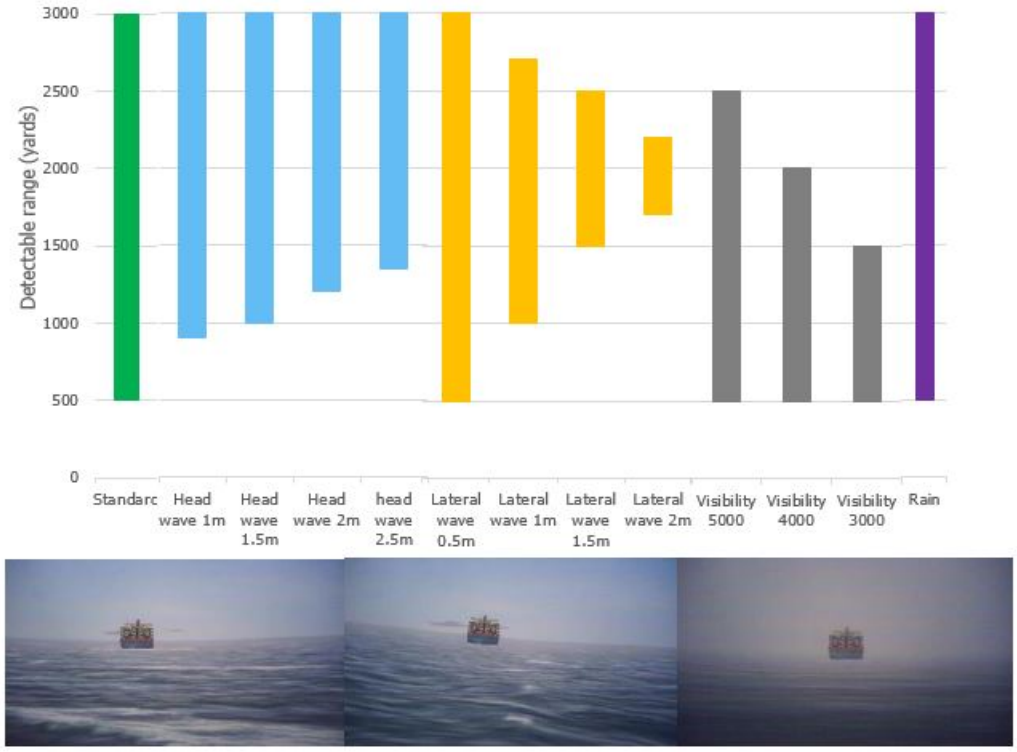

Figure 5.50: Graph showing the range for different operations.

In the graph each type of condition has another colour. The normal operational condition is coloured green, head waves blue, lateral waves brown, fog gray and rain purple. This graph immediatly show the impact for the different environmental conditions. Three images are added to show the influence of different conditions on the observations.

The first image shows the operation in head waves of 2 meter. In this image the relative large waves are clearly visible. Beacause these waves interfere with the vessel, this image shows why the minimum detectable range is increased. The second image shows what lateral waves of 1.5 meter do to the vessel. This image shows the rolling motion caused by the waves. Beacause of this rolling motion the system can only operate in a very small range. To close, the waves interfere with the target vessel and to far the system becomes to inaccurate. The final image shows the influence of fog on the contrast. The maximum detectable range is reduced because the system cannot distinguish the vessel from the back ground any longer.

The final influence on the operability that was researched is the ammount of ambient light. An illustration was made to show the influence on the system during twilight. During twilight the system will switch from operational to not operational and vice versa. The daily operational window can be found in figure 5.51.

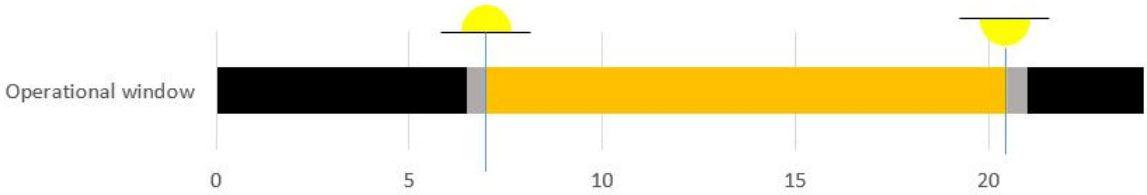

Figure 5.51: Graph showing operational window.

The image shows the operational window on the fourth of May. On the x-axis the numbers indicate the time. The black areas indicate that it is too dark to detect a vessel. The two gray areas indicate the twilight which last half an hour. The time of sunrise and sunset are indicated by the two suns, as the are usually used for nautical journals. Finally the yellow area is the normal operational window during daytime.

On the fourth of May the system is operational for 14 and a half hour. In summer time, during the longest day, at the 21st of June the operational time is increased to 17 hours and 45 minutes. However on the shortest day, the 21st of december, the system is only operational for 8 hours and 45 minutes.

These operational limits will be influenced by sensor properties. First of all the maximum detectable range can be increased by changing the pixels on the receiver. In order to change the camera parameter and the maximum range, the pixel density has to be increased. Thus a camera chip has to be used with either more pixels in the same space or with the same amount of pixels in a smaller space. Thus the pixel diameter will have to be reduced, which leads to a larger value for the camera parameter. When this is done the target will consist of more pixels in the image. Hereby making the target better distinguishable for the video processing software. Thus by reducing the pixel diameter with 50 percent, twice as much pixels will be used to capture the vessel at the same distance. In theory the maximum detectable range will then also double, but this has to be investigated more thouroughly.

The binary image shows noise around the edge of the image, for example in figure 2.5. By increasing the number of pixels the size of the noise will be the same in number of pixels, but will take up less space in the image. Therefore the system will be able to detect closer targets. The minimum detectable range will be smaller, which will increase the operational range of the system.

In seastate the minimum detectable range can not be reduced by increasing the number of pixels. This because in the image the waves and the vessel are interfering. For head waves the maximum range will be increased by using a sensor with a higher pixel density. For lateral waves the maximum detectable range is influenced by vessel motion. Hence in this case the maximum detectable range will not increase. In this case a stabilized camera will be the solution. Also for foggy conditions the maximum detectable range will not be increased. because here the contrast between the vessel and the back ground is the limiting factor. Finally on reduced light conditions the pixel density will also not be of an influence to the operability. Again the contrast is the limiting factor. Therefore the operational time can not be increased by changing the pixel density or camera resolution.

The operational limits can also be translated to the small scale model. For scale testing the noise around the edges is not present. It could be that the noise in the simulator is caused by the fact that the refreshing frequency of the simulator screen is interfering with the camera observations. On the scale vessel the camera is placed as about 25 centimeter from the water level. This means that the system theoratically can detect targets as close as 90 centimeter. The maximum range is not directly known, because this will depend on target size and contrast with the back ground.

6 Small scale model development process

In the previous chapters the development and testing of offline and simulator models was discussed. These models will be expanded in order to develop a fully autonomous small scale vessel. In this chapter the development process will be discussed. A few system concepts were examined. Each new concept was used, because the previous concept proved to have some major flaws. For each concept the main principle will be discussed. As well as the challenges for each concept, including the challenge that proved too big. Each concept is based on the use of the Seabex as autonomous vessel. This vessel is shown in figure 6.1.

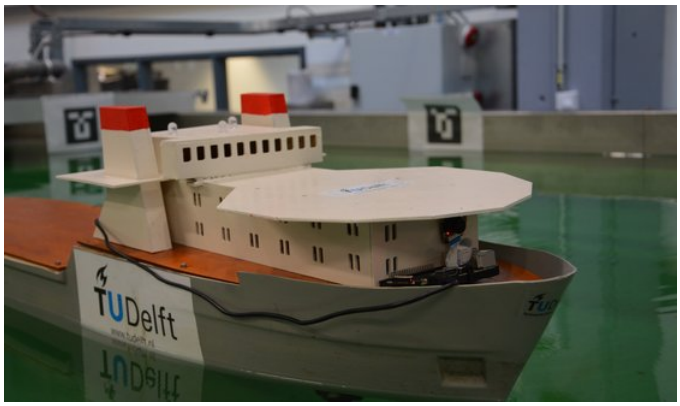

Figure 6.1: Image of the scale model.

For the development of the scale model one or more arduino boards will be used. An arduino board can connect to multiple sensors and actuator, which can be controlled by the build in microcontroller. In order to controll these components a program needs to be loaded to the board. The code for reading sensor data and to control actuators is open source. The developer only needs to add code in order to process the data as it is required for the application. Thus the arduino board is a easy solution for developing and prototyping projects. This solution does not require extensive knowledge in electronics and programming[24].

6.1 Video streaming

The first concept for an autonomous vessel was based on the wireless streaming of the video feed. This model required a few additional pieces of hardware. First of all the camera to capture the image. Secondly a system that is able to stream the feed. Finally to know the heading of the vessel an additional heading sensor is added. The original scale model already uses an arduino board to control the actuators. Figure 6.2 shows this equipment and how they should be connected for this concept.

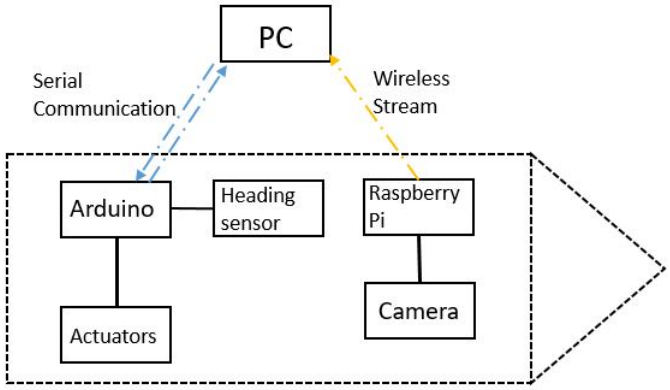

Figure 6.2: Model concept with video streaming.

In this figure different communication methods are indicated in different colours. First of all black lines indicate a standard cable connection. The blue lines indicate a serial communication protocol and the yellow line indicates a wifi connection. For the last two, the dotted lines indicate a wireless connection. If the blue line was solid, a cabled serial communication would be indicated. This colour scheme will be used throughout this chapter.

For the concept of video streaming, presented in figure 6.2, a Raspberry Pi is used for the streaming. The camera is connected to the Raspberry by cable. The Raspberry takes the video feed and will upload it to a private web page, only accesable from within the private network. From the mechatronics course the control model to connect the actuators with a arduino to the host computer is used. To this model the heading sensor shall be added. The Arduino should send actuator data and heading to the computer according to the serial communication protocol. On the computer the video feed should be taken from the web page and loaded into simulink. Then video processing should calculate distance and heading to the target vessel as it was done for the simulator model in the previous chapter. With this information the model should calculate new actuator settings. These settings will be send to the arduino again by serial communication.

Serial communication proves to be the key to the control of the autonomous vessel. In the previous paragraph the serial communication protocol was mentioned. So first this protocol should be discussed more thoroughly. This protocol is based on sending bytes. First a byte should be received before a response can be send. To initiate this protocol the computer will send a byte, which contains the information of the new task. Depending on the task the arduino will respond with different information. Then the simulink model on the computer calculates new actuator settings, which will be send to the arduino one at a time. The arduino will confirm with an acknowledgement byte, after which the computer can send the next byte. After the final acknowledgement the computer knows it can start a new task.

First of all the connection of the camera to the Raspberry Pi was established. In order to do this a small code had to be written, which starts the camera. An additional code made a web page to show the video feed. Then all devices connected to the network are able to open the web page with the IP adres of the camera. With the use of a guideline these steps were performed quite easily[25].

Next the challenge is to connect the heading sensor to an Arduino board and to obtain correct measurements. In appendix E the arduino code for the IMU is presented. In the first part of this code all parameters are declared. The second part is the setup of the system. In this part the serial communication is set. Also the speed of the communication is set. In this case a baud rate of 9600. Which means that 9600 bits per second can be transfered. The final part is the loop, where the execution of the model is performed. The first line of this part will start the sensor. The second line is to obtain the heading from the sensor. This code was obtained from the available software library from the sensor manufacturer[26]. The final part of the code was added in order to fix the output string. Depending on the heading, the output will have 4, 5 or 6 characters. With these different sizes the position of the dot will shift from the second to the fourth position. In order to fix the position of the dot and the size of the string one or two extra zeros in front of the string are added if necessary. By this, the string has always six characters with the dot at the fourth position. Each caracter will automatically be transformed to an ASCII value[27]. Because all positions of the characters are known, the transformation back to the original character can easily be made in simulink. Figure 6.3 shows the simulink transformation.

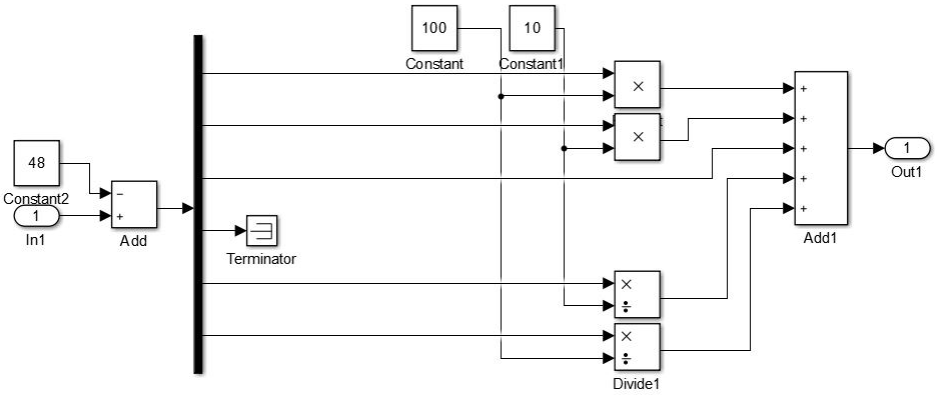

Figure 6.3: Model to transform a ASCII value to the correct number.

Because an ASCII value of 48 represents the character 0 and all numbers follow each other in the ASCII table, first the value of 48 is substracted. Each line in the figure represents one character of the heading with two decimals. The dot is indicated by a value of 46, but this line is not needed and hence terminated. In order to obtain the correct value for each character the first value will be multiplied by 100 and the second by 10. The third value already has the correct value and is not multiplied. Finally for the decimal numbers the character values are divided by 10 or 100. Hereby also the dot is placed back. All numbers will be added to obtain the correct heading.

In order to get this model operational the heading sensor has to be added to the original arduino for the scale model and the video stream has to be loaded into simulink. Both of these tasks proved to be quite difficult. The main problem with connecting the heading sensor was the amount of sensors and actuators that already were connected to the board. Also the code which controls all these components is quite complex. In order not to mess with the original hardware or software the choice was made to use an additional arduino board for the heading sensor.

It is possible to load and view a live feed from a web page to Matlab. However it is not possible to process the feed live. It is posssible to take a snapshot and thereafter process the snapshot. But this has to be done in two separate models. It is however not posssible to alternate between two active models, one to take the snapshot and another to process the image and calculate the output. The simulink model then stops the first time the other model captures a snapshot, because simulink cannot open an active file. Because of these problems it was decided to take a step down in complexity and use cables for all communications.

6.2 Cable connection

Due to the problems discovered during the development of the first system a new concept had to be found. The first change was an additional arduino for the heading sensor. Also the Raspberry Pi was removed. For this concept, both arduinos and the camera will be connected with an USB cable. The model scheme for this concept can be found in figure 6.4.

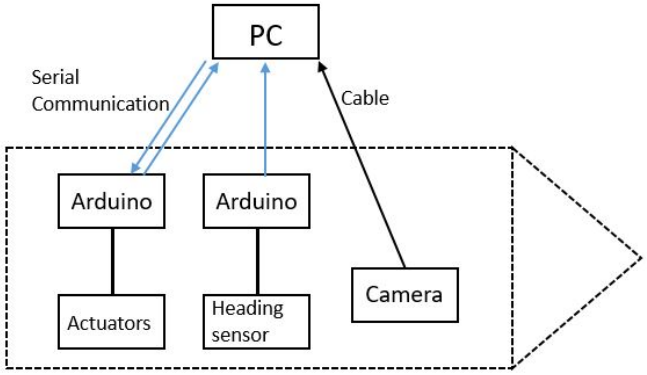

Figure 6.4: Model concept with cables.

When comparing this image to the first scheme, the component change can be observed. Both arduino boards will use a cable for the serial communication. A slight difference is that the second arduino only sends heading measurements through the communication link. This code will continuously write a measurement to the serial port. The webcam will be connected to the computer with the attached USB cable.

By eliminating the Raspberry and the wireles video stream the video feed kan directly be used in simulink. The same method was used for the simulator models in the previous chapter. Therefore this system can calculate the distance and heading with the same blocks as they were developed for the simulator model.

With the knowledge from the previous models it was quite easy to develop and use this concept. These tests were conducted in a small flume tank. This tank was surrounded by a lot of objects. Also the ambient lights were causing reflections in the water. Due to these facts the system was not able to obtain accurate and stable measurements. Therefore a marker on the target vessel was used to improve the system. Figure 6.5 shows an image of the target vessel with a marker and a specific image of the marker.

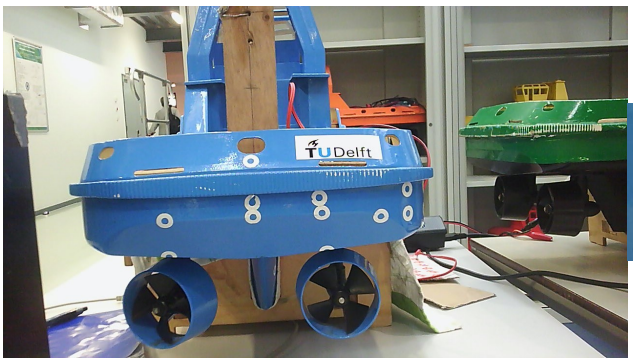

(a) Image from target vessel.

(b) Zoomed image of the marker.

Figure 6.5: Images showing Vessel with marker and only the marker.

A matlab script was used that takes these two images and than can point out the marker in the main image[28]. In appendix F this code is presented. First of all both images are loaded and transformed to an intensity image in accordance with equation 2.3. Then the algorithm will detect strong specific features from both images. These features will be used as reference points for the marker. The features for both images will then be matched to see which features are located in both images. Some of these pairs could have an odd placement with respect to the other pairs. These pairs are made up from a box feature and a similar feature on a different location in the main image. Therefore these pairs are disgarded. Then the final part of the standard program will draw a box polygon around the remaining points in the main image.

The next part of the program was added to point out the marker in order to use it in the autonomous system. The polygon has four sides, but the shape is not fixed. In order to make sure the full marker is visible the shape should be rectangular. Therefore the most upper, right, lower and left coordinates are obtained by finding the minimum or maximum values from the corners of the polygon. Next the intensity value of the most lower left corner is saved. Finally a straight line is obtained by setting all pixels above the most upper coordinate to the saved value. The same can be done for the three other lines, which results in a rectangle. The marker should be located in this rectangle. By giving all pixels outside the rectangle the same value, the autothreshold block should only output a white blob for the marker. Then the real size of the marker has to be used to calculate heading and distance from the blob. Finally in the matlab code the final image is saved, which should point out the marker. Figure 6.6 shows the result of the matlab code.

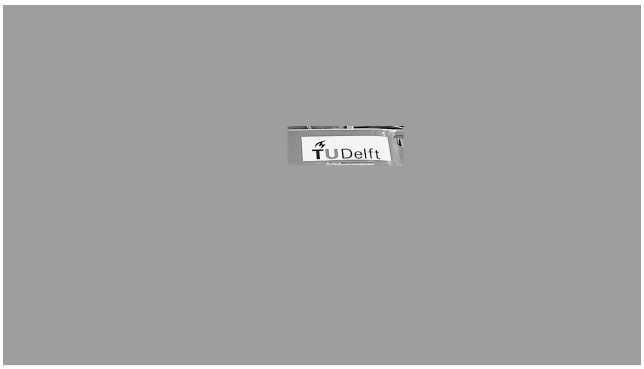

Figure 6.6: Intensity image focussed on the marker.

From this image the marker is clearly visible. Just a small area around the marker is from the original image and the rest is blanked out. This image shows that the code operates as expected. Unfortunately the code is not compatible with simulink. Even implementing this code as a matlab function in simulink did not work. A solution could be to only use matlab code instead of the simulink model. However then all standard simulink functionalities have to be coded in matlab. Therefore the choice was made not to move forward with this concept.

6.3 Serial communication

For the new concept the Raspberry Pi was brought back again. Only this time the Raspberry will be used in a different role. Again with this concept two arduino boards will be used. One for the communication from the vessel control and one for the heading sensor. Figure 6.7 will show the concept scheme.

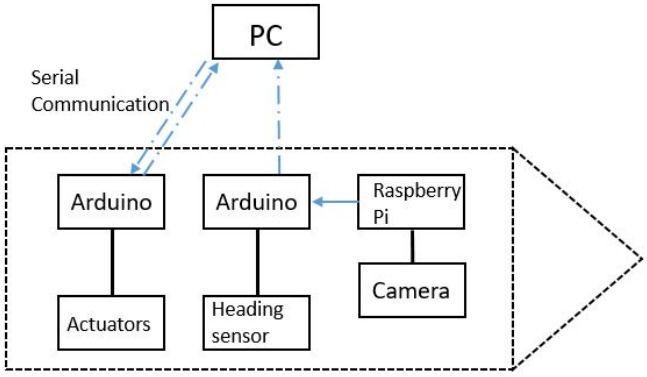

Figure 6.7: Model concept with serial communication.

Again a marker will be used for the detection and tracking of the target vessel. This time all video processsing will be performed by the Raspberry. For this concept a different type of marker is used. The marker used for this concept will help to determine the heading and bearing depending on the orientation of the marker. Figure 6.8 shows an example of such a marker.

Figure 6.8: Marker design to calculate heading and bearing.

By serial communication the raspberry will send target bearing, heading and distance to the arduino. These values will be taken from one serial port on the arduino board. Then these values will be increased in order to always have the same size. Then these values will be added to the string from the heading sensor. So only one string will be send to the computer by a second serial port. Because the size and order of all parameters are known the information can be extracted in simulink. The control communication with the other arduino will be established on another communication port on the computer. This enables that both arduino boards can communicate in the same simulink model.

The first test for this concept was to discover the influence of two arduino boards in the same model. Therefore the Drymodel for the scale model was taken. A dry model is a model to test the working of the vessel without placing it in the water. The Drymodel is placed in the appendix G, in figure G.1. The scale model has two stern thrusters and two bow thruster. In this model for each thruster the azimuth and the speed can be changed during a simulation. These settings are taken to the arduino block. This block takes care of the serial communication protocol. The output of this block are three measured rotational speeds. One for each stern thruster. And one for the two bow thrusters, which are driven by the same engine. The second arduino is connected at the third COM port, as can be seen in the image. For this test only the vessel heading was transmitted. Therefore the communication block will output six values based on the six received bytes. Then the model from figure 6.3 wil calculate the actual heading.

To this point the communication from the Raspberry to the arduino is not yet established. Also the transformation in the Raspberry which calculates the heading and bearing is not yet developed. Therefore in this research no further scale test will be conducted. However with this research most work to start testing is already done.

Conclusions and recommendations

This graduation thesis was focussing on the use of a camera system as a sensor for autonomous operations at sea. The research questions were formulated in chapter 1. First, with the results from the research, the support questsions will be answered. Thereafter the main research question can be answered with the results from the support questions.

When considering the results for the collision avoidance operations the first research question can be evaluated. With the use of a collision avoidance system, safety at sea can be improved. The test showed that the system is able to detect the other vessel. The detected vessel can be tracked, by which the threat is evaluated. Finally when the approach appears to be too close, the system is able to take evasive action. Due to sensor properties this system cannot act as an early warning system. But when the watch personel is not responding, this system can act as a final resort. The system is responding relatively late, but the evasive action proves to be sufficient to prevent a collision.

Next the second supporting research question, which consists of two parts, will be discussed. The first part is whether the system is able to take over the task of humans on vessels. The collision avoidance operation, but also the other operations, show that the control system together with the camera system can calculate vessel responses. So the decision making part can be performed by the system. For the second part, tests have shown that the camera system is able to perform target detection and tracking. So the camera system can also take over tasks from traditional sensor systems. However in terms of accuracy and stability the camera system still needs improvement, when compered to the traditional sensors.

The environmental conditions prove to limit the operational availability of the system. First of all head waves will influence the total range in which targets can be detected. An increasing wave height will increase the minimum distance from which targets can be detected. So in head waves the operational range is reduced. Due to vessel motion, the measurements will oscillate around the actual distance. These oscillations will reduce measurement stability. Lateral incoming waves influence both minimum and maximum detectable distance. Therefore these waves are largely limiting the operational range. Again vessel motion will also destabilize the measurements. Fog and visibility also limit the maximum detectable range for the vessel. The contrast between the back ground and the vessel is fading, which results in the fact that the system loses the target at a closer distance. Rain however does not negatively affect the performance of the system. Finally the available ambient light also limits the operability. From half an hour before sunrise to half an hour after sunset the system is operational. A remarkable discovery was that the system is better able to detect the vessel during twilight, while the reduced light causes a dark shade on the target.

The development of offline models for different ship types and operations proved to be a valuable tool in the development of the models for testing. By the use of an accurate offline model the control system can be tuned in order to give the system the desired response. A valuable insight was that no matter the vessel dimensions, the control parameters solely determine the response of the system. Also when the propulsion configuration is changed the same control parameters can be used. However the offline model also show that when the configuration is changed too drasticly these systems can become unstable. By bypassing some thrusters the moments and forces will not always be balanced, thereby causing the vessel to react unstably.

Next the evaluation is made on the different type of operations that can be performed with this system. This system is able to perform platform approach operations. However the camera resolution causes large gaps at larger distances. Because the control system experiences a fast change in distance it will react. Hence the system will reverse the thrust in order to slow down the vessel. This happens quite fast and will therefore destabilize the approach. For the replenishment operation the fluctuations are less significant, because the speed difference is smaller. However this system proves to be unstable during heading changes. For the heading control in order to reach a desired lateral distance the system is behaving very well. However the control of the distance is again possible, but difficult. The follow the leader operation was not tested, because small scale tetsing was not yet possible. However from the result for the other operations it is expected that the system should be able to perform this operation. Distance and heading measurements are possible, thus

with this information the system should be able to calculate the required vessel respons in order to follow the target. The ability to perform collision avoidance operations was already discussed when evaluating the influence on safety at sea.

The final supporting research question was to investigate the importance of video processing and video enhancement. From the simulator tests the importance of video enhancement was discovered. In order to obtain a stable measurement first the feed should be enhanced by histogram equalization. This method enhances the contrast between dark and light pixels. By doing this, the system will be able to distinguish the targets better from the back ground. A filter will finally remove all remaining noise peaks. Resulting in a more stable and constant distance measurement. The same method does not work for the heading measurement. The heading measurement however already proved to have a relatively stable behaviour.

So all in all this research proves the feasibility of a camera as a sensor for nautical systems. Tests have shown the posibility of detecting and tracking of target vessels. From the simulator the realistic conclusion was that the system works for relatively large vessels at a medium range. However small vessels cannot be detected in system noise. Therefore the camera can be a reliable sensor for autonomous operations at sea. However the operational range will have to be improved and environmental influence on the operability of the system will have to be limited in order to use this system on a large scale.

Recommendations

First of all, for the prove of concept the choice was made to use a simple webcam as camera for the testing. Thus in order to improve the performance of the system, a better camera should be used. The camera used for testing was full HD, which results is a resolution of 0.8 MP. However these days cell phones already have cameras up to 20 MP. However with only increasing the resolution the system behaviour will not improve significantly. Also pixel density should be increased in order to reduce the step size at larger distances. When pixels are packed closer together the transfer to the next pixel will be made sooner. Another limiting factor was the viewing angle of the camera. In order to improve the system, especially for the collision avoidance operation a camera coverage of 360 degrees is required. With such a system all vessels and objects, around the vessel can be detected. In this way the system will be able to react to all upcoming collision threats. A 360 degree coverage can be obtained in two ways. First of all by using multiple cameras facig in different directions. The video processing software should than cope with the overlap of the multiple inputs. A second solution is the use of a rotating camera mount. The benefits of a rotating mount is that no software is needed to cope with the overlap. Secondly the distance measurement for targets can always be performed when the camera is exactly facing towards the target. This will result in a more accurate distance measurement. Finally the camera position can then be used in order to obtain the target heading directly. Next in order to obtain a round the clock operability night vision cameras or infra red cameras should be used. These systems will be capable of detecting unlit vessels even in pitch dark. When staying with the environmental conditions the system should also be able to reduce the influence of vessel motion. Therefore the camera system should be gyro stabilized in some way. The Royal Dutch Navy already uses a rotating infrared camera which is stabilized[29]. For the Navy it could be valuable to investigate the use of this sensor in combination with the models for autonomous operation.

Initially the plan was to make use of a database consisting of vessel types in oreder to develop a collision avoidance system that fully complies with the IMO regulations. However due to the complexity the choice was made to only prove the concept of collision avoidance. So without the database the system is only required to act in case that the threat is approaching straight ahead or from starboard. Thus in order to fully comply with the regulations a self learning database should be developed. This database should detect and recognise different vessel types. Because special vessels usually have the right of way no matter from what direction they are approaching.

The main problem for developing a realistic scale model is the communication from the sensors on the vessel to the external computer. Also the communication between multiple programs that have to cooperate for the vessel control is hard to obtain. Durig testing the background is full of small and medium large

objects close to the size of the target vessel. These objects reduce the detectability of the target vessel. The use of markers on the target will help to destinghuish the target. However the additional programming and communication again will make the model more complex. Due to these problems and developed solutions, for these problems, it was not yet able to perform small scale tests. Therefore further small scale testing is requierd in order to assess the full operational potential of the system.

The ability to control every aspect of the test in a simulator resulted in the choice to mainly use the ship handling simulator for this research. However before this system can be used on full scale a lot more testing has to be done. Next to small scale tests of course also at full scale. However when a new and better camera will be used it will be valuablle to first go to the simulator again. In this way the calculated camera parameter can be evaluated. But also new operational limits can be established. In this research an assumption was made on how the operational limits will change when the camera is changed. But the relation will probably not be liniear. Thus when the resolution and pixel density are doubled, the range of the system will probably not be doubled. Therefore the simulator can help in determining the new limits.

For this research the assumption was made that the camera system would be used indipendently on the autonomous vessel. However it is of course also possible to use the camera next to the traditional sensors in order to get the most accurate measurements. The use of multiple sensors in order to calculate the most probable value can be done by sensor fusion. This method uses sensor accuracy, measurement uncertainty and sensitivity to environmental influences for all sensors. A filter then takes all these values and will calculate the most likely measurement value, which can be used for the control system. Therefore it could be valuable to investigate the use of sensor fusion in a multi sensor configuration.

With the results of small scale tests, full scale tests and simulator tests the models can be validated. Model validation is required in oreder to assess the usefulness of the models. Because of the unavailability of these test results the validation of these models and the offline model could net be performed. Also an uncertainty analysis will give insight in the usefulness of these models and sensors. After these analyzes have been performed a better insight will be obtained on vessel behaviour. Herby the operator can choose to reduce the level of autonomy when the conditions cause inaccurate measurements or an unstable behaviour.

Finally for this research a vessel configuration was chosen with two fixed stern thrusters and a bow thruster. The fixed stern thrusters were chosen to reduce model complexity. Heading changes were performed by a yaw moment when one stern thruster is applying forward thrust and the other thruster is applying backward thrust. However when one of these stern thrusters becomes unafailable the vessel behaviour becomes unstable. But when the azimuth of the stern thruster is allowed to change the vessel is still abble to operate stably. Therefore the model should be expanded with the introduction of stern azimuth changes.

References

[1] International Maritime Organization. *http : //www.imo.org/en/About/Pages/Default.aspx* [16-05-2017].

[2] Equations of motion. *http : //www.real−world−physics−problems.com/equations−of−motion.html*. real world physics problems. *http : //www.real − world − physics − problems.com/* [17-05-2017].

[3] Autonomous operations at sea, what and how? N. Jacobsen. Delft, November 2016.

[4] COLREGs - Preventing Collisions at Sea. *http : //www.imo.org/en/OurWork/Safety/Navigation/Pages/Preventing − Collisions.aspx*. International Maritime Organization. *http : //www.imo.org/en/Pages/Default.aspx* [12-01-2017].

[5] A Review of Multisensor Data Fusion for ADAS. *https : //lichaoma.com/*2016/02/14/*a − comprehensive − review − of − multisensor − data − fusion − for − adas/*. Malcolm's Technical Blog. *https : //lichaoma.com*. [25 October 2016].

[6] Advanced Techniques for Centimeter-Accurate GNSS Positioning on Low-Cost Mobile Platforms. K. M. Pesyna. Austin, December 2015.

[7] A robust vision-based moving target detection and tracking system. A. Behrad, A. Shahrokni, S.A. Motamedi, K. Madani. Januari 2001.

[8] Vision Based Target Tracking and Collision Avoidance for Mobile Robots. A. Tsalatsanis, K. Valvanis, A. Yalcin. Journal of Intelligent and Robotic Systems, January 2006.

[9] Autonomous Vehicles Navigation with Visual Target Tracking: Technical Approaches. Z. Jia, A. Balasuriya, S. Challa. Algorithms, 15 December 2008.

[10] A Robust Method for Computing Vehicle Ego-motion. G.P. Stein, O. ano, A. Shashua. Intelligent Vehicles Symposium 2000.

[11] A Monocular Vision Advance Warning System for the Automotive Aftermarket. I. Gat, M. Benady, A. Shashua. 29 September 2004.

[12] Vision-based ACC with a Single Camera: Bounds on Range and Range Rate Accuracy. G.P. Stein, O. Mano, A Shashua.

[13] CCD and CMOS sensors. *http : //www.techbriefs.com/component/content/article/*20063. NASA Tech Briefs. *http : //www.techbriefs.com/*. [25 October 2016].

[14] Sensor Fusion and Observer Design for Dynamic Positioning. Z. Liu. Delft, January 2015.

[15] CMOS Is Winning the Camera Sensor Battle, and Here's Why. *http : //www.techhive.com/article/*246931/*cmos*$_i$*s*$_w$*inning*$_t$*he*$_c$*amera*$_s$*ensor*$_b$*attle*$_a$*nd*$_h$*eres*$_w$*hy.html*. TechHive. *http : //www.techhive.com*. [25 October 2016].

[16] CMOS Image Sensors: Electronic Camera-On-A-Chip. E.R. Fossum. Institute of Electrical and Electronics Engineers. Vol 40, no 10, October 1997.

[17] Verkeersregels op zee, Bepalingen ter voorkoming van aanvaringen op zee. K. van Dokkum. 3rd, DOKMAR, Enkhuizen, 2008.

[18] Feedback Control of Dynamic Systems. G.F. Franklin, J.D. Powell A. Emami-Naeini. 6th, Pearson, Upper Saddle River, 2010.

[19] Design of Propulsion an Electric Power Generation Systems. H. Klein Woud, D. Stapersma. Reprint (1st), IMarEST, London, 2013 (2002).

[20] MT44000 Mechatronics in Maritime Technology. M. van den Boogaard, M. Overbeek, J. le Poole. Delft, November 2016.

[21] The interaction between diesel engines, ship and propellers during manoeuvring. P.J.M. Schulten. Delft, May 2005.

[22] Wetted surface area - approximate formulas. $https://www.boatdesign.net/threads/wetted-surface-area-approximate-formulas.930/$. $https://www.boatdesign.net/$. [09 May 2017].

[23] Time zone map. $https://www.timeanddate.com/time/map/$. https://www.timeanddate.com/. [02 June 2017].

[24] What is Arduino? $https://www.arduino.cc/en/Guide/Introduction$. Arduino. $https://www.arduino.cc/$. [20 June 2017].

[25] How to Make Raspberry Pi Webcam Server and Stream Live Video —— Motion + Webcam + Raspberry Pi. $http://www.instructables.com/id/How-to-Make-Raspberry-Pi-Webcam-Server-and-Stream-/$. Instructables. $http://www.instructables.com$. [07 June 2017].

[26] Adafruit BNO055 Absolute Orientation Sensor. $https://learn.adafruit.com/adafruit-bno055-absolute-orientation-sensor/overview$. Adafruit. $https://learn.adafruit.com/$ [07 June 2017].

[27] ASCII Table and Description. $http://www.asciitable.com/$. [07 June 2017].

[28] Object Detection in a Cluttered Scene Using Point Feature Matching. $http://nl.mathworks.com/help/vision/examples/object-detection-in-a-cluttered-scene-using-point-feature-matching.html$ MathWorks. $http://nl.mathworks.com/$ [07 June 2017].

[29] Sirius. $https://www.thalesgroup.com/sites/default/files/asset/document/DS007_09_06\%20SIRIUS.pdf$ Thales. $https://www.thalesgroup.com/$. [08 June 2017].

A Full offline model

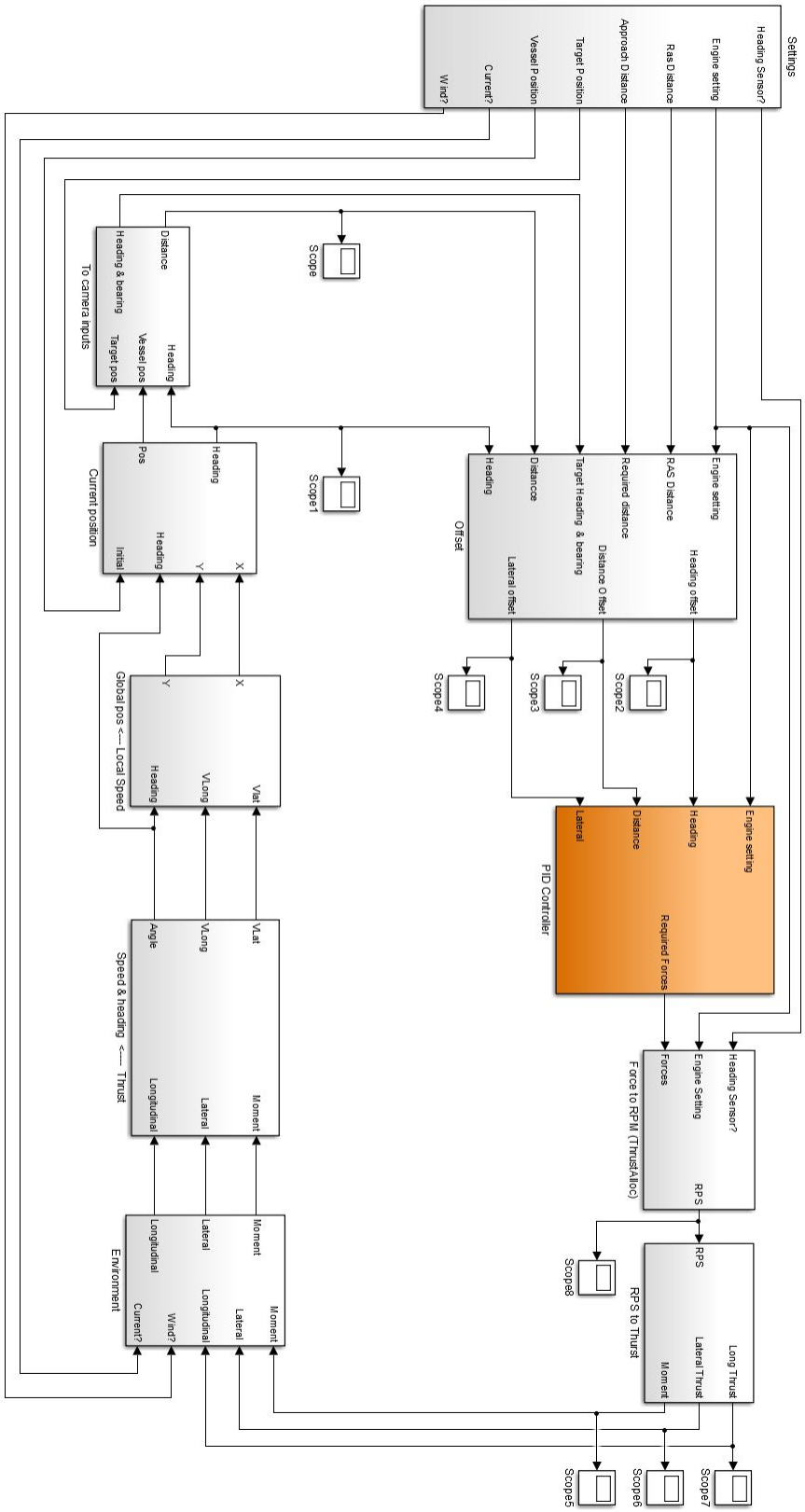

Figure A.1: Full offline model.

B Full model for offset calculation

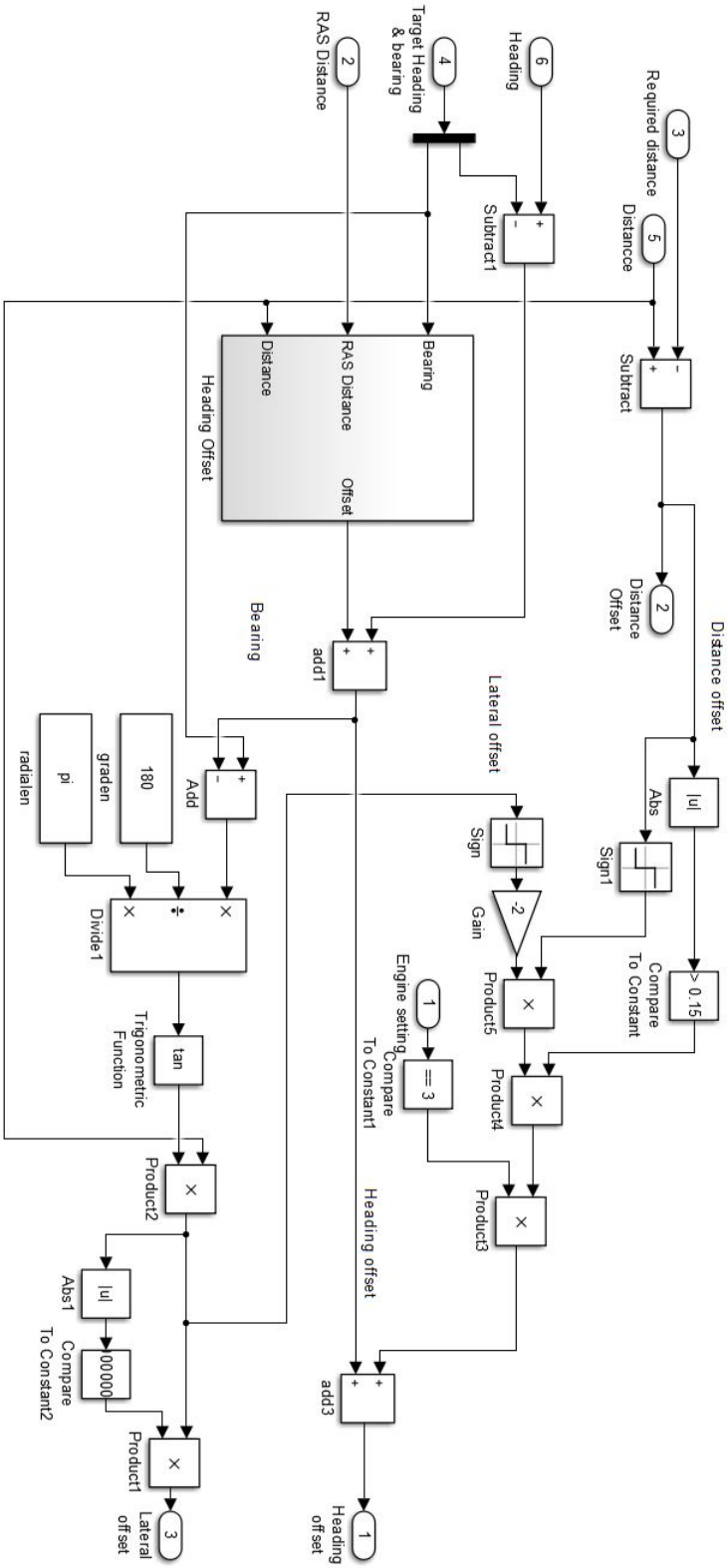

Figure B.1: Model to calculate all offsets.

C Offline model thrust allocation

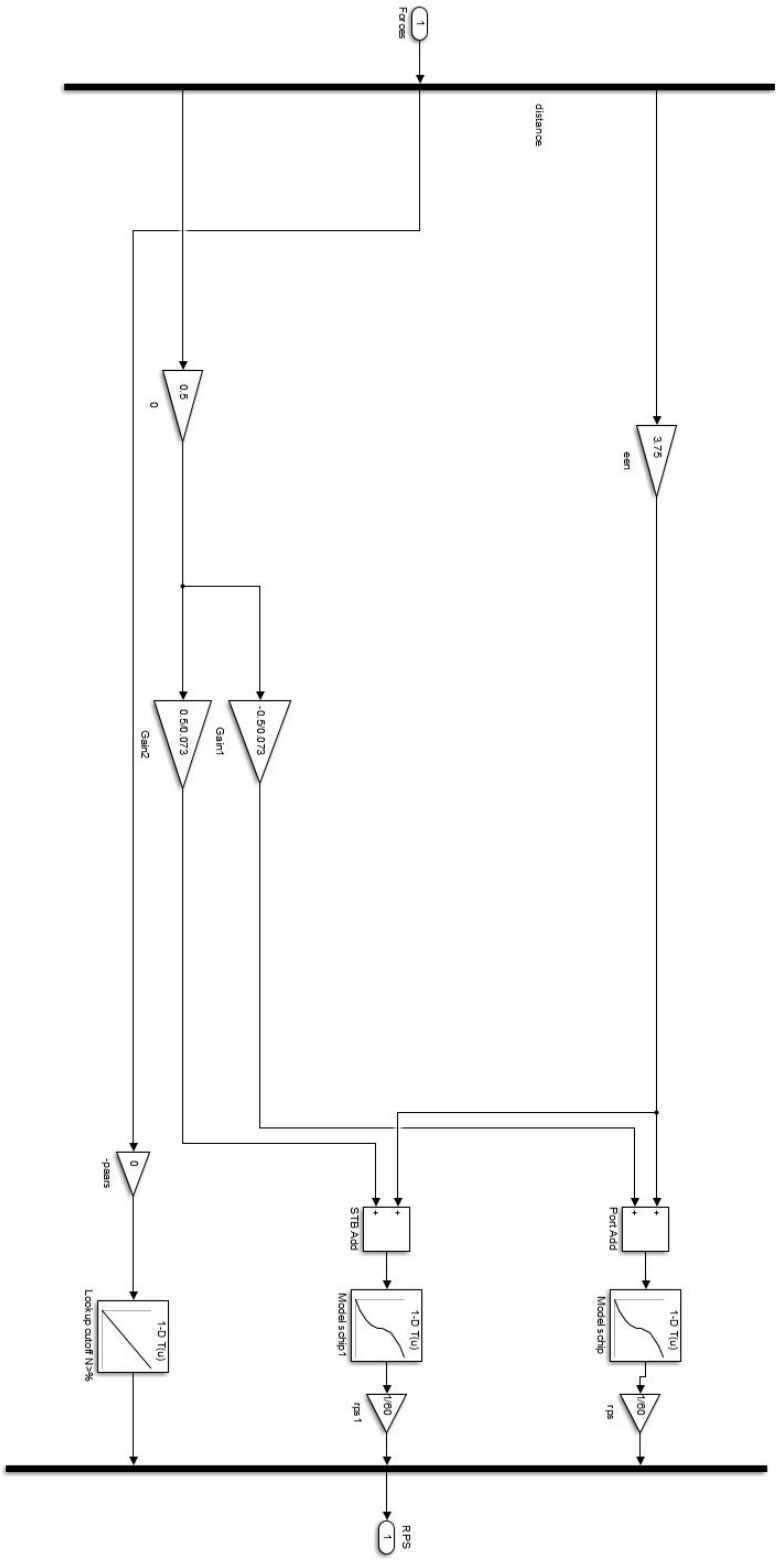

Figure C.1: Thrust allocation for the offline model with port and starboard thruster.

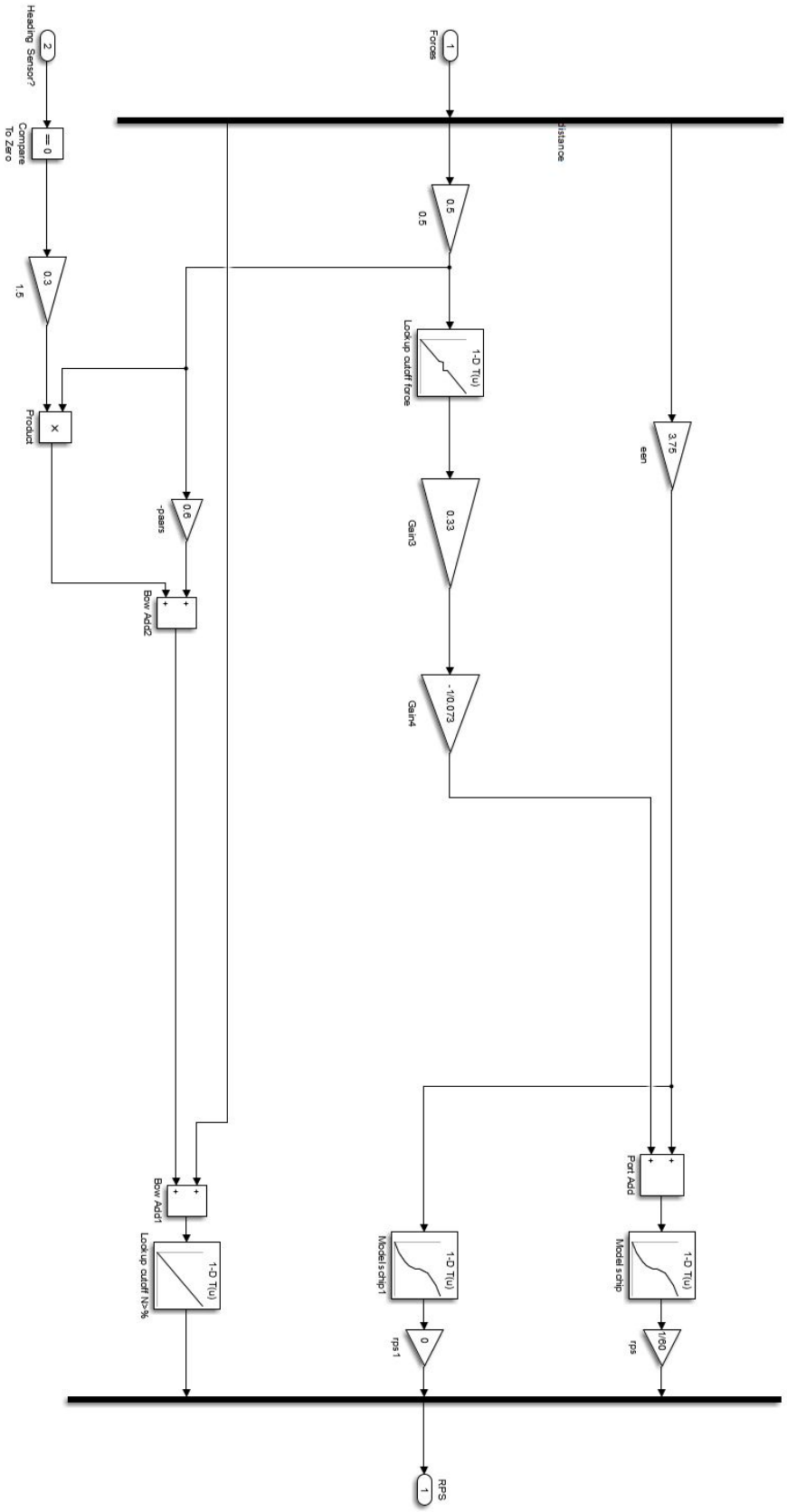

Figure C.2: Thrust allocation for the offline model with port and bow thruster.

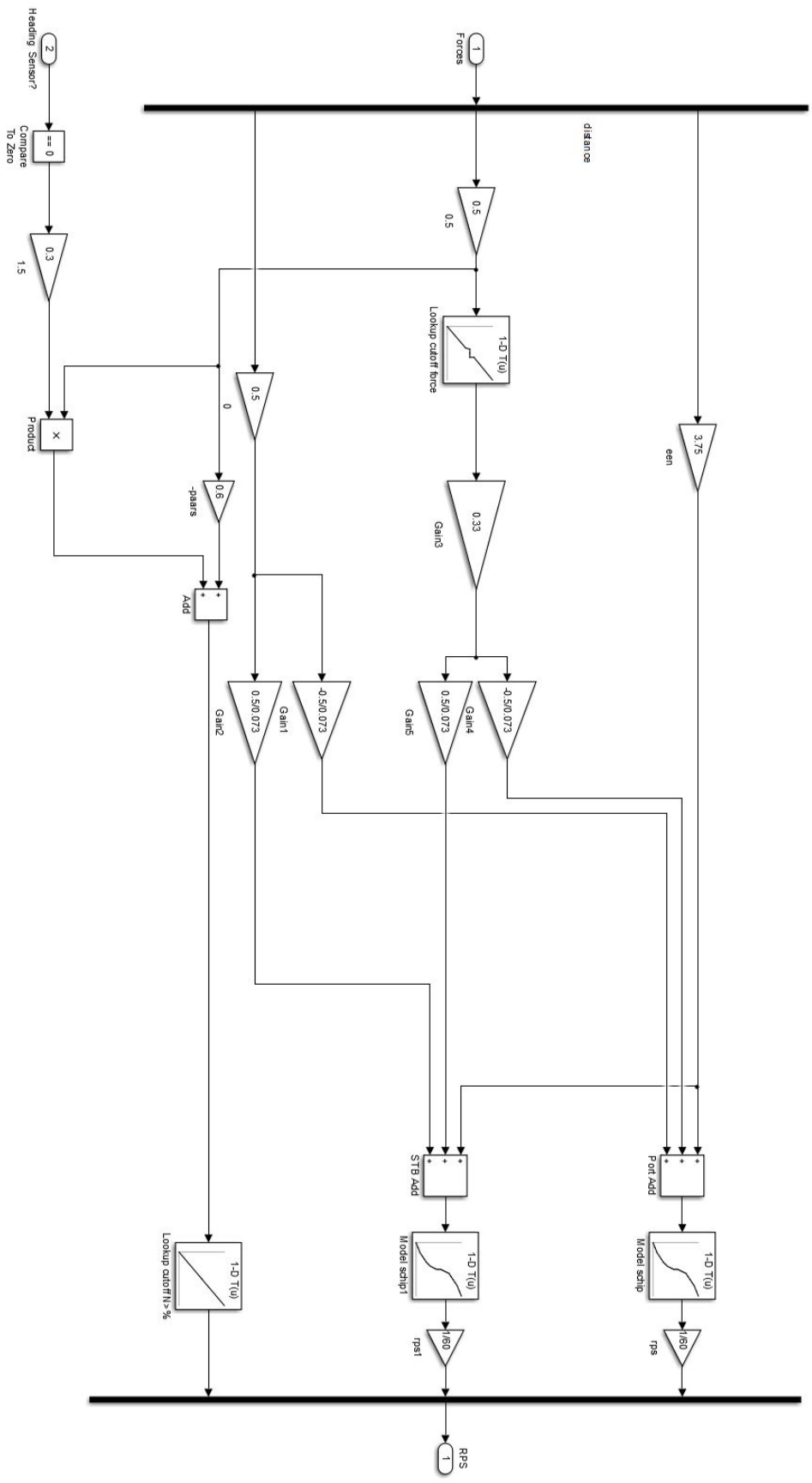

Figure C.3: Thrust allocation for the offline model with all thrusters.

D Simulator models

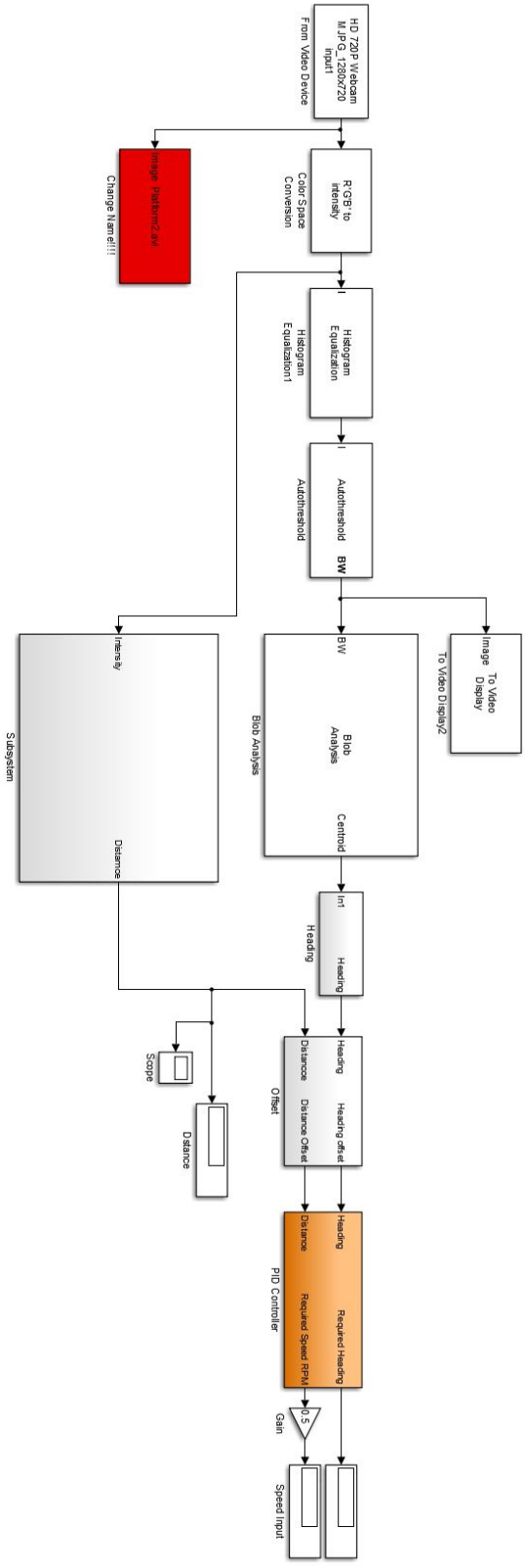

Figure D.1: Simulink model for the platform approach operation.

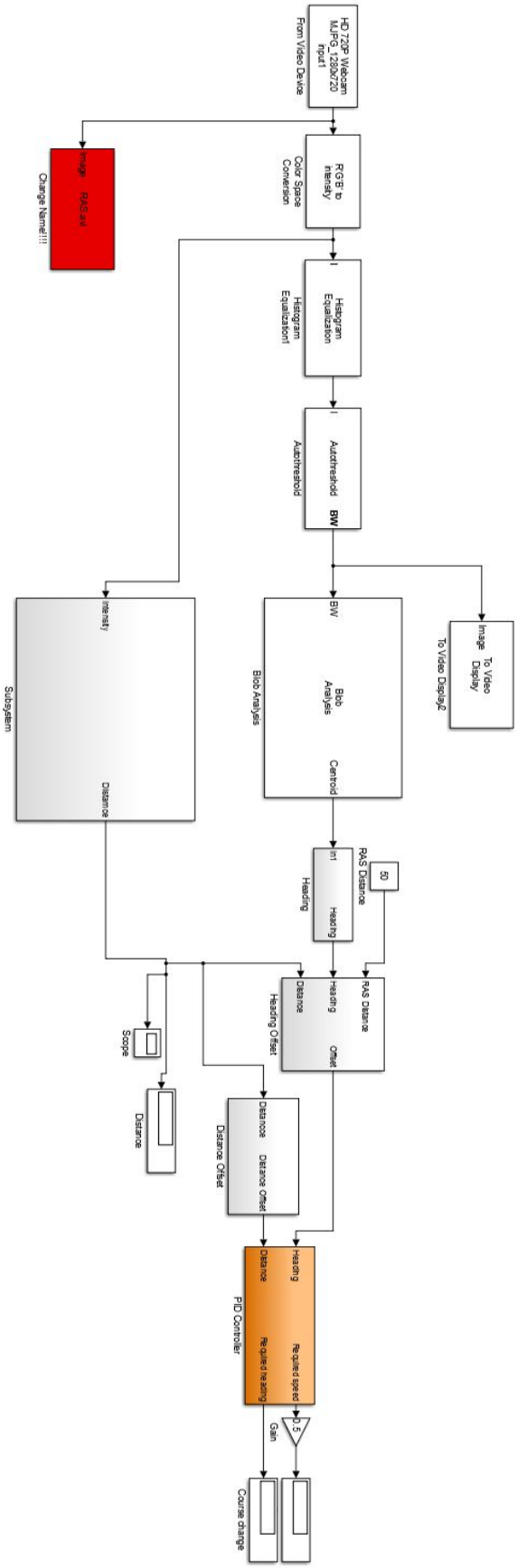

Figure D.2: Simulink model for the RAS approach.

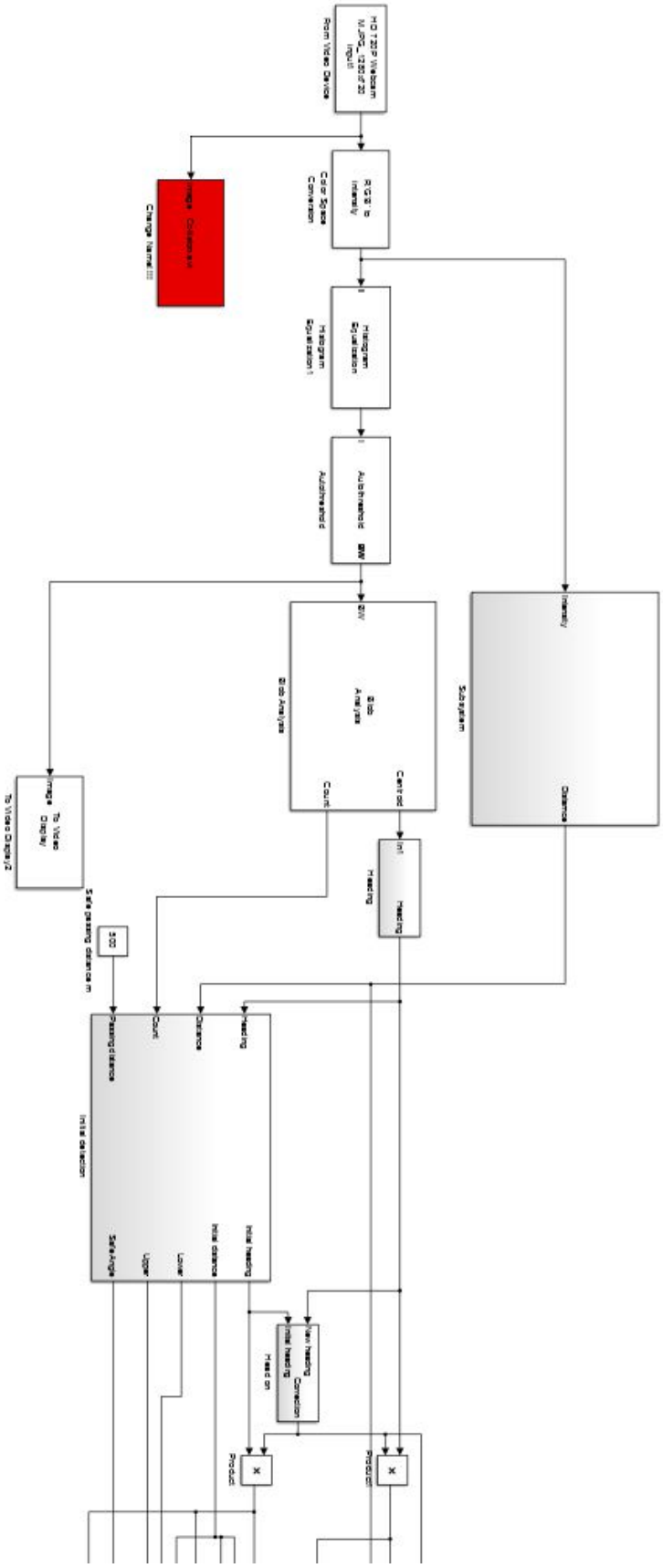

Figure D.3: First part of the simulink model for collision avoidance.

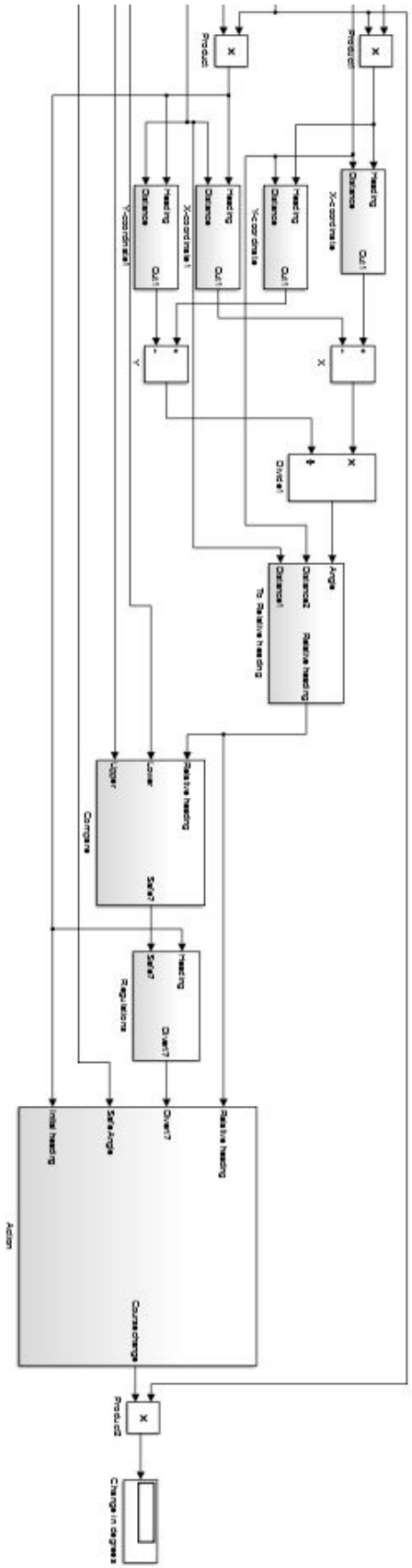

Figure D.4: Second part of the simulink model for collision avoidance.

E Arduino code to operate the IMU

The code from this appendix shows how the IMU obtains the heading and how this is send to simulink.

```
#include <Wire.h>
#include <Adafruit_Sensor.h>
#include <Adafruit_BNO055.h>
#include <utility/imumaths.h>

String Heading;
String test;
int Aantal;
int AantalSB;
int AantalP;
String Een;
String Output;


Adafruit_BNO055 bno = Adafruit_BNO055(55);
char msg[3];

void setup(void)
{
  Serial.begin(9600);
  /*Serial.println("Orientation Sensor Test"); Serial.println("");*/

  /* Initialise the sensor */
  if(!bno.begin())
  {
    /* There was a problem detecting the BNO055 ... check your connections */
    /*Serial.print("Ooops, no BNO055 detected ... Check your wiring or I2C ADDR!");*/
    while(1);
  }

  delay(1000);

  bno.setExtCrystalUse(true);
}
void loop(void)
{
  /* Get a new sensor event */
  sensors_event_t event;
  bno.getEvent(&event);

  /* Display the floating point data */


 test = String(event.orientation.x,2);
 Aantal = test.length();
 Een = String(0);
```

```
 if (Aantal == 4)
 {
  Heading = Een + Een + test;
 }
 else if (Aantal == 5)
 {
  Heading = Een + test;
 }
 else
 {
  Heading = test;
 }


Output = Heading;

 Serial.print(Output);



  delay(1000);
}
```

F Matlab code to focus on the marker area

This appendix shows the code that takes an image of a marker and will point out the area in which this marker is located in the main image.

```
Image = imread('Marker2.jpg');   % Marker
boxImage = 0.2989 * Image(:,:,1) + 0.5870 * Image(:,:,2) + 0.1140 * Image(:,:,3); %Intensity
Image2 = imread('Main.jpg'); % Full image
sceneImage = 0.2989 * Image2(:,:,1) + 0.5870 * Image2(:,:,2) + 0.1140 * Image2(:,:,3); %Intensity
% Capture strong features.
boxPoints = detectSURFFeatures(boxImage);
scenePoints = detectSURFFeatures(sceneImage);
[boxFeatures, boxPoints] = extractFeatures(boxImage, boxPoints);
[sceneFeatures, scenePoints] = extractFeatures(sceneImage, scenePoints);
% Match feature from both images.
boxPairs = matchFeatures(boxFeatures, sceneFeatures);
matchedBoxPoints = boxPoints(boxPairs(:, 1), :);
matchedScenePoints = scenePoints(boxPairs(:, 2), :);
% Disgard points that not correspond with box dimensions.
[tform, inlierBoxPoints, inlierScenePoints] = ...
    estimateGeometricTransform(matchedBoxPoints, matchedScenePoints, 'affine');
% Draw box around the marker in the full image.
boxPolygon = [1, 1;...                           % top-left
        size(boxImage, 2), 1;...                 % top-right
        size(boxImage, 2), size(boxImage, 1);... % bottom-right
        1, size(boxImage, 1);...                 % bottom-left
        1, 1];                   % top-left again to close the polygon
newBoxPolygon = round(transformPointsForward(tform, boxPolygon));
% Calculate the largest values of the box.
upper = min(newBoxPolygon(1,2),newBoxPolygon(2,2));
right = max(newBoxPolygon(2,1),newBoxPolygon(3,1));
lower = max(newBoxPolygon(3,2),newBoxPolygon(4,2));
left = min(newBoxPolygon(4,1),newBoxPolygon(1,1));
% Safe intensity value from lower left point.
value = sceneImage(lower,left);
FinalImage = sceneImage;
% Give each pixel outside the box limits the same value
for i = 1:upper
    FinalImage(i,:) = value;
end
for j = 1:(720-(lower-1))
    FinalImage((lower+(j-1)),:) = value;
end
for k = 1:left
    FinalImage(:,k) = value;
end
for l = 1:(1280-(right-1))
    FinalImage(:,(right+(l-1))) = value;
end
imshow(FinalImage);
```

G Drymodel for communication with additional arduino board

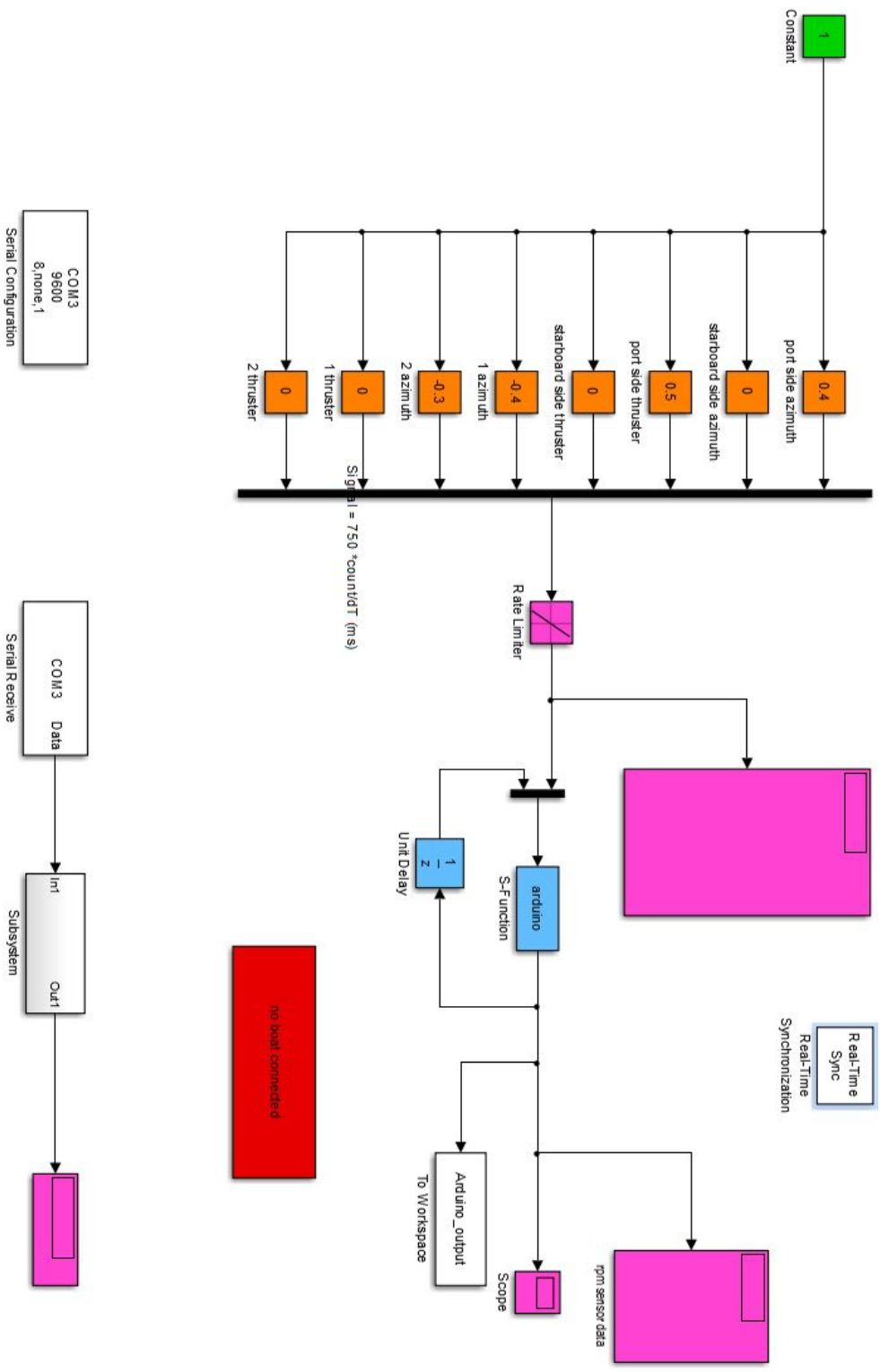

Figure G.1: Model to test the vessel with the dry model.